Evolutionary and Developmental Survey of Genes Involved in Chordate Pigmentation

Thesis

For guidance on citations see FAQs.

oro.open.ac.uk

EVOLUTIONARY AND DEVELOPMENTAL SURVEY OF

GENES INVOLVED IN CHORDATE PIGMENTATION

Ugo Coppola

Sponsoring Establishment:

STAZIONE ZOOLOGICA ANTON DOHRN

NAPOLI, ITALY

February, 2018

EVOLUTIONARY AND DEVELOPMENTAL SURVEY OF

GENES INVOLVED IN CHORDATE PIGMENTATION

A thesis submitted to the Open University of London for the degree

of

DOCTOR OF PHILOSOPHY

By

Ugo Coppola

Director of Studies:	**Dr. Filomena Ristoratore**
External Supervisor:	**Dr. Prof. Sebastian Shimeld**

Sponsoring Establishment:

STAZIONE ZOOLOGICA ANTON DOHRN

NAPOLI, ITALY

February, 2018

DEDICATION AND ACKNOWLEDGEMENTS

ABSTRACT

The pigmentation represents one of the most interesting topics in animal life because it is a decisive factor for the evolutionary success and the conquest of new ecological niches. Through the combination of developmental biology and comparative genomics, some aspects of pigmentary dynamics have been studied.

Given Rabs regulate a plethora of trafficking steps, the members belonging to this family are central to the transport of molecules involved in pigmentation. Moreover, comprehending the evolution of Rab family is relevant to understand the establishment of eukaryotic cellular organization and for its implication in many human pathologies. For the first time, I reconstructed the evolutionary scenario of Rab family in eleven species of metazoans, spanning from cnidarians to human. Phylogeny, intron code and synteny conservation prompted me to depict Rab evolution, with a special focus on chordates that exhibit a highly dynamic evolutionary pattern.

I clarified the evolution of Rab32/38 subfamily, fundamental in regulation of trafficking related to melanogenesis. It has been clarified the evolutionary history of Rab32/38 genes in deuterostomes and the expression pattern in key species as zebrafish and amphioxus, demonstrating how events as whole-genome duplications have influenced their role during embryogenesis.

In order to find new genes involved in pigmentation, I analyzed a Kelch-like member in ascidian *Ciona robusta* (*Cr-Klhl21*). My results point at this gene as a marker of pigmented cells, with a dynamic expression profile during embryogenesis: from middle tailbud stage, it is expressed specifically in the otolith. Moreover, *Cr-Klhl21* shows an intricate regulatory scenario with the possible intervention of a

transcription factors combination (*Cr-Mitf*, *Cr-msxb*, *Cr-Dmrt*). This work contains first data about a Kelch-like member in ascidians, providing new insights in pigmentation or pigment cell specification. This encourages further analyses on its gene regulatory network and possible function.

TABLE OF CONTENTS

LIST OF FIGURES

LIST OF ABBREVIATIONS

α-MSH (α-Melanocyte-Stimulating Hormone)

AP (adaptor protein complex)

BLOC (biogenesis of lysosome-related organelles complex)

cAMP (cyclic AMP)

DHI (5,6-dihydroxyndole)

DHICA (5,6-dihydroxyindole-5-carboxylic acid)

Dmrt, DMRT (Doublesex and mab-3 related transcription factor)

EFcab (EF-hand calcium-binding domain-containing protein)

GRB (genomic regulatory block)

Hpf (hours post-fertilization)

Klhl (Kelch-like)

LECA (Last Eukaryotic Common Ancestor)

LRO (Lysosome-related organelles)

MAPK (mitogen-activated protein kinase)

MC1R (melanocortin-1 receptor)

Mitf, MITF (microphtalmia-associated transcription factor)

ML (Maximum Likelihood)

Msx, MSX (msh homeobox)

NC (neural crest)

NM (neuromelanin)

Rab, RAB (Ras-related in brain)

Rab32LO (Rab32 Lost In Olfactores)

RASEF (RAS And EF-Hand Domain Containing)

RPE (retinal pigmented epithelium)

SOCS (suppressor of cytokine signaling)

Tyr, TYR (Tyrosinase)

Tyrp, TYRP (Tyrosinase-related proteins)

TSGD (Teleost-specific genome duplication)

WGD (whole-genome duplication)

CHAPTER 1

INTRODUCTION

1.1 – A multitude of molecules and cells for pigmentation

Pigmentation is one of the most fascinating and variable phenomena in the animal kingdom, in fact its evolution has attracted scientific community attention for centuries. The perceived colour is the net result of many interacting elements like nervous, hormones and environmental controls, rendering animal colouration a really interesting process to study, with different approaches and tools from ecology to physiology and developmental biology. Although the enormous differences existing between the animal phyla, invertebrates and vertebrates continuously use biological pigments contained in chromatophores for their survival and adaptation to a plethora of ecological niches. Pigment cells, albeit show different developmental origins and functions in distant animal phyla, are present in all the metazoans. As a matter of fact, all of them are characterized by formation and storage of biological pigments. All vertebrate pigment cells derive from the neuroectoderm and the most studied cell type is the black/brown melanocyte, present in birds and mammals containing the black pigment melanin. Other vertebrates possess more chromatophores whose names depend on the stored pigment, such as xanthophores, leucophores and cyanophores, which influence their pigmentary pattern, with an extraordinary colour explosion in teleost fishes (Fujii, 1993; Bagnara, 1998). Furthermore, several types of chromatophores have also been detected in distantly-related non-vertebrate metazoans from cnidarians as jellyfish to mollusks as octopus.

1.2 - Melanin: evolution, function, biosynthesis

Melanin represents the most successful biological pigment across animal evolution, probably for its physical and chemical features: its presence and diverse fundamental roles has been demonstrated in prokaryotic and eukaryotic domains. Indeed, melanin and its intermediates are crucial for maintaining the structure of cells in plant seed pods and insect cuticles (Riley, 1992) and increasing virulence in bacteria and fungi (Riley, 1997; Plonka and Grabacka, 2006). Animals possess cells containing melanin granules employed for a multitude of physiological processes that can be important in ecological strategies of species, in particular regarding inter/intra specific behaviors as sexual display and mating (Wittkopp et al., 2002).

Essentially, three kinds of melanin are known: the eumelanin, the most common divided in black and brown, the pheomelanin, that is responsible for red hair and the neuromelanin (NM), accumulated in the primate brains with an unknown function. Along the tree of life, melanin formation takes place in extra or intracellular environments. In bacteria, this pigment is synthesized in the external space for antitoxic and chemo-protective effects (Claus and Decker, 2006) whereas some phytopathogenic and pathogenic fungi accumulate melanin granules on the cell wall increasing the resistance to environmental damage (Eisenman and Casadevall, 2012). On the other hand, vertebrates present cells whose cytoplasm contains specialized organelles called melanosomes to store melanin granules (Marks and Seabra, 2001).

In prokaryotes, melanin originates from a series of reactions catalyzed by a single melanogenic enzyme while in vertebrates it is produced through the Raper-Mason pathway starting from the phenolic amino acid precursor L-tyrosine, with the succession of many biochemical reactions (Borovanský and Wiley, 2011). Tyrosinase (TYR) and Tyrosinase Related Proteins 1 and 2 (TYRP1, TYRP2) are

considered the mammalian key enzymes in this multi-step process, in fact the activity of these metalloproteases is crucial for melanin biosynthesis (Figure 1.1). Tyrosinase has a central role in the pathway, given that it promotes the first and rate-limiting reaction steps: the L-tyrosine hydroxylation to 3,4-dihydroxyphenylalanine (DOPA) and its subsequent oxidation in DOPAquinone. Moreover, it catalyzes also the oxidation of 5,6-dihydroxyndole (DHI) to indole-5,6-quinone. TYRP2, together with metal ions as Zinc and Copper, converts the red DOPAchrome in 5,6-dihydroxyindole-5-carboxylic acid (DHICA) rather than 5,6-dihydroxyindole (DHI) (Palumbo et al., 1991), whilst TYRP1 is implicated in DHICA oxidation to indole-5.6-quinone carboxylic acid (del Marmol and Beermann, 1996). The stability, activation and folding of tyrosinase are finely controlled by the cell modulating redox state (in particular Cu^{2+} ions), cysteine concentration and pH conditions. On top of this, melanin pigments and pathway intermediates directly inactivate melanogenesis (Slominski et al., 2004). TYRP1 and TYRP2 are enzymes considered as regulators of melanin production and tyrosinase activity (Slominski et al., 2004).
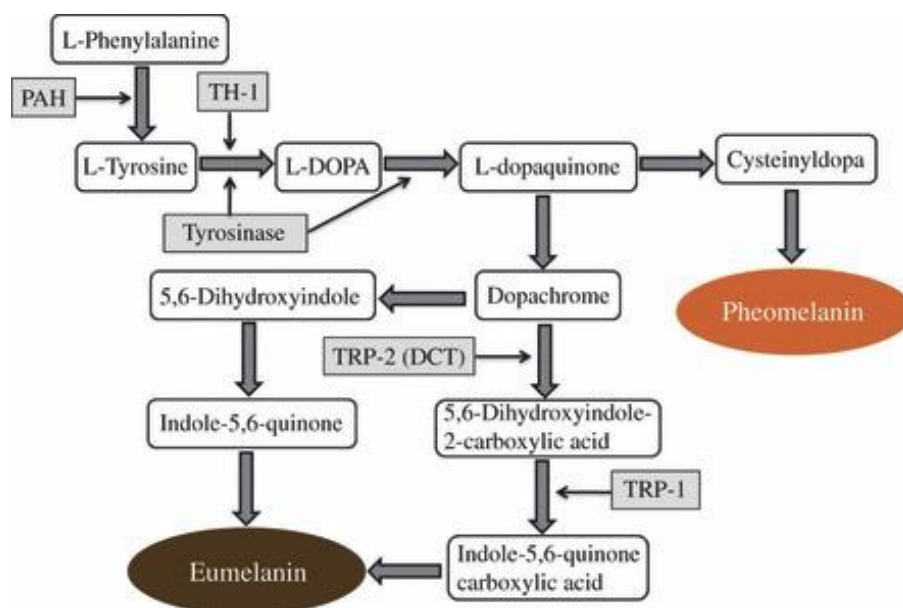
Figure 1.1. Scheme of melanogenic pathway. Here is represented the multi-step reaction series for the biosynthesis of melanins in the vertebrates (adapted from Gillbro and Olsson, 2011).

Eumelanin is a black/brown pigment constituted by DHI and DHICA whereas pheomelanin is a sulphate yellow-reddish macromolecule which comprises cysteinyl-3,4-dihydroxyphenylalanine (cysteinyl-DOPA), produced from the condensation of DOPAquinone and L-cysteine (Meredith and Sarna, 2006). Used in animals for protection against UV radiation (UVR), the two components of melanin granules are different in their UV response: eumelanin detoxifies from reactive oxygen species (ROS) derived from UV light (Bustamante et al., 1993) and transforms light into heat energy (Meredith and Riesz, 2004) whereas pheomelanin is involved in redox-buffering (Kim et al., 2015). The majority of melanin pigments present in nature are a mixture of eumelanin and pheomelanin (Ito and Wakamatsu, 2008), whose ratio is defined by tyrosinase functioning and disposability of tyrosine and cysteine; in addition, it can have consequences for human skin pigmentation (D'Mello et al., 2016). It has been suggested an involvement of TYRP1 and TYRP2 activity in the increase of eumelanin percentage with respect to pheomelanin (Slominski et al., 2004). Concerning the latter, its presence in vertebrates has been demonstrated in birds and mammals and not in teleosts and other poikilotherms (Fujii, 1993). Neuromelanin is a dark polymer of 5,6-dihydroxyindoles present principally in substantia nigra and locus coeruleus (Fedorow et al., 2005) for which has been suggested a role in neuroprotection or senescence. Because melanin biosynthesis is influenced by a myriad of factors like transcription factors and hormones and is a process implicated in many human diseases, the knowledge of melanogenic regulation could be fundamental in cellular and biomedical research.

1.3 - Animal melanin-containing cells

Across animal evolution, many types of melanin-producing cells have been recognized. Regarding this field, most of the energy has been spent on vertebrate pigment cell structure, function and development: many data have been collected about the bridge between human pathologies and genes related to melanogenesis (Goding, 2007). Melanogenic genes are implicated in several forms of albinism, deafness and vitiligo and their deregulation is linked with melanoma skin cancer (Goding, 2007). Under normal conditions, in vertebrates melanin granules are synthesized and stored only in membrane-enclosed organelles known as melanosomes, lysosome-related organelles (LROs) identified in mammalian skin melanocytes, in choroidal melanocytes and in retinal pigment epithelial (RPE) cells of the eye, but also in melanophores belonging to teleosts and amphibians (Nilsson Skold et al., 2013). The structure of melanosomes depends on the melanin typology accumulated, indeed eumelanosomes present elliptical shape and contain fibrillary matrix whereas pheomelanosomes are gaping circles with vesiculoglobular matrix (Nordlund et al., 1998). Melanosome biogenesis encompasses four steps (I-II-III-IV, Figure 1.2): during stage I-II occur matrix organization, in stage III melanin storage starts and in stage IV the melanosomes are completely darkened (Slominski et al., 2004; Bultema and Di Pietro, 2013). Pathological states can cause alterations of ordered melanogenesis and erroneous melanosome formation, with the absence of completely formed matrix or melanin not bound with matrix (Slominski et al., 2004).
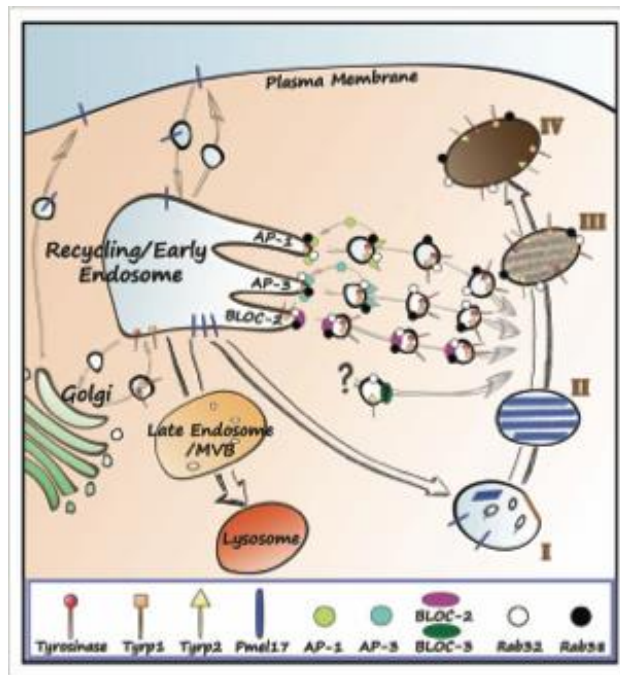
Figure 1.2. Melanosome biogenesis in melanocytes. The figure presents a model for the formation of melanosomes in vertebrate's melanocytes, with the proteins implicated in melanosomal vesicular trafficking (adapted from Bultema and Di Pietro, 2013).

The melanocytes present in RPE and eye choroidal cells are crucial for vision and the defense of photoreceptor layer (Marks and Seabra, 2001) while those comprised in *stria vascularis* of the inner ear are required for a proper hearing (Steel and Barkway, 1989). Skin melanocytes cover 5-10 % of epidermis basal cell layer where they serve to safeguard from ultraviolet radiations (Sulaimon and Kitchell, 2003) and each one is encircled by about 36 keratinocytes of squamous cell layer (Lin and Fisher, 2007). The skin colouration is due to pigment-filled melanosome transportation from melanocytes to surrounding cells through arm-like cytoplasmatic structures known as dendrites, along microtubules (Lin and Fisher, 2007). Before distribution, melanosomes need a maturation process depending on extracellular pH growth from 5.0 to 6.8. Chemical interaction between melanocytes and keratinocytes is intense but they are sensitive also to many extrinsic factors, in particular they are strongly influenced by extracellular glutamate concentration (D'Mello et al., 2016). Teleost melanophores, together with other clade-specific cell types like leucophores and

cyanophores, are fundamental for their social and ecological behavior. Furthermore, the melanin-producing cells comprised in kidney and spleen of teleosts are involved in immunity response (Press and Evensen, 1999). It supports the use of pigments for many challenges relevant for vertebrate's ecology and physiology. Similarly to vertebrates, invertebrates show a myriad of pigment cells covering disparate functions. Insects and other protostomes synthesize melanin in haemolinph cells and hemocytes for external tasks as egg tanning, cuticle biogenesis and innate immunity (Nappi and Christensen, 2005). The cuttlefish *Sepia officinalis* possesses an ink gland with melanin-containing cells used for escaping defense: these ectodermal cells contain particulate melanosomes deemed as rudimentary intracellular structures if compared to fibrillar melanosomes of vertebrate melanocytes (Fiore et al., 2004). Inside invertebrate chordates, there are various structures which include melanin-producing cells. Cephalochordates as amphioxus, have a complex photoreceptive system formed by different cells: among them, it has been shown that some pigmented cells are homologous to vertebrate melanocytes (Vopalensky et al., 2012). The ascidian unique pigmented sensory organs, otolith and ocellus, house melanized cells implicated in perception of light and gravity (Tsuda et al., 2003; Sakurai et al., 2004). Except these, multiple examples of structure and function of invertebrate pigment cells are registered in the literature, specifically it is well-known the conservation of genetic developmental pathways across evolution. In light of this and their lower complexity, invertebrates can represent a significant tool for understanding mechanisms of pigment cell development. In order to comprehend vertebrate pigment cell biology, the early-branching chordates with their ease of manipulation, simple pigmentary organs and evolutionary proximity to vertebrates, can be really important.

1.4 - Melanogenesis: transcriptional and hormonal regulation

The pigmentation process is thought to be influenced by more than 100 genes (Bennett and Lamoreux, 2003). Within the tyrosinase family, Tyr is the key enzyme in melanin biosynthesis and ultra-conserved in all the metazoans while Tyrp represent important Tyr-derived accessory proteins arisen in chordates, (Esposito et al., 2012). The expression of these genes is upregulated by α-Melanocyte-Stimulating Hormone (α-MSH) binding to melanocortin-1 receptor (MC1R) that activates adenylate cyclase producing cyclic AMP (cAMP). The α-MSH cleavage is operated by pro-opiomelanocortin (POMC) synthesized by the pituitary gland and the keratinocytes (D'Mello et al., 2016). Through the phosphorylation of CREB, the cAMP-dependent protein kinase A (PKA) is responsible for the positive effects of cAMP high levels (Edelman et al., 1987). The absence of cAMP response elements (CREs) in Tyrp promoter regions speaks in favor of a direct microphtalmia-associated transcription factor (MITF) involvement. Among other functions, MITF or bHLHe32 represents a fundamental regulator of tyrosinase family members recognizing tyrosinase distal elements (TDEs) of promoters (Yasumoto et al., 1994). It has been demonstrated the incidence of many distinct factors on MITF transcription encompassing PAX3, SOX9, LEF1, ONECUT-2 (Levy et al., 2006). MITF activity in melanocytes is post-transcriptionally dictated by receptor tyrosine kinase pathway SCF-KIT, in fact it is phosphorylated by kinases as ribosomal S6 kinase (RSK), mitogen-activated protein kinase (MAPK) and p38, depending on environmental stimuli; other pathways modulating MITF activity are Wnt and RAS/MEK signaling (Levy et al., 2006). Not only tyrosinase genes, but also other genes involved in melanogenesis are finely regulated by MITF, implying a leading

role in pigmentation control for this gene. Additionally, the findings in insects and ascidians support the conservation of Mitf's role during evolution (Yajima et al., 2003; Halsson et al., 2004). In summary, melanin production is an extremely complex biological pathway that is at the center of different types of regulation, probably for its extraordinary ecological and physiological importance.

1.5 - Pigmentation: a complex molecular machinery

Aside from the tyrosinase family, melanosome formation and melanogenesis need the intervention of a plethora of proteins. Melanosomes are LROs present exclusively in specialized cells as melanocytes where they normally co-exist with classical lysosomes, in fact these two organelles have in common the major part of their molecular machinery (Fig. 1.2, Figure 1.3). In mammals, the stage I melanosomes rise by sorting of transmembrane structural protein Pmel17 to early endosomes. Pmel17 is responsible for proper melanosome biogenesis through the genesis of amyloid fibrils. Two other melanocyte-specific proteins, fundamental for early melanosome structure (stages I-II), are the G-protein-coupled receptor 143 (Gpr143) and the small integral membrane protein Mart1, in fact mice with mutations in DNA encoding these three proteins are characterized by hypopigmentation (Sitaram and Marks, 2012). Melanin production and deposition begins at the third melanosome stage, thanks to melanogenic enzymes delivered and packaged in transport clathrin-vesicles by adaptor protein complex (AP-1 and AP-3) and biogenesis of lysosome-related organelles complex (BLOC-1 and BLOC-3). Defects in these molecular machineries cause wrong deposition of melanin polymers in melanosomes, with many functional consequences potentially linked to human diseases. Melanogenic enzymes trafficking after exit from the trans-Golgi network

(TGN) to active melanosomes is a crucial step, which is regulated by some specialized small-GTPases. Tyrosinase family member transport is mediated by Rab32 and Rab38 (Wasmeier et al., 2006), in collaboration with the ubiquitous lysosomal machinery composed by BLOC-2, AP-3 and AP-1 (Bultema and Di Pietro, 2013). A further Rab connected to pigmentation is Rab27A, expressed in melanocytes and responsible for the melanosome motility, through its effector melanophilin (Wu et al., 2001; Wu et al., 2002). For their centrality in trafficking machinery, it has been supposed a role for other small GTPases such as Rab11 and Rab9 (Sitaram and Marks, 2012). However, solute carrier family (Slc) includes many genes potentially involved in pigmentation. For instance Slc45a2, implicated in oculocutaneous albinism type 4 (OCA4) and melanoma, regulates melanosome pH affecting tyrosinase activity (Bin et al., 2015): indeed, its expression is conserved in pigment cells of evolutionary distant animals like ascidians and zebrafish (Racioppi et al., 2014; Thisse and Thisse, 2004). Moreover, in human several SLC24 genes play a role in pigment cells (Schnetkamp, 2013). Highly conserved multisubunit complexes like ESCRTs and TRAPPs are considered noteworthy in melanogenesis regulation because they actively participate in mechanisms connected to vesicle formation and cargo trafficking, though the exact mechanisms remain to be elucidated (Sitaram and Marks, 2012).
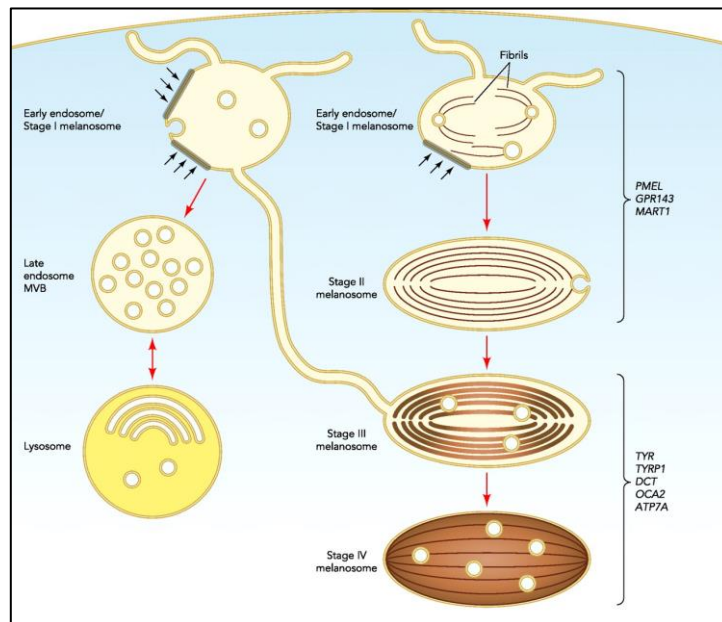
Figure 1.3. Gene families involved in melanosome biogenesis. Representation of gene families which are implicated in diverse steps of melanosome life (from Sitaram and Marks, 2013).

Hence, melanogenesis appears as key process for the proper functioning of pigment cells containing melanin with the intervention of several proteins. Moreover, melanosome biogenesis can be fundamental for the comprehension of mechanisms related to vesicle trafficking and intracellular transport, to understand which genes are involved and to discover new players in membrane trafficking.

1.6 – Pigment cell development and function in vertebrates

Pigment cells of vertebrates represent the best characterized in the animal kingdom. Recently, the term of vertebrate "pigment cell" has been applied not only to primarily pigmented cells possessing membrane-bound organelles (as melanosomes) with chromophoric substances or structures but also to their non-pigmented precursor cells and pathological derivatives (Schartl et al., 2015). This definition excludes cells characterized by secondary pigmentation that depends on the pigment uptake from *bona fide* pigment cells, as happens in keratinocytes or some macrophage lineages.

Other cells out from this classification are nervous cells accumulating waste pigments as neuromelanin or lipofuscin. In synthesis, considered as "pigmented" are those cells, pigment-containing, which are responsible for light absorbing to provide pigmentation visible to other organisms or ameliorate vision skills (Schartl et al. 2015). As previously said, vertebrate pigment cells are neuroectodermal derivatives which are distinguished for their embryonic origins: the RPE and the pineal gland deriving from the optic cup of the developing forebrain while the neural crest (NC) pigment cells, forming skin melanocytes, inner ear melanocytes and other chromatophores (Quevedo and Fleischmann, 1980). Notwithstanding pigment cell types present distinct timing processes and final destinations, and analyses from diverse model systems sheds light on conserved developmental modes amongst vertebrates. Teleosts, as zebrafish, present some experimental advantages which render them very interesting as model organisms, especially for the pigment cell development and pigmentation-related diseases.

In the vertebrate eye, the cells of RPE descend from the multipotent optic neuroepithelium and form an ultra-specialized multifunctional epithelium. These cells are strictly connected to eye during embryo and adult phases, in fact RPE layer and neural retina represent a functional unit (Bharti et al., 2006). The RPE layer has several functions, spanning from light absorption and epithelial transport to phagocytosis of photoreceptor outer segment (POS) membranes (Straus et al., 2005). In zebrafish, the optic primordium consists of a flat wing constituted by a cellular bilayer which cavitates forming the optic cup (Li et al., 2000). The RPE cells originate from the medial layer and approximately at 16 hours post-fertilization (hpf) dorsalmost cells start to modify their shape from columnar to squamous and flat, coinciding with a dorso-ventral migration. At 24 hpf, all the RPE occupies the whole

outermost retina layer, while pigment granules are visible. During these transitions, *mitf*, *tyrp* and *tyrosinase* representatives are clearly expressed (Li et al., 2000) .

Neural crest cells are a vertebrate-novelty with a great evolutionary relevance (Shimeld and Holland, 2000). They are a cellular population deriving from neural tube that, from the boundary existing between neural plate and surface ectoderm, migrate ventrally and differentiate in distinct subpopulations of sensory, connective and pigment cell types. Neural crest-derived pigment cells migrate following a dorso-lateral pathway while the other subpopulations follow a medial pathway. Albeit some differences (Raible et al., 1992), the mechanisms governing NC cells development are conserved between teleosts and higher vertebrates. In zebrafish, neural crest induction is orchestrated during gastrulation by bmp2b/swirl pathway, mechanisms shared with other vertebrates (Nguyen et al., 1998). Moreover, zebrafish NC cells present the same vertebrate markers, as for instance *pax3* and *foxd3*/*fkd6* (Seo et al., 1998; Odenthal and Nusslein-Volhard, 1998). The pigment cells are one of the best-known derivatives of neural crest because they are not central to viability, in fact non-lethal mutations led to study the developmental modes in zebrafish and other vertebrates. Melanophores (analogous to melanocytes) are the first cell type to appear during embryogenesis, starting at 24 hpf laterally on both the sides of the ear then expanding down the trunk. Soon after they are visible on the head dorsal side the xanthophores, whose yellow aspect is caused by pteridine accumulated in peculiar organelles called pterinosomes. After that, it begins the iridophores appearance in the tail and in two stripes over the yolk: these are reflecting and round cells that contain platelets with purine crystals (Kelsh et al., 1996; Lister, 2002). The final pattern of zebrafish larva is based on three melanophore lines alternated with iridophores while xanthophores remain positioned dorsally along all the embryo.

Ventrally to the yolk there is a layer formed melanophores and iridophores (Kelsh et al., 1996; Lister, 2002). Aside these cell types in common with tetrapods, teleosts as zebrafish possess also blue cyanophores and whitish leucophores whose embryonic origins are not documented. By contrast, their ultrastructural organization and shape suggested to enclose them to the NC-deriving pigment cells (Braasch et al., 2007). Interestingly, experiments conducted on medaka (*Oryzias latipes*) leucophores lead to consider them developmentally related to xanthophores (Kimura et al., 2014). Several studies on mutants have provided insights regarding the pigmentation scenario in teleosts, as shown by zebrafish larvae (Moreira and Deutsch, 2005).
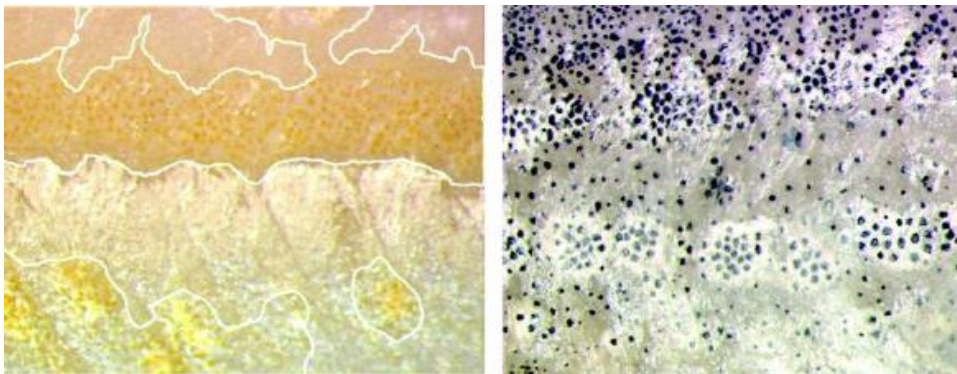
Figure 1.4. Zebrafish pigmentary cell diversity. *Nacre* mutants (left) show areas with concentration of xanthophores surrounded by the white line, while zebrafish *fms* mutant (right) are rich of melanophores which form clusters (adapted from Moreira and Deutsch, 2005).

The well-known melanogenic enzymes *tyr* and *tyrp2* are expressed specifically in melanoblasts (Figure 1.5), from early developmental stages (Kelsh et al., 2000; Camp and Lardelli, 2001). The xanthoblasts are characterized by mRNA presence of xanthine dehydrogenase (*xdh*), the last enzyme of pteridine synthesis (Parichy et al., 2000) whereas pnp4a is the causal gene of medaka iridophore guanine (Kimura et al., 2017). Other genes, as GTP cyclohydrolase I (*gch*) and Endothelin receptor b1 (*ednrb1*) mark more than one pigment cell type precursor (Lister, 2002). Apart from

Bmp, also Wnt/ β-catenin signaling is very important for pigment cell development in zebrafish, as in higher vertebrates: in fact it has been suggested as responsible for the early pigment cell restriction fate of NC precursors by regulating directly *Mitf* transcription factor expression, via Tcf (Dorsky et al., 2000; Takeda et al., 2000). The SRY-containing transcription factors Sox9 and Sox10 are involved in early development of pigment cells, promoting their differentiation and survival (Silver et al., 2013).
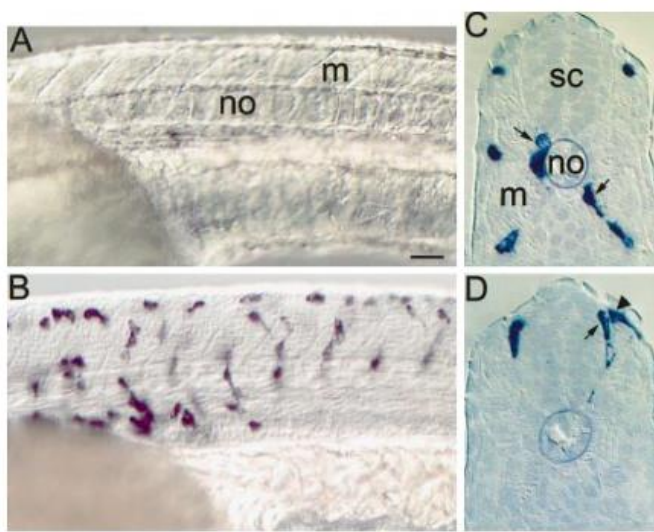
Figure 1.5. *Tyrp* **expression in zebrafish.** While 25 hpf embryos have no melanin in posterior trunk, WISH using *Tyrp* mRNA shows strong expression in NC cells (A, B); transverse sections (C, D) hint the presence of these cells (arrowheads) along the migratory pattern of NC cells (adapted from Kelsh et al., 2000).

The study of pigment cell development in teleosts like zebrafish and medaka has confirmed several data obtained from mammals but the analysis is more interesting because this group have evolved new cell types to face new challenges, probably for the adaptation to new ecological niches. With more than 32000 species, teleosts are the largest group in vertebrates showing a myriad of pigmentary pattern.

1.7 – Pigment cell development and role in amphioxus and ascidians

In the chordate phylum, vertebrates co-exist with other two important subphyla, cephalochordates and urochordates, which can be instrumental to improve knowledge on pigment cell evolution. Considered as the closest living relative of the chordate ancestor, cephalochordates such as amphioxus, possess an unduplicated genome that encompasses all the main vertebrate gene families (Putnam et al., 2008). Among cephalochordates the more intensely studied models are the species belonging to the *Branchiostoma* genus, having a photoreceptive system constituted by Joseph cells, dorsal ocelli (Hesse cells), lamellar body and frontal eye (Lacalli, 2004). The ciliated Row cells of frontal eye are similar to vertebrate eye photoreceptors (mainly Row1) whereas the adjacent pigment cell seem to be homologue to vertebrate RPE cells (Figure 1.6), as suggested by common expression profiles of genes involved in pigmentation (Vopalensky et al., 2012). Moreover, the primary pigmented spot of the amphioxus neural tube is marked by different genes belonging to the tyrosinase family (Yu et al., 2008).
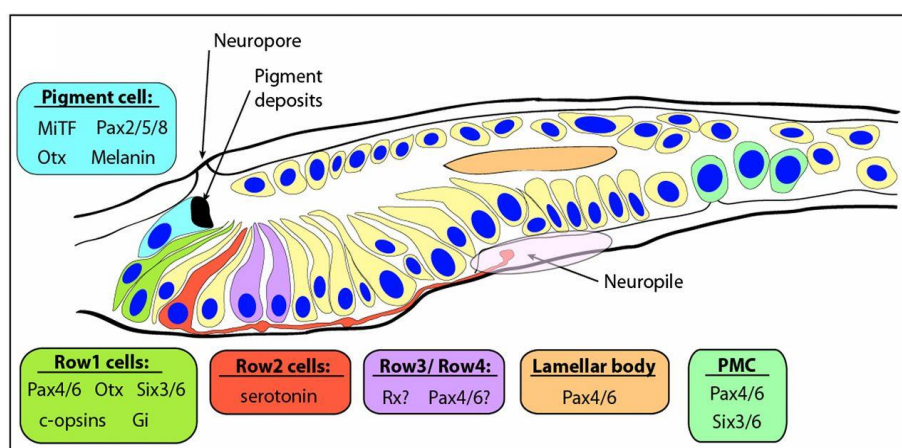
Figure 1.6. Photoreceptive system of amphioxus. This map describes the pigmented and photoreceptor cells of cephalochordates characterized by genes common to vertebrates (adapted from Vopalensky et al., 2012).

The *Urochordata* subphylum, subdivided into ascidians, appendicularians and thaliaceans is characterized by the presence of canonical features of the chordate bauplan like a notochord and a dorsal hollow nerve cord, during larval stageBy employing diverse phylogenetic urochordates have been described as the closest living relatives of vertebrates. However they showgreat morphological divergence that has been correlated to fast rate of genome evolution (Delsuc et al., 2006). The members of the ascidian class, also named sea squirts, are solitary or colonial animals which spend the first part of life as swimming planktonic larvae and then attach to a substrate. After this, they undergo metamorphosis to become adult sessile filter feeders. The most common ascidian used in developmental biology, is *Ciona robusta*, formerly known as *Ciona intestinalis* type A (Brunetti et al., 2015). With well-known embryogenesis it is suitable for gene expression studies, while a quite compact genome with regulatory regions short and near to coding sequences render *C. robusta* a good system for promoter analysys. Moreover, the experimental advantages (Satoh et al., 2003) are enhanced from the availability of genomic resources (Dehal et al., 2002). Together with the solitary ascidian *Halocynthia roretzi*, *C. robusta* represents the best source of information on pigment cell specification in ascidians. Given the extraordinary conservation of cleavage program in solitary ascidians, data extracted from these two species could be extended to other genera such as *Phallusia* and *Molgula*. Ascidian pigment cells are contained in the anterior sensory vesicle, a cavity located in the larval trunk, belonging to central nervous system (CNS) that in Ciona is constituted approximately by 335 cells (Nicol and Meinertzhagen 1991). Because sensory vesicle derives from neural plate rolling into neural tube during neurulation, and expresses marker genes of vertebrate CNS, it has been proposed as a homologue to the vertebrate prosencephalon and

mesencephalon (Wada et al., 1998). This structure is composed mainly by ependymal cells (Nicol and Meinertzhagen 1991) but harbors two sensory structures, the otolith and the ocellus, containing pigment cells (Dilly, 1969; Eakin and Kuda, 1971). They are involved in perception of gravity and light stimuli, fundamental functions for ascidian larvae (Tsuda et al., 2003; Sakurainet al., 2004). According to molecular and functional similarities, diverse members of scientific community have hypothesized a common origin for ascidian sensory organs and eye of vertebrates (Kusakabe et al., 2001; Lamb et al., 2007). After the larval stage, pigment cells comprised in sensory organs undergo apoptosis and reabsorption between metamorphosis and adulthood. They are necessary for the first part of ascidians' life, with central function in the proper swimming behavior of larvae: during the first 3-4 hours after hatching larvae are not able to perceive the light and thus depend on gravity information from otolith which causes upward swimming. The beginning of downward swimming coincides with the perception of light stimuli by larvae (Tsuda et al., 2003): as in vertebrates, photoreceptor cells of ascidians are implicated in the light perception through membrane hyperpolarization (Gorman et al., 1971). Because ascidian adults are sessile, swimming behavior due to pigment cells is extremely important from an ecological perspective, so larvae can be diffused in the surrounding environment and exploit new territories, far from adult settling location. It is linked with the occupation of new niches allowing the large colonization of all the seas operated by these sessile species. Several studies have explored ascidian development, producing a deep knowledge about the destiny of every single blastomere. Experiments on *H. roretzi* show that pigment cells originate from the a4.2 blastomeres lineage (Nishida, 1987). During gastrulation two descendants of the a4.2 blastomeres (a8.25 cells), become influenced, by the underneath A-line

blastomeres (Nishida, 1991) to pigment cell fate. At the late gastrula stage the a9.49 cells, derivided from a8.25, are fate-restricted to pigment cell fate as shown by mechanical ablation experiments (Nishida and Satoh, 1989). a9.49 cell pair division give rice to a10.97 and a10.98 pairs that divides againforming a11.193 (otolith and ocellus precursors) and a11.194 pairs . These four cells, at the neural tube closure, migrate and intercalate forming a single row, along the anterior-posterior axis (Figure 1.7). At this time the specification of the two pigmented cells occurs (a10.97) under the control of positional information driving the development of the anterior otolith and the posterior ocellus (Nishida and Satoh, 1989; Darras and Nishida, 2001).

Traditionally, ascidian embryogenesis has been considered as a canonical example of mosaic development, where embryonic territories have been decided from the zygotic stage through ooplasmic segregation of maternal determinants (Jeffery and Meier, 1984). Nevertheless, it has been shown the involvement of diverse inducing signal events due to cell-cell interaction (Kawaminani and Nishida, 1997; Kim and Nishida, 1999). FGF signaling plays a fundamental role during embryogenesis, such as cell proliferation, nervous system development and differentiation: for instance, FGF is central to the activation of tissue-regulatory genes in heart specification through final pathway effector, Ets1/2 transcription factor (Davidson et al., 2006).

Although ascidians are known for deterministic development, their pigment cell lineage specification is governed by inductive signals (Kawaminani and Nishida, 1997; Kim and Nishida, 1999). The formation of anterior neural tissue is governed by early inductive signals from anterior vegetal cells (A-line) (Lemaire et al., 2002). Coherent with data collected in vertebrates such as *Xenopus* and chick (Hongo et al., 1999; Streit et al., 2000), neural induction in ascidians is influenced by fibroblast

growth factor (FGF) signaling (Hudson et al., 2003). In fact, morpholino-mediated knock down experiments have demonstrated the direct implication of endogenous Ffg9/16/20 in nervous system commitment, through MAP Kinase signaling and GATA and Ets transcription factors (Bertrand et al., 2003). The specific expression of *Fgf8/17/18* and *Fgf9/16/20* in six A-line cells of the neural plate row II surrounding pigment cell precursors (PCPs), together with inhibition and immunohistochemical experiments, indicate the FGF pathway as central to impose discrete fates of neural precursors in ascidians (Hudson et al., 2007). Given FGFs are implicated in the induction of ascidian and vertebrate mesoderm, it has been supposed that similar signals are unfolded differently by presumptive territories (Nishida, 2002). Thus, FGF signaling has been suggested to be involved in pigment cell determination of ascidians, with a role possibly conserved in vertebrate melanocytes (deOliveira et al., 1998). Belonging to a superfamily expanded during metazoan evolution (Popovici et al., 2005), FGF members are involved in processes linked to vertebrate development: for instance, some FGFs and related receptors (FGFr) play a fundamental role in retina formation (Yang, 2004). The presence of only of six FGFs and one receptor in the *Ciona* genome, (Satou et al., 2002) has encouraged the analysis of their role in tunicate ontogenesis. Several studies conducted in the lab where I did my thesis demonstrated that the FGF/MAPK pathway orchestrates pigment cell induction in *C. robusta* through Ets1/2, from gastrulation to neural tube closure (Squarzoni et al., 2011). Using a dominant negative form of the unique *Ciona* FGFr under control of the Tyrp1/2 regulatory region, larvae without pigment cells were constituted, whereas the constitutive active form of Ets1/2 produced overpigmented larvae. FGF *via* MAPK regulates transcription of TCF, a well-known Wnt effector, in the otolith and ocellus, in turn

the perturbation of TCF is able to disrupt the pigment cell program (Squarzoni et al., 2011), similar to tcf-3 perturbation experiments in zebrafish neural crest cells (Dorsky et al., 1998). It has been elucidated the implication of both FGF and Wnt pathways in ascidian pigment cell specification (Squarzoni et al., 2011), In order to decipher the machinery influenced by FGF pathway in ascidians, a microarray experiment at two stages (neurula, tailbud) in two different conditions was conducted: down-regulation of FGF and hyper-activation of Ets1/2 (Racioppi et al., 2014). From the microarray experiments several genes involved in anterior nervous system or pigment cell differentiation were isolated. Taken together, data showed that FGF cascade imposes pigment cell identity in neural territories (Racioppi et al., 2014). Moreover, FGF influences the specific expression of many factors in pigment cell lineage with a slightly different localization in the lineage. Among the FGF-dependent genes identified, there are the transporters Slc45a2 and Rab32/38, known for their role in melanosomal logistics (Newton et al., 2001; Bultema et al., 2012), and others (Doc2a, Bzrap, Piwi, Klhl21) that have never been associated to pigmentation.
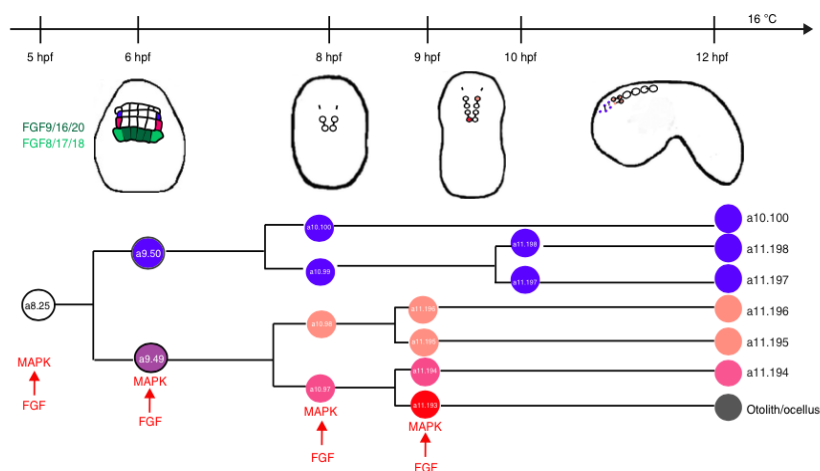
Figure 1.7. Pigment cell lineage during Ciona embryogenesis. The scheme resumes the embryonic origin of Ciona pigment cell precursors (PCPs) and FGF signaling involvement in their specification (adapted from Racioppi et al., 2014).

CHAPTER 2

2.1 – General aim of the thesis

The transcriptomic approach carried out in the lab where I did my thesis work, generated a list of genes with different expression pattern. Starting from these data, my PhD project aimed to identify how the potential to give rise to pigmentation program is regulated in *Ciona* pigment cell lineage during development and to investigate the evolutionary scenario of gene families implicated in pigmentation dynamics (*Rab*, *Klhl*). We focused our analyses on chordates (Figure 2.1), combining comparative genomics with molecular and developmental biology techniques.
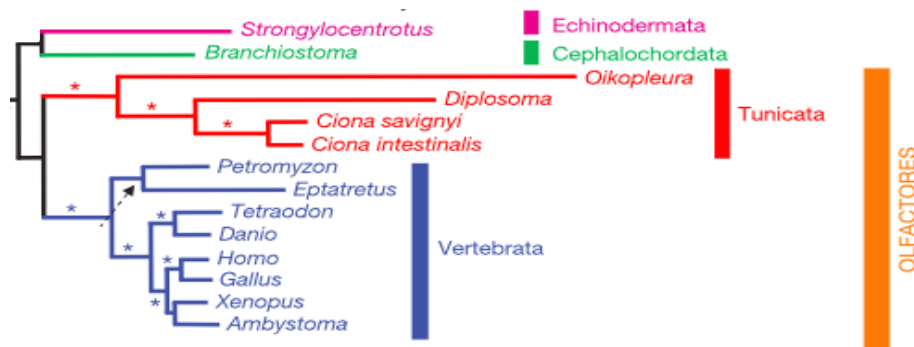
Figure 2.1. Evolutionary relationships among chordates. The cladogram shows the phylogenetic positions of organisms employed in my thesis: the early-branching cephalochordates (*Branchiostoma*) are at the base of Olfactores the clade comprising tunicates, as *Ciona*, and vertebrates, as *Danio rerio*. (adapted from Delsuc et al., 2006).

2.2 - Aim 1: Rab family evolution

Given the involvement of several Rabs in trafficking events connected to pigmentation process in numerous animals, it has been decided to investigate the molecular evolution of entire Rab family in metazoans. Through phylogenetic, intron conservation and domain analyses I aimed to elucidate the Rab evolution towards eleven species, ranging from cnidarians to human, with a great attention to genomic

events occurred during chordate evolution. Nevertheless, understanding Rab molecular evolution could be relevant not only for the pigmentation dynamics but also for the understanding of Rab-dependent trafficking processes during metazoan evolution. Moreover, providing insights into a Rab family could be instrumental to shed light on human diseases related to these small GTPases.

2.3 - Aim 2: *Rab32/38* involvement in chordate pigmentation

In light of its implication in pigmentation dynamics of several organisms (fly, ascidians, mouse) and in diseases as melanoma and albinisms, Rab32/38 subfamily has been targeted for a deep evo-devo study through a detailed evolutionary analysis regarding *Rab32/38* genes in metazoans, with a focus on the expression of *Rab32/38* gene of Mediterranean amphioxus (*B. lanceolatum*) and *Rab32* and *Rab38* genes of zebrafish (*Danio rerio*). This study has the objective of understanding the possible pigmentary role of this subfamily in early-branching chordates as amphioxus and in multi-pigmented teleosts as zebrafish.

2.4 - Aim 3: *Klhl21*, a new potential player in pigmentation

In order to find new genes involved in ascidian pigment cell development, we aimed to investigate deeply the *Klhl21* behaviour in *Ciona* development, a Kelch-like family member traditionally considered as a regulator of eukaryotic cytokinesis that in *Ciona* is down-regulated when FGF signaling is blocked. It is the first time that a Kelch-like gene seems to be implicated in pigmentation with a specific expression in sensory organs as otolith and ocellus: for this reason, we decided to study its promoter region and the combinatorial pattern of transcription factors which seem to work in two distinct regulatory modules.

CHAPTER 3

Evolution of Rab family in metazoans: new insights from *Chordata* phylum

3.1 - Background

The setting-up of a complex endomembrane system (ES) has been doubtless a fundamental evolutionary step for the eukaryotic organisms, compared to Archea and Bacteria clades. Intracellular compartmentalization, i.e. the existence of membrane-bound organelles such as the nucleus and Golgi, represents a distinguishing feature of the Eukarya domain (Cavalier-Smith, 2002). The presence of these structures is due to autogenous evolution, different for the endosymbiotic evolution of mitochondrion and plastids (Embley and Martin, 2006; Keeling, 2010). Despite the presence of many differences, compartments have followed a sort of Bauplan across evolution, composed mainly by endoplasmic reticulum (ER), Golgi apparatus, trans-Golgi network (TGN) and nuclear envelope (Elias, 2010). The ES system is formed by an extremely high number of compartments with a variegated protein and lipid composition, necessary for specific import/export mechanisms of ions, macromolecules and particles. Eukaryotic organelles have been linked to a plethora of diseases and pathologies (Olkkonen and Ikonen, 2006).

Cellular compartments need the contribution of a highly organized system of proteins regulating intracellular transportation, with many gene families involved. Among these, Rabs are considered as crucial players for communication inside eukaryotic cells in collaboration with coats, tethers and SNAREs (Cai et al., 2007; Sudhof and Rothman, 2009). Initially recognized as membrane traffic regulators in yeasts and then discovered in mammalian brain (Touchout et al., 1987), Rab ('Ras-

related in brain') proteins form by far the largest and most diversified family inside the Ras superfamily (small G proteins) and are emerging as the main hallmarks of vesicle and organelle identity (Stenmark, 2009; Hutagalung and Novick, 2011).

In eukaryotic cells, Rab proteins are attached to lipid bilayers through a long and flexible ultra-variable domain characterized by a prenylated C terminus, called hypervariable C-terminal domain (HVD). As evidenced by recent findings, it acts not only as pliable spacer but also as organellar determinant and positive regulator of membrane affinity (Li et al., 2014). Despite some differences, Rabs exert their role of cargo transporters through a continuous cycling between their GTP/GDP-bound states with the decisive provision of several accessory proteins. This molecular shift depends mainly on the P-loop domain (also called "G-domain"), a short and well-known guanine binding motif present also in other Ras superfamily members and considered a "landmark" of Rab functioning that is harboured in a six-stranded β sheet (Park, 2013). Two other fundamental domains are Switch I and Switch II: in a three-dimensional structure they lie on the Rab surface and are central to proper conformational folding of Rabs in trafficking dynamics (Park, 2013). Many mutations have indicated the putative Switch as instrumental for the interplay between Rabs and their effectors (Stenmark and Olkkonen, 2001). Through extensive sequence-analysis, it has been unraveled the existence in and around Switch regions of five amino-acid stretches (RabF regions) probably implicated in Rab interactions with effectors (Moore et al., 1995). These proteins are able to work in their GTP-form and need a complex pathway to be activated. After GTP hydrolysis operated by specific GTPase activating proteins (GAP), each Rab protein is extracted from its original lipid membrane through the intervention of carriers named GDP dissociation inhibitors (Lee at al., 2009; Barr and Lambright, 2010). At this point, the ultra-

specialized GTP exchange factors (GEFs) activate Rabs in cohabitation with GAPs, in order to impose a precise intracellular position for each linked family member. This GTP-bound form represents an hub for recruiting all the effectors necessary to carry out a specific step of intracellular trafficking, such as tethering factors and motor proteins (Klopper et al., 2012). Concerning Rab connection to eukaryotic membranes, a post-translational modification of their terminal cysteine motif by Rab escort proteins (REPs) is necessary, specialized in Rab delivery to proper membranes together with geranylgeranyl transferases (Alexandrov et al., 1994; Anant et al., 1998). By employing affinity chromatography and mass spectrometry on *Drosophila*, it has been shown the existence of a complex system of interactions for ten distinct Rabs: the list of effectors comprises motor linkers, tethering complexes, Rab regulators and proteins related with human pathologies (Gillingham et al., 2014). In short, Rab proteins co-ordinate eukaryotic cellular trafficking together with a multitude of accessory proteins, resulting in a network involving all the cellular environments, far from being completely understood (Barr, 2013).

Although they share many structural and functional elements with other Ras proteins, Rabs show unique characteristics rendering them a monophyletic grouping inside the Ras superfamily, closest to the putative family of Ran nuclear transporters (Colicelli, 2004; Rojas et al., 2012). Rab family evolution and its contribution to trafficking dynamics have been considered as decisive events for the success of eukaryogenesis (Brighouse et al. 2010). The Rab toolkit exhibits an extremely variable number across the tree of life, with more than 60 members in *Homo sapiens* (Stenmark, 2009): although linkage between Rab number and cellular function remains to be elucidated, a larger Rab complement could indicate an increase of trafficking mechanism complexity. In order to shed light on Rabs already present in the Last

Eukaryotic Common Ancestor (LECA), efforts have been made to investigate the bulk of Rab complement in unicellular eukaryotes. It has been hypothesized the LECA Rab toolkit encompasses 14 proteins, even if only 10 are phylogenetically supported (Pereira-Leal and Seabra, 2001; Pereira-Leal, 2008; Bright et al., 2010); nonetheless, several unicellular eukaryotes possess totally 20-30 Rabs (Saito-Nakano et al., 2005; Carlton et al., 2007; Bright et al., 2010). Using deeper phylogenetic methods, it has been possible to enlarge the ancient and complex family toolkit with the LECA comprising 20 or 23 Rabs (Klopper et al., 2012; Elias et al., 2012). Rabs belonging to the original LECA dataset probably are the result of duplicative events pre-dating eukaryotic diversification (Klopper et al., 2012) involving an original set of five "core" Rabs (Rab1, Rab5, Rab6, Rab7, and Rab11) which could represent the origin of 5/6 groups or supergroups (Dunst *et al.,* 2015). The ancient dynamism of Rab evolution is suggested by the presence of putative pre-LECA paralogue's couples like Rab1/Rab8, Rab20/24, Rab32A/Rab32B (Elias et al., 2012). Coherently with these results, it has been shown the existence of a small Rab toolkit already in the Archea (Surkont and Pereira-Leal, 2016). Moreover, LECA Rabs have been categorized in six groups or supergroups depending on their cellular localization (Figure 3.1; Klopper et al., 2012). On the other hand, multicellular eukaryotes present multiple Rab members probably originated through different duplicative events leading to Metazoans considered as a hotspot for Rab diversification (Elias et al., 2012). Nevertheless, as suggested by toolkit discrepancies of distinct invertebrates (*Nematostella vectensis*, *Caenhorabditis elegans*, *Drosophila melanogaster*), the impact of gene gains and losses on Rab evolution has been strong with probable functional consequences (Gallegos et al., 2012; Elias et al., 2012). For instance, the role of secondary losses needs to be better investigated for their possible

connections with cell functioning (Albalat and Canestro, 2016): it could be a partial effect of particular structure loss across evolution (Klopper et al., 2012). Worthy of being analyzed from an evolutionary perspective, the Rab repertoire appears characterized by a strong variability in animals with a variable phylogenetic distribution for many subfamilies. The current Rab family results from a balance continuously influenced by the loss of ancient members and the addition of lineage-specific paralogues, with a patchy pattern in different phyla (Elias et al., 2012). As well as metazoans, also in plants have been evidenced differences in terms of Rab complement but the evaluation is less supported because the scarcity of available plant genomes (Klopper et al., 2012). Inside Metazoans, a further hotspot in Rab diversification could be the origin of vertebrates, due to duplication events that occurred early during their evolution (Abi-Rached et al., 2001; Dehal and Boore, 2005). To shed light on trafficking evolution, the Rab toolkit history has been compared with those of other gene families implicated in eukaryotic transportation dynamics such as transport protein particle (TRAPP) and SNARE. Rab family evolution appears much more animated by gains and losses, with a sort of "evolutionary calm" disclosed by other families of membrane players during evolution (Klopper et al., 2012).
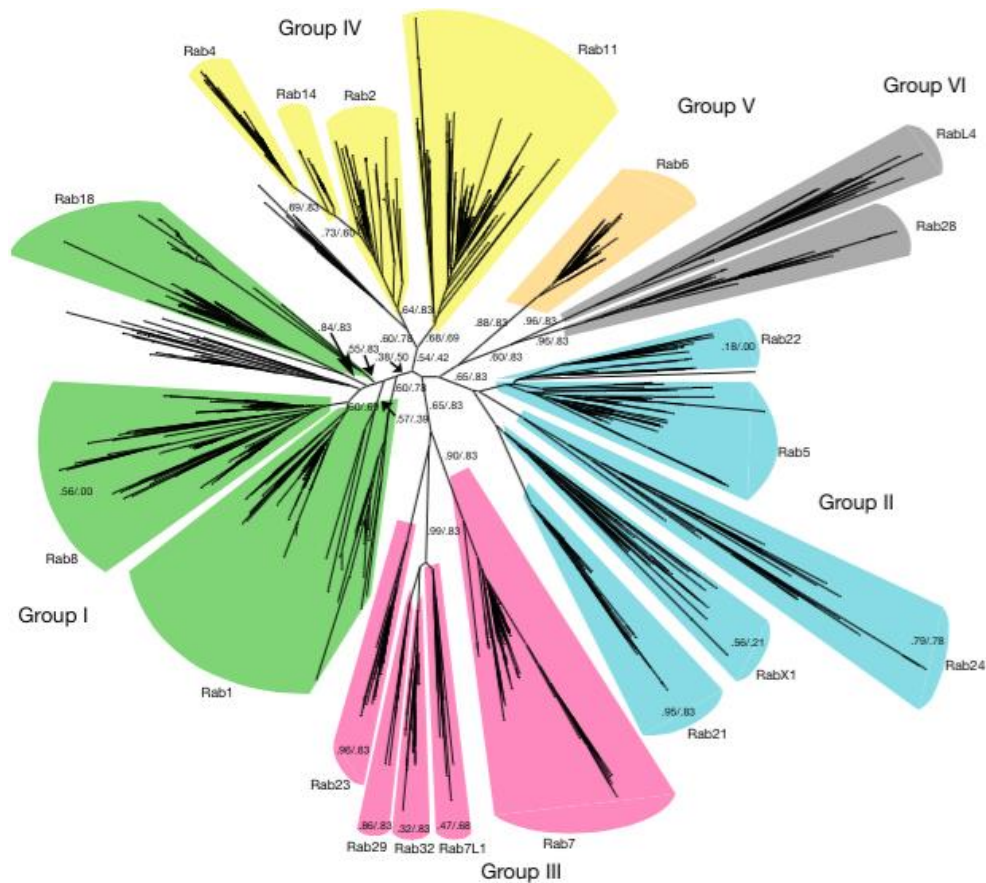
Figure 3.1. Evolutionary history of putative LECA Rabs. This phylogeny encompasses Rabs attributed to Last Eukaryotic Common ancestor and divided in six supergroups depending on their putative cellular localization (from Klopper et al., 2012).

Notably, Rab orthologs in such evolutionary distant species as yeast, plants, insects and humans perform functions highly superimposable; this is coherent with a conservation of trafficking roles played by Rabs in eukaryotes. In *H. sapiens,* many Rab proteins are present in each tissue, and some are expressed in particular tissues, reflecting that Rabs participate to a myriad of trafficking processes (Zerial and McBride, 2001; Bock et al., 2001). Pigmentation represents an interesting field of study from ecological, biochemical and evolutionary viewpoints. Pigment cells of vertebrates are characterized by an intense vesicular trafficking, whose regulation needs the involvement of different protein families (Sitaram and Marks, 2012). The

most studied mechanism for pigment formation is melanogenesis, a conserved biosynthetic pathway where a plethora of proteins are involved, but the most important are tyrosinase family members as Tyr and Tyrp, considered markers for pigmentation (Esposito et al., 2012). This multi-reaction process needs a fine regulation and requires an intense transport of molecules, mainly for the formation of melanosomes: amongst a myriad of proteins, Rab32 and Rab38 exert a fundamental role in pigmentation because they transport tyrosinase family members between trans-Golgi network (TGN) and immature melanosomes (Wasmeier et al., 2006). In co-habitation with classical lysosomal proteins these Rabs, partially redundant functionally, are fundamental for melanocyte pigmentation (Bultema et al., 2012; Bultema and Di Pietro, 2013) as confirmed also by functional experiments conducted in ascidians (Racioppi et al., 2014). Rab9A, belonging to group III as Rab32/38 genes, is indispensable for the recycling of cargos during melanosome biogenesis; it has been proposed a functioning scheme in concert with Rab32 and Rab38 (Mahanty et al., 2016). Indeed, Rab27A is implicated in the orchestration of melanosome distribution inside melanocytes, together with myosin Va (Wu et al., 2001; Wu et al., 2002), in fact is considered as a key gene for the determination of human skin (Yoshida-Amano et al., 2012). Regarding melanosomes, the regulator of endocytosis Rab11b is fundamental for their membrane formation and transfer to keratinocytes (Tarafder et al., 2014); this step is regulated by filopodia, whose formation requires Rab17 protein (Beaumont et al., 2011). The incidence exerted by Rab family members on pigmentation mechanisms is demonstrated also by a number of cases in which has been reported a linking between certain Rabs and human pathologies associated to pigmentary defects. Griscelli syndrome, an autosomal recessive disorder causing partial albinism, is caused (in its immunological variant) by a

missense mutation in gene that encodes for Rab27A (Menasche et al., 2000). On the other hand, Rab38 mutation on chocolate mouse and ruby rats (Loftus et al., 2002; Oiso et al., 2004) is at the base of Hermansky-Pudlak syndrome (HPS), a human disease characterized by oculocutaneous albinism and lipofuscin accumulation (Wei, 2006). Moreover, defects in Rab38 expression produces not completely functional RPE in eye of mouse (Lopes et al., 2007).

The Rab family is thought as one of the most important players in the trafficking inside eukaryotic cell and understanding its evolutionary landscape could represent a fundamental aid to study multicellularity establishment. Probably because of their key role as traffic regulators, Rabs constitute vital players also for pigmentation dynamics and credible candidates for studying human diseases implicating pigment cells. These elements, together with irregular and unfocused studies available, prompted me to analyze in depth the Rab family using eleven species of metazoans, ranging from cnidarians to human. By employing phylogeny, synteny and intron analysis, I provide the most up-to-date and comprehensive study about the Rab evolutionary history in animals describing the toolkit and the mechanisms driving the evolution of this family: it represents an important platform for evolutionary biologists interested in transportation and pigmentary dynamics. This part of my Phd thesis has been carried out together with Dr Salvatore D'Aniello (Biology and Evolution of Marine Organisms, Stazione Zoologica Anton Dohrn, Naples) and Prof. Ricard Albalat Rodriguez (Departament de Genètica, Microbiologia i Estadística, Universitat de Barcelona).

3.2 - Results

3.2.1 - Rab phylogeny in Metazoans

In order to gain insights in the evolutionary landscape of metazoan Rab family, we performed a thorough and detailed genome search starting from available databases and focused on the connection between Rab complement and eukaryotic membranes (Elias et al., 2012; Klopper et al., 2012). According to their strategic evolutionary positions, I selected eleven species for surveying this family in metazoans: the cnidarian starlet sea anemone *Nematostella vectensis*, the nematode *Caenorhabditis elegans* (Ecdysozoa), the segmented annelid worm *Capitella teleta* (Lophotrochozoa), the mollusk owl limpet *Lottia gigantea* (Lophotrochozoa), the acorn worm *Saccoglossus kowalevskii* and the purple sea urchin *Strongylocentrotus purpuratus* for the ambulacrarians, the early-branching Mediterranean amphioxus *Branchiostoma lanceolatum* (Putnam et al., 2008), the appendicularian *Oikopleura dioica* and the ascidian *Ciona intestinalis* from the fast-evolving Urochordata subphylum (Bernà and Alvarez-Valin, 2014), the anole lizard *Anolis carolinensis* and the primate *Homo sapiens* from vertebrates. To indicate species names I have used the first initial letters, i.e. *Nematostella vectensis* Rab2 is Nv_Rab2. This species catalogue has been employed to shed light on Rab diversification from early-branching metazoan and invertebrate's genomes, concentrating the analysis on chordate Rab toolkit evolution (totally five species). Rab proteins have been retrieved from public (NCBI, Ensembl, JGI) and private (European Amphioxus Genome Project) databases using human sequences as queries for Blast searches. Totally we obtained a dataset of 486 proteins consituting the most updated catalogue of bilaterian Rabs thus far. After discarding short and divergent sequences identified by analyzing the alignment, I constructed a phylogenetic tree with the Maximum

Likelihood (ML) method comprising 457 non-redundant Rabs (Figure 3.2), subdivided in 42 gene subfamilies. The majority of these are present from cnidarians to vertebrates supporting the hypothesis of a great Rab diversification occurred at the root of metazoans (Elias et al., 2012; Klopper et al., 2012). Interestingly, phylogeny demonstrates the existence of 38 Rab subfamilies pre-dating the rise of eu-metazoans with the remaining part formed by new members appeared in different times of animal evolution. Rab40 and RabX6 seem to be appeared before the split of bilaterians, while Rab46 and Rab12 represent deuterostome- and chordate-specific novelties, respectively. Moreover, this evolutionary survey robustly supports the orthology among the members belonging to each subfamily from *N. vectensis* to *H. sapiens*. It is noteworthy that urochordate Rabs often occupy more basal positions in the tree than expected from their phylogenetic relationships: a "long-branch attraction" artifact caused by the fast evolutionary rate characterizing tunicate genomes (Bernà and Alvarez-Valin, 2014). Besides, the topology of phylogenetic tree supports the existence in metazoans of 5-6 groups of Rabs as previously suggested (Klopper et al., 2012, Stenmark, 2012). I have employed a color code to distinguish among the groups: I (green, the most diversified), II (blue), III (red), IV (violet), V (orange), VI (yellow). Interestingly, Rab6 (Group V) includes also Rab34/36 subfamily, previously attributed to Group I (Klopper et al., 2012). The Rab family dimension is due to duplication events, which are particularly numerous in chordates and involve mainly certain subfamilies, as exemplified by Rab40. It could be interesting to investigate the impact of gene losses on Rab family: a phenomenon that is evident in organisms as *O. dioica* and *C. elegans*. Gene losses could be studied from a functional prespective because potentially connected to the absence of some specific trafficking step inside cell.
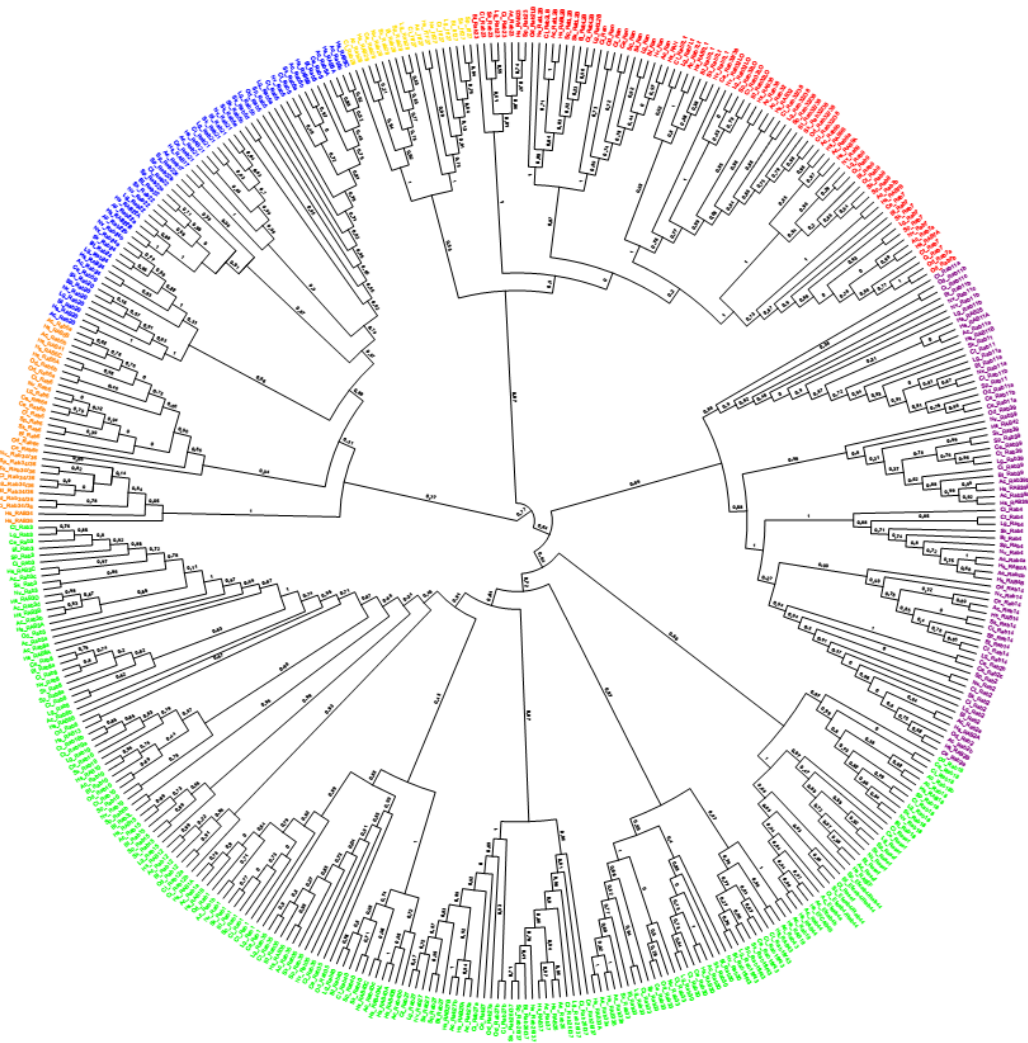
Figure 3.2. Phylogenetic reconstruction of metazoan Rab family. Maximum likelihood tree obtained using 457 proteins from eleven metazoan species, subdivided in three distinct groups represented with different colours: I (green) II (blue), III (red), IV (violet), V (orange), VI (yellow).

In short, phylogenetic analysis confirms Rabs as a dynamic family reaching a major degree of modification in chordates, where a mixture of evolutionary events such as duplications and losses modelled heavily this family. The detailed genome's search and the phylogenesis represent the most comprehensive survey concerning Rabs, in particular for the attribution of precise orthology to several genes from different metazoans. This phylogeny provides essential information to analyze evolutionary history of Rab family, representing an improvement of knowledge about that. It is focused not only on LECA proteins as past studies (Elias et al., 2012; Klopper et al.,

2012) but it covers a large amount of Rabs from eleven animal species, with some never investigated.

3.2.2 - Introns: an evolutionary signature for Rabs

In order to gain more insights concerning Rab evolution, I performed a survey on the intron/exon structures of Rab subfamilies. Since splicing sites are affected by a slow gain/loss degree, they can be a fundamental tool for studying the evolution of genes (Irimia and Roy, 2008). For the first time, it is described in deep the intron code of entire Rab family from early-branching metazoans such as cnidarians to primates. Splicing site conservation has been evaluated using genomic information from available databases and the intron junctions have been mapped on protein alignment of distinct Rabs belonging to six Groups. Employing intron/exon structures, I designed a model comprising all the Rab subfamilies characterized by distinct classes of introns (Figure 3.3) that are intra-group (blue), inter-group (red) and subfamily-specific (black) introns. This survey highlights an extraordinary conservation of Rab gene structure, in particular each subfamily retains specific intron positions across all metazoans analyzed supporting the existence of an intron code for the Rab family. All the bars shown in Fig. 3.3 represent a Rab with the outcome of all selected species, except *O. dioica* proteins excluded due to scarcity of available information about its genome. The unique gene not surveyed is the intron-less Rab9, belonging to the group III (red in Fig. 3.2). Interestingly, the conserved splicing sites are subfamily-specific signatures coherent with the phylogenetic-based classification of chordate (and non-chordate) genes. Moreover, shared intron positions and phases represent a tool to depict the orthology among invertebrate and vertebrate genes supporting duplication events, as shown by several cases in Rab

family such as Rab34/36 with Rab34 and Rab36 or Rab26/37 with Rab26 and
Rab37.
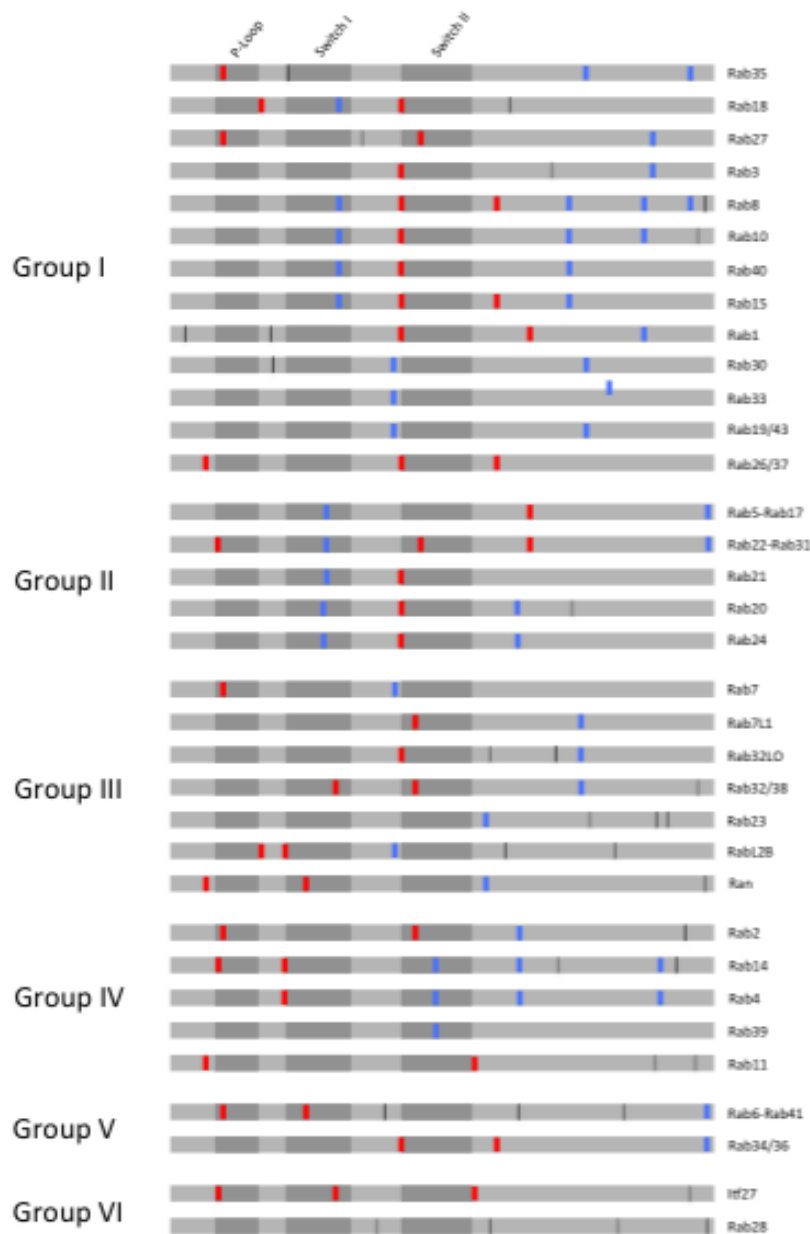
Figure 3.3. Intron code of Rabs. The figure shows the splicing sites of all Rab subfamilies (long gray bars) in Metazoans, which present three typical functional domains (dark boxes). Intron/exon junction have been classified using different colors: intra-group (blue), inter-group (red), member-specific (black).

In general, all the members of each subfamily share a common intron code, spanning from cnidarians to human. Because intron gain/loss is a slow evolutionary phenomenon, introns may be used more reliably than protein alignments typical of

phylogenies to trace back the history of highly divergent genes. For instance, intron code has been used to clarify the orthology of RabX6, present only in mollusks and ambulacrarians, and excluded from the tree for their fast evolutionary rate. As suggested by previous explorations inside group III (Fig. 2.3; Coppola et al., 2016), the preservation of intron code among distinct subfamilies is a clear hallmark of an ancient common origin as happens in Group I for Rab8, Rab10 and Rab40 or in Group II for Rab5 and Rab22. The presence of many conserved inter-group introns, however, reinforced the idea of a complex gene structure for the ancestral eukaryotic *Rab* gene. Here we show the first map concerning intron code of Rab family, demonstrating as the intron/exon structure is a diagnostic tool for recognizing the members of each Rab subfamily, supporting strongly the phylogenetic analysis. Moreover, intron positions shared by members belonging to distinct groups suggest that "modern" Rabs derive from one or few ancestral molecules.

3.2.3 - Duplications sculpted Metazoan Rab repertoire

Phylogenetic analysis and intron code, taken together, allowed depiction of Rab repertoire evolution in the eleven species selected across metazoans. A model was designed describing Rab toolkit and the identity of all family members, with a comprehensive scheme of Rab evolution in animals (Figure 3.4). Starting from LECA Rab genes, all the subfamilies have been visualized in the surveyed organism with a black and white symbols used to show the dichotomy between presence and absence for a gene. Rab repertoire analysis evidences the great variability in terms of metazoan Rab number that becomes more dramatic in the chordate phylum. First, this survey provides an update about Rab complement of species with respect to past Rab evolutionary investigations (Gallegos et al., 2012; Elias et al., 2012; Klopper et

al., 2012): *N. vectensis* with 52, *C. elegans* with 32, *L. gigantea* with 41, *S. purpuratus* with 40, *H. sapiens* with 66 Rab family members. Besides, this schematisation introduces in the Rab evolutionary scenario the genomes of novel species as the annelid *C. teleta* (37), the acorn-worm *S. kowalevskii* (43), the amphioxus *B. lanceolatum* (45), the appendicularian *O. dioica* (30) and the reptile *A. carolinensis* (60). It illustrates duplications inside the Rab family in all the selected species, but mainly in anole lizard and human (vertebrates). However, the impact of gene losses is clear comparing the Rab complement size of cnidarians to nematodes and annelids or, similarly, the Rabs possessed by amphioxus to *C. robusta* and *O. dioica*, with the latter having the smallest Rab repertoire among the analyzed species. Tunicates show a dynamic Rab toolkit due to a combination of duplications and losses in comparison with originary amphioxus 41 subfamilies, with many differences between ascidians and larvaceans, even if some losses which could be due to low-quality of genomes. Given the impact of duplications on Rab family during metazoan evolution, I also performed a syntenic survey to shed light on the nature of these duplicative events in vertebrates and invertebrates (Catchen et al., 2009). Together with phylogeny and intron code, this kind of approach is able to reconstruct unequivocally evolutionary history of Rabs from early-branching metazoans to vertebrates (Supplementary Table 3.1; Fig. 3.4). Regarding vertebrates, a synteny study on human chromosomes allowed to distinguish between extra-copies deriving from whole-genome duplications or WGDs (green in Figure 3.4) and gene duplications (blue in Fig. 3.4). Chromosomal conservation data indicate the presence of 40 WGD-originated Rabs in vertebrates (mainly comprised in Group I), with seven of them absent in *Anolis*. The genes derived from whole-genome duplications are: Rab1A-Rab1B, Rab3B-Rab3C, Rab8A-Rab8B-Rab13, Rab19-Rab43, Rab26-

Rab37, Rab27A-Rab27B, Rab33A-Rab33B, Rab39A-Rab39B and EFcab4A-EFcab4B-Rab44 for the Group I; Rab5A-Rab5B-Rab5C and Rab22A-Rab22B for the Group II; Rab32-Rab38 for the Group III; Rab2A-Rab2B, Rab4A-Rab4B, Rab11A-Rab11B-Rab25 for the Group IV; Rab6A-Rab6B-Rab6C-Rab41 and Rab34-Rab36 for the Group V. Then, I recognized ten genes phylogenetically related but without common syntenic surrounding genes, probably they are arisen from local duplications occurred at the stem of vertebrate's class, with only one not possessed by reptiles. All the syntenic relationships are listed in Suppl. Table 3.1.
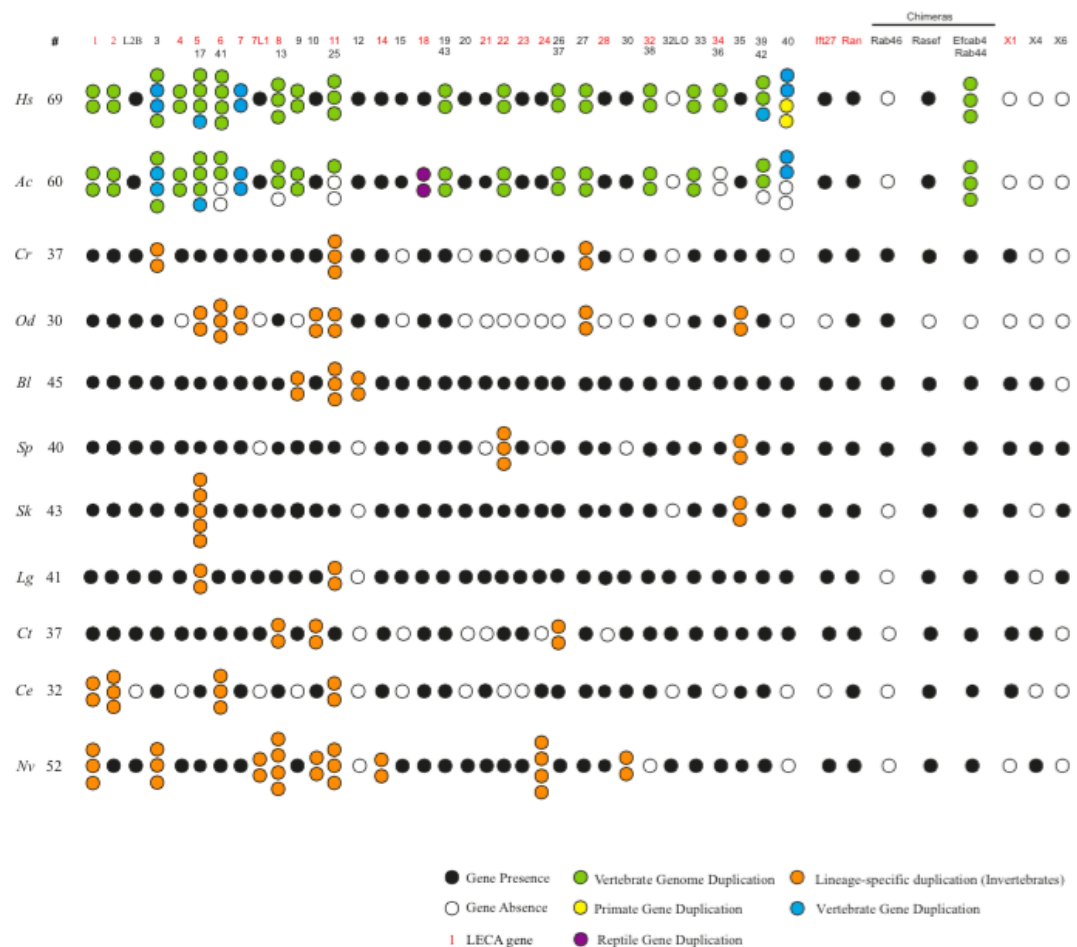
Figure 3.4. Rab repertoire in metazoans. Rab toolkit schematization of all metazoans present in this survey, respect to LECA genes (written in red). The species are indicated with initial letters of their name. All the genes are represented by circles (without color in case of absence). Using a color code, we evidenced distinct duplicative events. Subtle lines under paralogues indicate tandem-duplications (Rab5 in *S. kowalevskii* and Rab40 in *H. sapiens*).

Among these, three derive from tandem duplications: Rab3A-Rab3D (human Chr 19) and Rab40A-Rab40AL of group I (human Chr X), Rab9A-Rab9B (human Chr X) of group III. The lack of introns in Rab40A and Rab40AL hints a retrotranscriptional origin for them; curiously, a genome search in mammals show that Rab40A and Rab40AL are present only in primates (yellow). Intriguingly, the original metazoan Rab toolkit of invertebrates has been affected by various specific duplications (orange) mainly in *N. vectensis* and *O. dioica* while amphioxus and owl limpet show general Rab stasis. In the hemichordates, it has been found a Rab5 cluster formed by five members (Suppl. Table 3.1). Moreover, we found some examples of Rabs "resistant to duplications" across the evolution (Ran, Itf27).

Here is reported a map about identity and origins of all metazoan Rabs, demonstrating a great impact of duplications in Rab complement sculpting, especially in chordates; moreover, this survey testifies also the relevance of gene losses in Rab family.

3.2.4 - Domain architecture: not only "Rabs"

For collecting information about the evolution of Rab proteins, I also investigated their domain organization in metazoans (Figure 3.5). The majority of Rabs typically present three fundamental domains: a short motif fundamental to bind guanine nucleotides named the P-loop, and two stretches crucial for proper protein folding named Switch I and Switch II (Park, 2013). Interestingly, there are several exceptions in the "canonical" Rab domain architecture. Inside group III there is a subgroup of proteins characterized by a FALK stretch downstream of Switch I, composed by Rab32/38, Rab32LO and Rab7L1 subfamilies (Fig. 2.2; Coppola et al., 2016). Placed in the same group from my phylogeny there is Ran (Rab-in-nucleus),

the unique member of Rab family known for its nuclear functions (Melchior et al., 1993; Moore and Blobel, 1993) which is as single-copy gene across the evolution showing slightly diverse domain amino acid composition respect to other Rabs. Within the large group I there is Rab40, a bilaterian-specific protein with many duplicates in vertebrates (Fig. 3.2 and Fig. 3.3) whose peculiarity is the SOCS box at the C-terminus of protein. The SOCS (suppressor of cytokine signaling) box is a 50-amino acid motif present in several proteins which confers to Rab40 a regulatory role in lipid droplets formation in *Drosophila* (Tan et al., 2013) and Varp proteasomal degradation in melanocytes (Yatsu et al., 2015). Moreover, inside the P-loop of Rab40 orthologues I detected remarkable amino acid variability, a further element rendering this subfamily attractive for evolutionary biologists. However, an interesting peculiarity is represented, within Group I, by a class of "giant" Rabs (approximately 700 amino acids) showing C-terminal canonical domains of Rabs (P-Loop, Switch I, Switch II) and one/two EF-Hand motifs, which are calcium-binding elements widespread in eukaryotes (Kawasaki and Kretsinger, 1995), at the N-terminal region. Because of the domain's combination, I called these proteins "Rab chimeras" (Rasef, EFcab4/Rab44, EFcab4A, EFcab4B, Rab44, Rab46). The first atypical big GTPase to be found has been Rab45/RASEF, in the perinuclear area of HeLa cells (Shintani et al., 2007). It has been demonstrated the implication of this gene in several diseases, such as melanoma (Maat et al., 2008; Kaplon et al., 2014). Mammalian genomes encode for a couple of chimeras (CRACR2A and CRACR2B, here respectively renamed EFCAB4B and EFCAB4A) partially similar to each other. Their name derive from regulation of CRAC channels operated by CRACR2A in T cells (Srikanth et al., 2010), central in the presynaptic vesicle trafficking (Srikanth et al., 2016). Given the similarity in terms of domain architecture, all the large Rabs

could be implicated in calcium binding within intracellular signalling pathways, a novel function for GTPases (Srikanth et al., 2016; Srikanth et al., 2017).
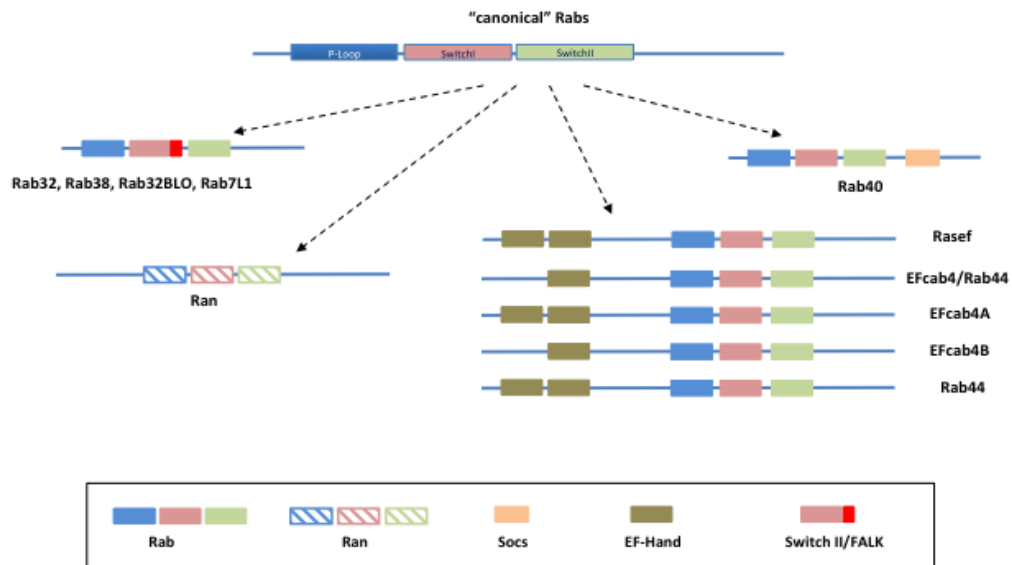
Figure 3.5. Domain organization of Rab family members. Here are classified all the metazoan Rabs, according to their domain combination. It has been established a colour code for all the protein motifs present in Rab family.

To shed light on Rab chimeras evolution and classification, I performed a ML phylogenetic reconstruction focused on metazoans (Figure 3.6). The sequences have been retrieved from public databases using human RASEF and EFCAB4B (CRACR2A) as queries and, successively, aligned by ClustalX (Larkin et al., 2007). In light of their shortness or divergence, several sequences have been excluded from the dedicated tree, which comprises 29 Rab chimeras from the following species: *C. elegans*, *C. teleta*, the oyster *Crassostrea gigas* (mollusk), the trematode *Schistosoma mansoni* (plathelmyntes), the Brachiopod *Lingula anatina*, the Holocephalan *Callorhinchus milii* (cartilagineous fish), *A. carolinensis*, the goose *Anser cygnoides* (bird), the mouse *Mus musculus* (mammal) and *H. sapiens*. I did not find Rab chimeras in the available genomes of unicellular eukaryotes. Each protein present in the tree is flanked by a schematic domain organization: 1st EF-Hand (orange

pentagon), 2nd EF-Hand (red pentagon), Rab (blue bar). The tree topology shows the existence of two big and phylogenetically robust subfamilies named Rasef (orange box in Fig. 3.6A) and EFcab4/Rab44 (light blue box in Fig. 3.6A). While the first is formed by single-copy gene for invertebrates and vertebrates, the latter has a quite complex evolutionary scenario. Phylogenesis suggests that invertebrate EFcab4/Rab44 is the ancestor of vertebrate-specific EFcab4A (Cracr2B), EFcab4B (Cracr2B) and Rab44, originated in two different rounds of genome duplication (Abi-Rached et al., 2001; Dehal and Boore, 2005), as supported by comparison among four human genomic loci (Supplementary Table 3.2). Analyzing the domain architecture of each large GTPase has permitted to prepare a classification in accordance to EF-Hand presence/absence (Fig. 3.6B). My survey demonstrated invertebrate's Rasef, EFcab4/Rab44 and Efcab4B have one whereas vertebrate's Rasef and Efcab4A have two calcium-binding motifs. The presence in some invertebrate's Rasefs of two EF-Hands (for instance *L. anatina*) supports the occurrence of several domain losses. The EF-hand presence/absence landscape could be parsimoniously explained with several loss events from an ancestor of all Rab chimeras clade characterized by two EF-Hands; genome search and alignments hint at the first EF-hand as that preferentially lost (orange pentagon). Surprisingly, Efcab4A of mammals and amphibians as *Xenopus tropicalis* (excluded from the phylogeny) lacks a C-terminal Rab domain. The orthology of these two genes with other vertebrate Efcab4A proteins has been confirmed using a synteny approach, evidencing a paralogon highly preserved in gnathostomes (Fig. 3.6C). Moreover, this class comprises a further member (Rab46) that probably is a deuterostome-specific duplicate, here absent for its fast-evolutionary rate (Fig 3.2).
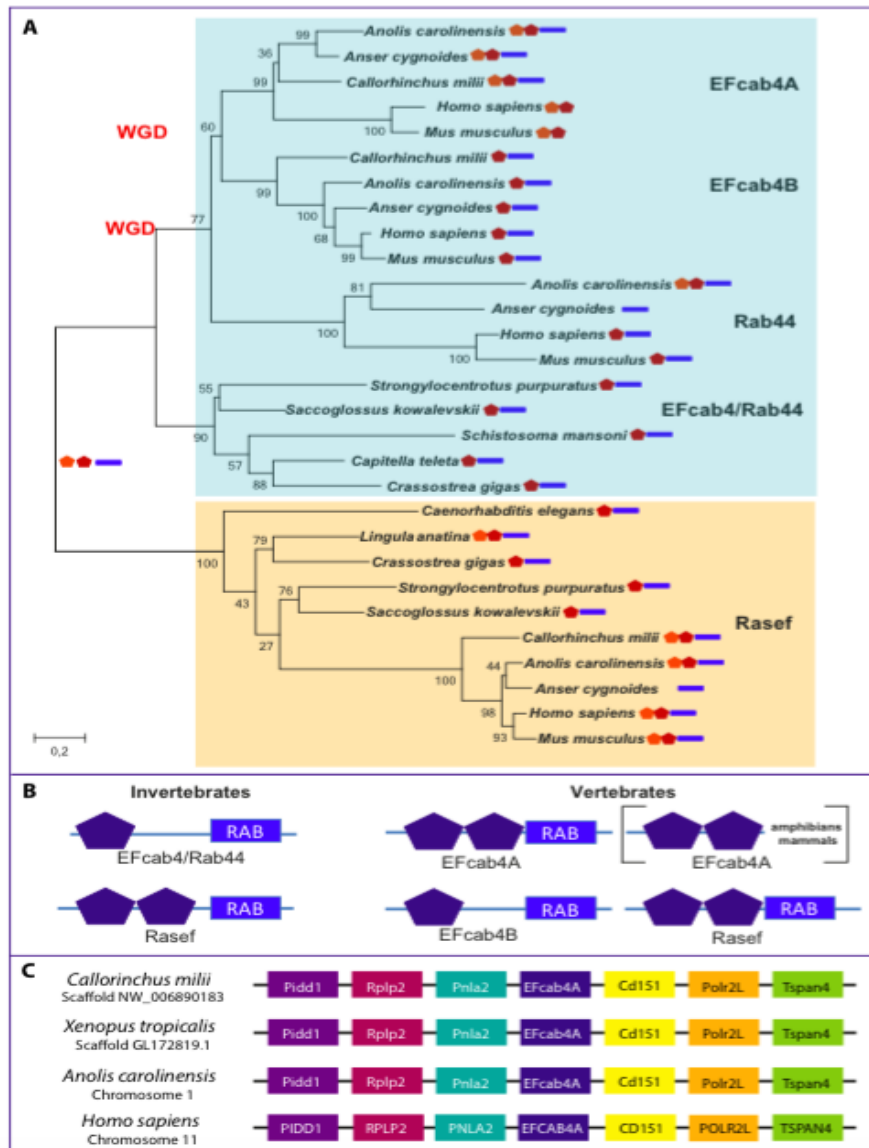
Figure 3.6. Evolution of Rab chimeras. A) ML phylogenetic tree shows Rasef (orange) and Efcab4/Rab44 classes; close to each protein are drawn EF-Hands (pentagons) and Rab (blue bar) motifs. B) Schematization of domain architecture in invertebrate and vertebrate Rab chimeras. C) Paralogon conservation of Efcab4A genomic loci.

My survey represents the first general and clear picture about Rab family domain organization in metazoan clade where is possible to find several exceptions, rendering this family extremely dynamic also from this perspective. Among these, Rab chimeras are the most fascinating for their complex evolutionary scenario (particularly in vertebrates) and for the possible functional implications due to the evolution of giant Rabs.

3.3 - Discussion

3.3.1 - The Rab family: a complex evolutionary scenario

Genome searches, phylogenetic tree analysis, intron code and synteny represented fundamental tools to investigate the evolution of the metazoan Rab family, the largest within Ras superfamily. Despite comprehension of Rab evolutionary history having been traditionally deemed instrumental for understanding eukaryotic evolution (Elias et al., 2012), here is reported the first comprehensive investigation on "animal" Rabs, under the hypothesis that a major complexity requires a more manifold trafficking machinery. In particular, I focused on Rab complement in chordates which can be considered as the most active "hotspot" for Rab variability inside metazoans. Phylogenetic reconstruction proved the existence of 42 Rab subfamilies in animals, with 36 already present in *Nematostella vectensis* (Fig. 3.1). The cnidarian Rab repertoire result is extremely interesting because it permits us to quantitate the increase in Rab number before metazoan split of 21 ancestral Rabs (Fig. 3.4, highlighted in red), as previously suggested (Klopper et al., 2012). The presence of two LECA genes, RabX1 and Rab32/38, in the demosponge *Amphimedon queenslandica* speaks in favor of their loss in the cnidarian ancestor. In light of this, the eu-metazoan Rab complement consisted of 38 subfamilies approximately conserved across animal evolution. To shed light on the mechanisms driving the evolution of Rab toolkit from LECA to animals, a challenging step will be to analyze Rabs across other basal animals as *A. queenslandica* (sponges), *Mnemiopsis leidyi* (ctenophorans) and *Trichoplax adhaerens* (placozoans). With its 41 subfamily members clustering with vertebrates and ambulacrarians, amphioxus is the best stand-in to study the ancestral Rab repertoire at the stem of chordates: in fact, *B. lanceolatum* has conserved all the subfamilies, except the RabX6 (excluded

from phylogeny for its evolutionary divergence). Interestingly, this Rab35-like gene has faced several losses as happens in chordates and my results indicate it as a bilaterian-novelty. Characterized by a complex story in vertebrates, also Rab40 arose before the split of bilaterians. With respect to the eu-metazoan subfamily set, the amphioxus set presents Rab46 and Rab12. The deuterostome-specific Rab46, lost in hemichordates and vertebrates, here is classified for the first time and belongs to the "Rab chimeras" class (not shown in Fig. 3.6A). Surprisingly, Rab12 represents the unique family member evolved by chordates and has been maintained in all vertebrates. Initially identified in rat testis (Iida et al., 2005), Rab12 regulates transferrin degradation therefore is fundamental for recycling endosomes to lysosomes (Matsui and Fukuda, 2011). It supports the specialization of chordate-specific Rab12 to orchestrate innovative trafficking routes. Curiously, all the novel subfamilies appeared after metazoans split belong to Group I (green), by far the largest inside the Rab family, encompassing 23 well-supported distinct subfamilies (57 % of total): taking all into consideration, it represents the most 'successful' group from an evolutionary perspective, maybe for the relevance of regulated pathways inside intracellular trafficking. Using phylogeny it has been possible to establish parsimoniously the orthology of several Rabs, whose identity and name were hitherto unknown, uncertain or wrong. Apart from a more stringent classification of many proteins belonging to known models, constructing this tree has allowed me to identify the entire Rab family of key species such as annelid *C. teleta*, ambulacrarian *S. kowalevskii*, appendicularian *O. dioica*. Intriguingly, the selection only of metazoan species and the exclusion of unicellular eukaryotes could have facilitated tree definition and the orthology of subfamilies. Finally, the phylogenetic tree shows the Rab family as, characterized by several duplications and losses which have

modeled the starting Rab toolkit across metazoan evolution, mainly in chordates. Although Rab intron codes give little information supporting the presence of distinct groups, it represented a valid tool to shed light on the orthology of Rab subfamilies. Given intron positions are rarely modified over time, splicing site conservation is more reliable than phylogeny, which can be affected by divergent evolutionary rates, or low signal-to-noise ratios of sequences (Irimia and Roy, 2008). Next I reported the first attempt for deciphering the intron code of Rab GTPases family (Fig. 3.3). Intron/exon structure is conserved in all the analyzed species, with a general preservation from eu-metazoan ancestor to vertebrates. I recognized subfamily-specific intron signatures retained (also in duplicates) during evolution, in spite of many protein modifications; this has been important to establishing chordate Rab orthology with other metazoan members. As suggested for the Rab32/38 subfamily (Coppola et al. 2016), the retention of intron positions traces back the evolutionary origins of vertebrate genes: for instance Rab34/36 with Rab34 and Rab36 and Rab26/37 with Rab26 and Rab37. Using this code will be instrumental to assess the orthology of Rabs from other species, in particular invertebrates. For instance, the conservation of the same intron has inferred the orthology among RabsX6 of *L. gigantea*, *S. kowalevskii* and *S. purpuratus* (not present in phylogeny). By contrast, inside groups there are subfamilies with common intron/exon structure: the most interesting and supported cases are Rab8, Rab10, Rab15 and Rab40 within Group I, Rab20, Rab21 and Rab24 inside Group II and Rab32/38, Rab32LO and Rab7L1 inside group III, already supposed as a subgroup (Coppola et al., 2016). The shared intron code exhibited by non-orthologous genes unveils common history for distinct subfamilies suggesting the existence of ancient duplicative events before radiation of eu-metazoans. Then, some intron sites can be used as key phylogenetic markers

which postulate ancient common origin, inherited from an ancestral Rab or, more probably, from a set of "core" Rabs (Dunst et al., 2015). Moreover, also intron absence is a significant evolutionary information: the lacking of introns in all the Rab9 genes prompted me to consider it as an ancient paralogue retrotranscripted from Rab7. Collectively, intron site data are an essential component to comprehend the evolutionary events (gene duplications, genome duplications, gene losses) which carved the Rab family, especially during chordate diversification. Albeit the introns do not give clear bias for "group-specific" codes, it has been discovered a number of splicing sites conserved in members belonging to distinct groups. The presence of many inter-group introns, however, reinforced the idea of a complex gene structure for the ancestral eukaryotic *Rab* genes, which would have unevenly lost introns during evolution.

Phylogenetic and intron/exon analysis permitted me to describe Rab complement in metazoans, with a particular attention on chordates. Adding synteny analysis, I deciphered the impact on duplications and losses on the Rab toolkit of chordates, with a plethora of vertebrate-specific members deriving from genome and local duplications. Surveying human chromosomes, it has been established clear relationship for 40 ohnologue (green) Rabs arisen at the stem of vertebrates (Abi-Rached et al., 2001; Dehal and Boore, 2005). Therefore, chromosomal conservation indicates the existence of 17 Rab invertebrate ancestors which represent the major source of Rab number increase in vertebrates, such as Rab19/43 and Rab34/36. Besides, for ten genes (Rab3A, Rab3D, Rab17, Rab42, Rab40B, Rab40C, Rab7A, Rab7B, Rab9A, Rab9B) absence of synteny speaks in favour of local duplications that occurred before vertebrate's split (blue), with two gene couples deriving from tandem duplications (Rab3A-Rab3D, Rab9A-Rab9B). Moreover, a tandem

duplication involves also two primate-specific genes, Rab40A and Rab40AL (yellow). The study of Rab40 demonstrates how unifying phylogeny, intron and synteny data can be helpful to understand the evolutionary history of such a complex lineage. The most parsimonious explanation is based on a local vertebrate duplication affecting Rab40B/C ancestor, with a successive retrotransposition before primate's split generating Rab40A/AL, as suggested by intron absence in all the primate sequences surveyed. The retrotranscribed sequence duplicated again giving rise to tandem Rab40A-Rab40AL. Regarding vertebrate duplicates, anole lizard does not possess seven WGD-Rabs (Rab11B, Rab25, Rab13, Rab6C, Rab41, Rab34, Rab36) and one local duplicate (Rab42) and exhibits an additional Rab18. A survey in other reptilian genomes demonstrates that Rab13, Rab34 and Rab6C are lost in all the reptiles whereas the other absences could be related to specific loss events or to low quality of genomes; reptiles present a duplication involving the Rab18 lineage (Rab18A, Rab18B). It suggests to investigate discrepancies in Rab complement amid vertebrates (cyclostomes, sharks, amphibians, birds) which could be extremely interesting from a functional perspective, in terms of gain/loss of cellular trafficking capabilities. Because teleost-specific genome duplication (TSGD or 3R) involving "modern fishes" (Hoegg et al., 2004; Kuraku et al., 2009), the analysis of fish Rabs appears to be really challenging. Moreover, this survey on teleost should give insights on the effects on functionality driven by duplications, as suggested by developmental diversification occurred in Rab32/38 subfamily of zebrafish (Coppola et al., 2016).

Interestingly, the vertebrate toolkit includes all the ancient subfamilies, except two, RabX1 and Rab32LO, whose function could result lost or attributed to other genes; for Rab32LO, the original role could be partially redundant with ancient paralogue

Rab32/38, specialized in pigmentation (Racioppi et al., 2014). Surprisingly, *N. vectensis* lacks Rab32/38 in place of Rab32LO evoking a common role in trafficking dynamics for these two genes, but is necessary to get information regarding Rab32LO. About Rab32/38, its presence in *Oikopleura dioica* results very interesting because speaks in favour of a function not necessarily related to pigmentation. This appendicularian does not show pigmentation, in fact we demonstrated it lacks tyrosinase family members (Racioppi et al., 2017). Given Rab32/38 subfamily is associated to pigmentation for its role in the transport of tyrosinases (Tyr, Tyrp), the Rab32/38 gene in *O. dioica* must bind some other cargo. Functional analysis in this model system could reveal other trafficking capabilities for Rab32/38 subfamily, not related to pigmentation (Omotezako et al., 2015).

Concerning invertebrates, I recognized many specific duplicates in all the selected species and this testifies to a strong impact of duplications on the Rab family also outside vertebrates. The highest number of duplications has been found in cnidarian *N. vectensis*, with 9 (or more) genes duplicated resulting in a toolkit of 52 Rabs. Moreover, the *S. kowalevskii* genome, harbours the largest Rab cluster found in metazoans, constituted by Rab5 genes. Importantly, we must comprehend how invertebrate duplications have encouraged the acquisition of new traffic capabilities.

The Rab repertoire highlights the existence of distinct opposing scenarios in chordates. With its 45 Rabs distributed in 41 subfamilies (close to ambulacrarian toolkits), amphioxus complement is the closest to chordate archetypal Rab dataset. Rab toolkit confirms the amphioxus proclivity to genomic stasis, in fact just three lineages are affected by duplications (Rab9, Rab11, Rab12). On the other hand, there are urochordates here represented by *O. dioica* and *C. robusta* with 30 and 37 Rabs, respectively, which can be considered as "Rab-losers". Since the chordate ancestor

possessed a full-set of 41 subfamilies, I compared amphioxus and tunicate repertoires distinguishing between 6 urochordate- (Rab15, Rab20, Rab22, Rab24, Rab30, Rab40B/C) and 11 larvacean-specific Rab losses (Rab4, Rab7L1, Rab9, Rab21, Rab23, Rab26/37, Rab28, Rasef, EFcab4/Rab44, RabX1, Itf27) whose role needs to be investigated. Among these, urochordates lack totally three original LECA genes (Rab22, Rab24, Rab32LO) while larvaceans have lost also other 5 LECA (Rab4, Rab7L1, Rab21, Rab23, Rab28, Itf27). Furthermore, this scenario supports two different periods of loss, one at the base of urochordates and a further in the appendicularian ancestor. Interestingly, *O. dioica* has the smallest Rab repertoire (30) in metazoans by losing a plethora of genes: it should be understood the functional impact of these losses. By contrast, the "Rab-loser" tunicates also show many duplications: in *Ciona* there are two Rab3 while in *Oikopleura* are duplicated Rab4, Rab5, Rab6 and Rab35. This could be connected to different functional needs of different urochordate species. However, *Oikopleura dioica* has the smallest Rab complement amongst metazoans surveyed here and in past analyses (Elias et al., 2012; Klopper et al., 2012): it represents probably the minimal set of Rabs necesessary for metazoan's trafficking.

Vertebrates have the largest and most diversified Rab toolkit in metazoans depending on whole-genome and specific duplications. In light of two WGD events and local duplications, the vertebrate ancestor had approximately 150 Rab members, a pattern severely modified by a myriad of gene losses demonstrating their strong impact also in vertebrates, even if they are qualitatively different because this massive loss concerns only recent duplicates. Nonetheless, the comparison between invertebrate chordates, lizard and human allowed me to observe dynamic variability inside vertebrate's complement, with many losses found in anole lizard. Moreover, toolkit

analysis indicates the existence of several clade-specific losses: chordates have lost RabX6, Olfactores Rab32LO and RabX4, vertebrates Rab46 and RabX1, whose role in the cell trafficking remains to be elucidated. Although it is necessary to survey the repertoire from other vertebrates (in particular agnathans), current information prompts me to believe that the ancestral vertebrate Rab complement was made of 37 subfamilies.

Comparisons among selected metazoan species allowed me to recognize not only the toolkit structure but also the most active lineages. In fact, the balance between gains and losses of genes remains elusive but it is apparent that expansion involved mainly some Rab subfamilies from cnidarians to vertebrates, as happened for Rab5, Rab6 and Rab11. The duplication in different models of the same subfamily alongside the evolution is a believable phylogenetic signal to indicate the relevance of that protein in transportation dynamics, as already suggested (Klopper et al., 2012). The unduplicated Rabs alongside evolution such as Ran and Itf27 could represent a case of study for their involvement in human diseases. It has been hypothesized that a major degree of Rab modeling across different phyla has been useful to modify intracellular traffic pathways: it is hard to duplicate tethering complexes and coats because they are formed by several independent proteins, while duplicating Rabs has represented an easier strategy to influence transportation dynamics (Klopper et al., 2012). In summary, my data lead to consider family variations across metazoans as driven by functional trafficking modifications. Among analyzed genomes, chordates exhibit the most active and dynamic Rab evolutionary landscape that has been influenced by diverse genomic events.

3.3.2 - Domains: a new tale from Chimeras

For the first time, we mapped the domain architectures of the entire Rab family across metazoans (Fig. 3.5), demonstrating that some particular trafficking steps depend on a partial change in "canonical" Rab domain organization. Three subfamilies belonging to group III (Rab32/38, Rab32LO, Rab7L1), possess an ultra-conserved stretch (FALK) downstream Switch I (Coppola et al., 2016). It could be functionally related with transportation steps regulated by Rab32/38 subfamily members in pigmentation (Bultema and Di Pietro, 2013; Racioppi et al., 2014). Sharing FALK could indicate a common origin for these three subfamilies, possibly associated with partially redundant functionality in pigmentation dynamics. Moreover, it could be interesting to evaluate the preservation of similar 'boxes' in related subfamilies. With its role in nuclear import-export, Ran represents a peculiarity in the Rab family, in fact it translocates several proteins through the nuclear pore complex (NPC) (Schlenstedt, 1996). By overexpression of RanBP1 (a Ran effector) in tissue cultures or *Xenopus laevis* cycling eggs, Ran pathway importance has been clarified also in mitotic progression (Battistoni et al., 1997; Kalab et al., 1999). Ran is a LECA gene present in all the selected metazoans and shows a modified Rab domain that could be responsible for its function in the cell.

Rab40 represents a bilaterian innovation of group I with a particularly active pattern in chordates, as exemplified by different gene gains and losses (Fig. 3.4). Proteins encoded by this gene are characterized by C-terminal SOCS box, formed by two blocks of well-conserved residues separated by 2 to 10 nonconserved amino-acids (Kamura et al., 1998). In *Drosophila* Rab40B/C regulates the lipid droplet formation (Tan et al., 2013) while in mammals its ortholog Rab40C is implicated in pigmentation dynamics, because it regulates the degradation of Varp (Rab32/38

effector) influencing Tyrp1 trafficking (Yatsu et al., 2015). A role has also been proposed in Wnt pathway regulation in amphibian gastrulation (Lee et al., 2007). Moreover, I discovered a high degree of variation inside the Rab40 P-Loop amongst metazoans (not only those used for my phylogeny) that could be linked to functional modifications. Given SOCS is known to be a suppressor motif and the diverse functions attributed, I hypothesize that Rab40 subfamily has been evolved and maintained for playing specific roles, slightly different from simple transportation. In light of this, the absence in tunicates could be linked with loss of Rab40 special functionality whereas the impact of duplications occurred in vertebrates should be investigated, with a particular focus on pigmentation mechanisms.

Among non-canonical Rabs, a noteworthy discovery has been the class of giant Rabs for their structure, evolution and function; therefore, I conducted a deep *in silico* analysis to comprehend the evolutionary history of "chimeras", so called because they seem a combination between Rabs and calcium-binding proteins (Fig. 3.6). Firstly, phylogeny supports the existence of two distinct subfamilies in metazoans, Rasef and EFcab/Rab44. A detailed genome search demonstrated the absence in unicellular eukaryotes as *Capsaspora owcarzaki* and *Monosiga brevicollis* of such arranged Rabs, while both Rasef and Efcab4/Rab44 are present in the demosponge *A. queenslandica*. This prompted me to time "chimeras" formation before Porifera split and to define Rasef and EFcab4/Rab44 as two animal-specific Rabs, evolved for particular functions central to multicellularity. This event could be associated to the presence of EF-Hand elements, present in many calcium-binding proteins and consisting of twelve residue loop between two α-helical domains which form a trap for a calcium ion (Kawasai and Kretsinger, 1995). In synthesis, all the Rab chimeras

could represent a "mixed" subgroup which are not only transporters as other Rabs, but also sensors for calcium ions.

Evolutionary analyses have demonstrated the presence of two ancestral subfamilies in the animal ancestor (Rasef, EFcab4/Rab44), both with two EF-Hands and a Rab-homologue domain. While Rasef has been maintained in one copy from sponges to primates, EFcab4/Rab44 lineage appears particularly dynamic, as reflected by four additional proteins generated during evolution. Phylogenesis and complement representation (Fig. 3.2; Fig. 3.4) show the existence of a novel subfamily (Rab46) deriving from a duplication event in the deuterostome ancestor, successively lost in hemichordates and vertebrates. Its exclusion from the phylogenetic analysis depended on its fast evolutionary rate, that, together with its absence in vertebrates, speak in favor of ultra-specialized function. Indeed, three other proteins (EFcab4, EFcab4B, Rab44) are vertebrate novelties arisen from two rounds of genome duplication, as supported by synteny conservation among human chromosomes 1, 6, 11, 12. I found Rab chimeras (blue) clustering with tetraspanins (TSPAN, yellow), potassium channels (KCNQ, orange) and cyclin-dependent kinase inhibitors (CDKN, green), as supported by dedicated phylogenetic reconstructions. Interestingly, I showed that chromosome 1 should be the position of a ghost chimera, i.e. the fourth member generated from WGDs. Collectively, data indicated Rab chimeras as a functional subgroup of six genes (Rasef, EFcab4/Rab44, EFcab4A, EFcab4B, Rab44, Rab46) comprised in three subfamilies (Rasef, EFcab/Rab44, Rab46), a diversification reflected by distinct domain architectures possibly linked to diverse roles in the cell. Organization of domains is diagnostic: Rasef (invertebrate), EFcab4/Rab44 and EFcab4B with one EF-hand, and Rasef (vertebrate), EFcab4B with two EF-hands. The presence of some exceptions to this classification and the

variable architecture characterizing Rab44 and Rab46 are consistent with specific losses of the first EF-Hand. Because of pairing EF-hands enables cooperative binding of Ca^{2+} ions, the lack of one EH-Hand could be driven by the requirement of calcium-binding tools in different animals. Interestingly, in avians as *A. cygnoides* only EFcab4A presents both calcium-binding elements: this scenario has to be investigated, since it could be related with functional differences among chimeras in this class. Besides, mammalian and amphibian EFcab4A orthologues do not include a Rab domain: these independent (but convergent) losses could be linked with some functional specialization or with function loss with respect to other gnathostomes, maybe transport capability that is the "classical" work done by Rabs: in this case, I can suppose a distribution of cellular skills to the rest of chimeras.

Domain architecture is a further example of evolutionary dynamism inside Rabs, which are actually much more than simple cargo transporters. This report shows how Rab family, chiefly in metazoans, acquired novel domains to play new specialized roles. The Rab Chimeras represent the most diversified amongst atypical GTPases, representing an innovation of animals with a probable double role. The chimeras evolutionary scenario is made interesting by diverse genomic rearrangements (gene gain/loss, domain loss) which reach the highest degree of complexity in vertebrates.

CHAPTER 4

Rab32/38 subfamily in pigmentation: insights from chordates

4.1- Background

The establishment of intracellular compartmentalization constituted a crucial step for the eukaryotic evolution and Rab family members, belonging to Ras superfamily, represent by far the main coordinators of vesicular trafficking existing among membrane-enclosed organelles (Diekmann et al., 2011). Rabs, the largest family inside small GTPases encompassing approximately 60 proteins in human (Stenmark, 2009), have a complicated evolutionary history (Elias et al., 2012) with an extremely variable number in unicellular eukaryotes (Saito-Nakano et al., 2010) to multicellular organisms (Pereira-Leal and Seabra, 2001; Rutherford and Moore, 2002). Given the importance of the endomembrane system for pigment processes, different Rabs have been associated to pigmentation, in particular melonosome biogenesis (Sitaram and Marks, 2012). Amongst them, particularly relevant for pigmentation dynamics, are members of the Rab32/38 subfamily belonging to supergroup III strictly involved in the life of melanosomes (Wasmeier et al., 2006), which are LROs deputed to synthesize, store and transport melanin granules. With the support of effectors such as AP-3, AP-1 and BLOC-2, the mammalian Rab32 and Rab38 regulate the transportation of pigmentation markers Tyrosinase (Tyr) and Tyrosinase related protein 1 (Tyrp1) from trans-Golgi network to rising melanosomes, during step II-III of their biogenesis (Bultema et al., 2012). Interestingly, Rab32 and Rab38 are able to redirect the canonical lysosomal machinery composed principally of AP-3, AP-2 and BLOC-2, loading melanogenic enzymes into specialized vesicles which co-exist with

other cargoes connected to lysosomal functioning. It evokes a central role for Rab32 and Rab38 in pigmentation, in fact they could represent factors specific of ultra-specialized cells as melanocytes and eye pigment cells (Bultema and Di Pietro, 2013). Moreover, it has been supposed a permanent physical interaction with vesicles by these two Rabs in order to increase their motility and fusion with maturing melanosomes. Conversely, the Tyrp2 transport conditions are not well-known but probably it is involved Rab32 in concert with BLOC-3: in fact depletion of Rab32, and not Rab38, is responsible for Tyrp2 decrease in MNT-1 melanocytes. It suggests a specific role for Rab32 protein in melanocytes and a functional cooperation with Rab38 in melanosomal logistics using the pre-existing clathrin-dependent typical of lysosomes (Bultema et al., 2012; Bultema and Di Pietro, 2013). Amongst regulators, in mouse melanocytes have been identified Rab9A and Rutbc1 as mediators of Rab32/38 spatiotemporal regulation that is essential for a proper melanosomal trafficking (Marubashi et al., 2016). On the other hand, Varp (VPS9-ankyrin-repeat-protein) represents a Rab32/38 effector specialized in Tyrp1 trafficking (Tamura et al., 2009) whereas Myosin Vc seems to co-work in the proper transport of both Tyrosinase-related proteins (Bultema et al., 2014). Concerning the adaptor proteins, their recruitment to membranes is controlled by membrane lipids, cytoplasmic tails and ARF proteins, constituting another family of small GTPases (Owen et al., 2004).

The implication of Rab32/38 subfamily members in pigmentation dynamics emerged from observations conducted on mice where a point autosomal recessive mutation inside P-loop domain of Rab38, arising spontaneously in some mice strains (Loftus et al., 2002). The *Chocolate* (*cht*) mutation in mice produces a phenotype characterized by an oculocutaneous albinism and hypopigmented color coat which

probably depends on the mistrafficking of tyrosinase family members operated by Rab38. Furthermore, Rab32 breakdown in cultured *cht* melanocytes causes strong hypopigmentation, showing combined effects for these two Rab proteins (Wasmeier et al., 2006). With the support of a 67 % amino acid identity, they are considered as a couple of paralogues (Wasmeier et al., 2006) deriving from the vertebrate whole genome duplication (WGD) occurred at the stem of Gnathostomata clade (Ohno, 1993; Abi-Rached et al., 2002; Dehal and Boore, 2005). The centrality of this subfamily to pigmentation has also been shown by analyzing diseases: for instance, the impact of Rab38 mutation on ruby rats (Oiso et al., 2004) which present features such as hypopigmentation platelet storage pool deficiency linked with Hermansky-Pudlak syndrome or HPS (Wei, 2006). It is a human pathology with different severe consequences such as oculocutaneous albinism, abnormal lipofuscin accumulation, and easiness of bleeding (Hermansky and Pudlak, 1959). Moreover, immunohistochemical experiments suggest an involvement for Rab38 in melanoma development (Zippelius et al., 2007). Inside vertebrates, many data corroborate the pivotal role attributed to Rab32/38 subfamily members in melanin production. According to cellular physiology data, the murine homologue of human RAB32 co-localizes with the Tyr and Tyrp1 enzymes in melanocytes (Cohen-Solal et al., 2003) even if, Rab32 of *Mus musculus* seems to be not involved in mithochondria functioning as registered in human (Alto et al., 2002). However, Rab38 is localized in the cells of rat lung (Osanai et al., 2001), in fact this protein is responsible for the size control of lung alveolar type II epithelial cells (Zhang et al., 2011). There are many examples of Rab32 and Rab38 implication in processes that are not pigmentation-related, suggesting other vesicular mechanisms regulated by the Rab32/38 members linked to distinct processes. Interestingly, strong *Rab32*

expression in melanophores, the skin pigmented cells of frog (*Xenopus laevis*) speaks in favor of its conserved role in pigment biogenesis (Park et al., 2007). This concept is enforced by data obtained from invertebrate model systems. In the fruit fly *Drosophila melanogaster* the phenotype called *lightoid* (*ltd*) is characterized by the depletion of eye pigmentation due to mutation of *Rab-RP1*, orthologue of *Rab32* (Ma et al., 2004); it marks specifically the eye lysosomes and lipid droplets that enrich the adipose tissue, suggesting its involvement also in authophagy processes (Wang et al., 2012). Besides, the formation of LROs present in the intestine cells of nematode *Caenorhabditis elegans* is governed by a Rab32 homologue, called GLO-1. Interestingly, it has been proposed a model for the gut granule biogenesis, with the direct involvement of GLO-3 protein that probably represent a guanine exchange factor (GEF) for GLO-1 (Delahaye et al., 2014). In the ascidian *Ciona robusta*, the closest living relative of vertebrates, it has been found specific expression of the unique *Rab32/38* gene during embryogenesis in four cells belonging to pigment cell lineage (Racioppi et al., 2014). Furthermore, functional investigations highlighted Rab32/38 importance for the development of otolith and ocellus pigment cells, acting as an "hub" for a complex network of genes influenced by FGF signaling (Racioppi et al., 2014).

To shed light on the Rab32/38 subfamily behavior during evolution we conducted a deep phylogenetic analysis with a focus on the deuterostome clade. Moreover, in order to obtain insights regarding Rab32/38 in chordate development we selected two key species, the cephalochordate *Branchiostoma lanceolatum* and the teleost *Danio rerio*. For their unique ensemble of genomic and anatomical characteristics, the cephalochordates such as Mediterranean amphioxus are considered key model systems to study chordate evolution. Amphioxus species represent a key stand-in for

evolutionary investigations: it is at the root of the chordates and possess an unduplicated genome comprising instead representatives from almost all typical vertebrate gene families (Putnam et al., 2008). The analysis of Rab32/38 subfamily in amphioxus pigmentation can be particularly interesting given its complex photoreceptive system consisting of Joseph cells, lamellar body, dorsal ocelli (Hesse cells) and frontal eye (Lacalli, 2004). For the presence of cilia, the latter has been traditionally thought as a structure homologous to the retinal pigmented epithelium (RPE) of vertebrates. Frontal eye shares with vertebrate RPE not only the melanin content but also a common regulatory signature, due to the co-expression of transcription factors and opsins typical of vertebrates (Vopalensky et al., 2012). Moreover, amphioxus frontal eye simple projections may represent the ancestral condition successively evolved in the complex neural circuitry observed in vertebrates (Vopalensky et al., 2012). A further point consistent with common photoreceptive origins, is represented by the expression of tyrosinase family members in the neural tube region where is visible the first pigment spot (Yu et al., 2008).

Fishes have colonized all the aquatic ecological niches thanks to their incredible variety of morphological and anatomical adaptations, which become exceptional in more than 32000 known species of teleosts. They show the largest set of pigmentary patterns among vertebrates, patterns that are fundamental for disparate social and sexual behaviours, instrumental to their diffusion in distinct habitats like oceans, rivers and lakes. A plethora of habits like warning, camouflage and threatening of predators are based also on extraordinary teleost colour variability (Fujii, 1993). While mammals and birds possess solely black/brown melanocytes and amphibians and reptiles enriched their pigment cell spectrum with yellow/red

xantho/erythrophores and reflecting iridophopores, teleosts are characterized by a major number of pigment cell types with lineage-specific novelties such as whitish leucophores and blue cyanophores (Braasch et al., 2007). Moreover, it has been hypothesized the presence of red fluorescent cells in some coral reef fish species (Michiels et al., 2008). The exploitation of this excellent pigmentation system for the adaptation to different environmental conditions requires a fine regulation: an example is given by the α-melanophore-stimulating hormone (α-MSH) whose pituitary secretion is governed by neurotransmitters such as norepinephrine (Sugimoto, 2002).

Apart from the polyploidization and rediploidization events which have affected vertebrate lineages and the whole-genome duplications (WGDs) occurred before gnathostomes split (Ohno, 1993; Abi-Rached et al., 2002; Dehal and Boore; Putnam et al., 2008), it is documented the existence of lineage-specific WGDs in different vertebrates (Otto, 2007). Teleosts have faced an extra-genome duplication providing genetic raw material for their explosion during the Mesozoic era (Jaillon et al., 2004; Taylor et al., 2001; Taylor et al., 2003). Inside actynopterigians, this phenomenon involved only this clade hence it has been defined "teleost-specific genome duplication" (TSGD), hypothesized as a driving force for teleost evolution (Hoegg et al., 2004; Kuraku et al., 2009), albeit the relation between the availability of new genetic material and evolutionary success is not totally clarified (Otto, 2007). TSGD has been connected to extraordinary difference in color patterning of teleost clade with an impact on pathways implicated in pigmentation (Mellgren and Johnson, 2005). Concerning fundamental enzymes such as tyrosinase and GTP-cyclohydrolase I (GchI), the teleost toolkit appear to be increased in comparison with other vertebrates (Braasch et al., 2007) and the expansion in terms of genetic material

implicates also genes not directly connected to pigmentary mechanisms like those related to melanosome biogenesis (Braasch et al., 2009). These data support the idea of the strong relationship existing between the TSGD and pigmentation complexity in the teleost clade that could be at the base of subtle functional divergences (Braasch et al., 2007; Braasch et al., 2009). For instance, the expanded opsin complement of Pacific bluefin tuna could be instrumental to acquire new capabilities as perception of blue-green light in pelagic ocean (Nakamura et al., 2013). In summary, teleosts have a greater repertoire of "pigmentation genes" with respect to other vertebrates, probably due to the effects of TSGD and small-scale duplications, this caused several cases of sub-functionalization and neo-functionalization (Braasch et al., 2009).

In this work, the first comprehensive study on the Rab32/38 subfamily evolution in metazoans is reported, with a special focus on deuterostomes. In addition, the role during development of entire Rab32/38 toolkit present in genomes of two chordates: Mediterranean amphioxus (*B. lanceolatum*) and zebrafish (*D. rerio*) has been investigated. The majority of results here shown has been published on BMC Evolutionary Biology in 2016 (Rab32 and Rab38 genes in chordate pigmentation: an evolutionary perspective).

4.2 - Results

4.2.1 - Molecular evolution of Rab32/38 subfamily

In order to untangle the evolutionary history of Rab32/38 subfamily a survey was performed employing a manually selected database made of Rab proteins belonging to the whole of group III, according to classification recently proposed (Klopper et al., 2012), which are Rab32, Rab38, Rab7, Rab7L1, Rab9 and Rab23. Given the high degree of similarity characterizing all the small GTPases, the reconstruction did not

include short and uninformative sequences. The tree infers 247 amino acid sites and comprises 65 sequences from vertebrates (*Petromyzon marinus*, *Callorinchus milii*, *Lepisosteus oculatus*, *Latimeria chalumnae*, *D. rerio*, *Xenopus tropicalis*, *Anolis carolinensis*, *Gallus gallus*, *Mus musculus*, and *Homo sapiens*), urochordates (*Ciona robusta*), cephalochordates (*B. lanceolatum*), hemichordates (*Saccoglossus kowalevskii*) and echinoderms (*Strongylocentrotus purpuratus*); outside deuterostomes, we selected the mollusk *Lottia gigantea* and the polychaete *Capitella teleta*.
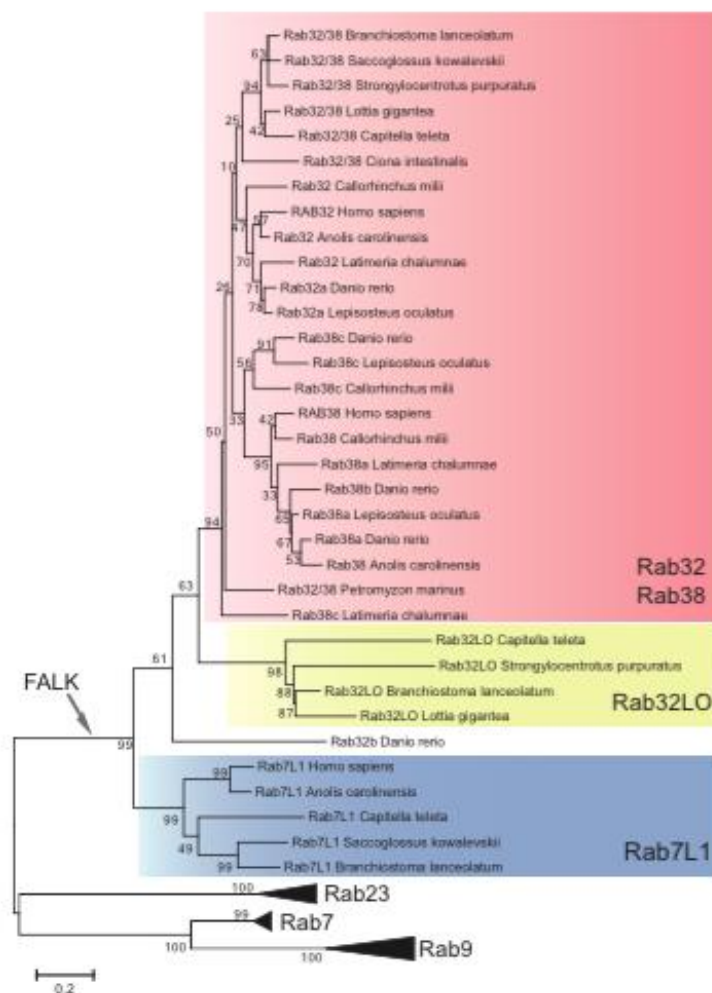
Figure 4.1. Phylogenesis of Rab group III focused on Rab32/38 subfamily. Maximum likelihood tree showing the existence of three phylogenetically robust classes inside Rab32/38 subgroup which are Rab32/Rab38 (red), Rab32LO (yellow), Rab7L1 (blue) which share FALK stretch.

The phylogenetic reconstruction clearly demonstrates the existence of four highly supported protein classes with Rab7, Rab9, Rab23 (collapsed in Figure 4.1) and Rab32/38. The latter is a phylogenetically robust Rab32/38 subgroup comprising three subfamilies (Rab32/38, Rab32LO, Rab7L1). In particular, Rab7L1 proteins constitute a sister class of Rab32LO and Rab32/38 groupages. The Rab32LO, previously called Rab32B (Elias et al., 2012), was found to be present from analyzed protostomes to amphioxus and absent in the urochordates and vertebrates, which together form the clade named Olfactores (Delsuc et al., 2006): for this reason, here it has been called Rab32LO (Lost in Olfactores). It is encoded by a gene already present in unicellular eukaryotes like the choanoflagellate *Capsaspora owcarzaki* and the early-branching animals such as the demosponge *Amphimedon queenslandica* and the sea anemone *Nematostella vectensis*: this speaks in favor of a gene loss after the split of the Olfactores. In the Rab32/38 grouping three distinct proteins are recognizable, Rab32/38 (protostomes, non-vertebrate deuterostomes) Rab32 and Rab38 (vertebrates). Concerning selected model species, amphioxus presents a single copy of Rab32LO and of Rab32/38, while zebrafish possesses two Rab32 (Rab32a, Rab32b) and three Rab38 (Rab38a, Rab38b, Rab38c), distinct from other gnathostomes like *H. sapiens* with just RAB32 and RAB38. Surprisingly, Rab32b of zebrafish is characterized by a position not consistent with canonical "tree of life" maybe for the occurrence of very fast evolutionary rate. Unfortunately, the Maximum Likelihood (ML) phylogeny here shown was not able to shed light on the evolutionary relationships between Rab32 and Rab38 of vertebrates, therefore a new vertebrate-dedicated tree including only vertebrate sequences plus an outgroup represented by *S. kowalevskii* Rab32/38 was constructed (Figure 4.2). Albeit some

low bootstrap values, the tree topology infers a common origin for the two vertebrate genes.

In synthesis, the survey regarding Rab32/38 genes and Rab group III highlights a very complex evolutionary history with the intervention of several events alongside tree of life, probably due to gene and genome duplications occurred mainly in vertebrates (WGDs), as shown by zebrafish extra-copy genes respect to other gnathostomes.
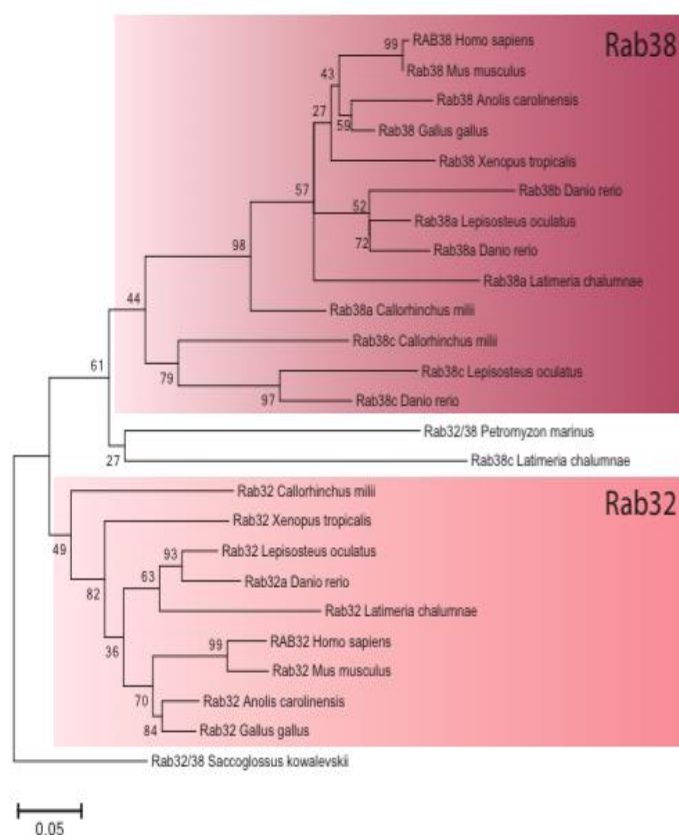
Figure 4.2. Phylogenetic tree of vertebrate Rab32/38 subfamily. ML phylogenetic tree dedicated to Rab32 (violet) and Rab38 (magenta) of vertebrates, with Rab32/38 of *Saccoglossus kowalevski* employed as outgroup; respect to vertebrates used for Fig. 4.1 survey, here has been added the amphibian *Xenopus tropicalis*.

4.2.2 - Analysis of main domains of Rab32/38 subgroup members

To comprehend the molecular changes occurred in the Rab32/38 subfamily, I aligned manually the members included in the phylogeny, focusing on three main domains

which allow Rab functioning, the guanine-binding motif (P-Loop), and Switch I and Switch II, crucial for the proper Rab conformational status (Park, 2013). Using the human RAB6A as reference (Park, 2013), I used a color code to evidence different domains: the green for P-Loop (20-27 aa), the turquoise for Switch I (38-49), the magenta for Switch II (69-81), while the changed residues are devoid of color (Figure 4.3). To have a more complete scenario about Rab32/38 protein conservation, I added to this survey the other human members of group III, the Rab7L1 present in the tree and one human representative for the remaining five groups. Concerning the Rab32/38, the degree of amino acid conservation is extremely high, spanning from protostomes to vertebrates. Though my alignment highlights the general conservation of G-domain core sequence alongside Rab evolution with the consensus GxxxxGKT(S), here it is demonstrated how the 2nd residue is diagnostic to discriminate between Rab32 (E, glutamic acid) and Rab38 (D, aspartic acid) proteins. The Rab32/38 exhibited an exceptional conservation also for Switch I (consensus FSxxYxxTIGVD) and Switch II (consensus DIAGxERFGxMTR) with some conserved modifications specific for Rab32LO class, from polychaetes to amphioxus. The retained "new" amino acids as two Histidines in the Rab32LO Switch II domain enforces the concept of its existence as different class inside group III. It is noteworthy the numerous modifications of zebrafish Rab32b, consistently with its divergent position in the phylogenetic analysis. For the first time, I observed the presence of ultra-conserved quartet downstream to Switch I (FALK, yellow) common to Rab32/38, Rab32LO and Rab7L1 supporting the monophyletic origin for all these classes within supergroup III, coherently with phylogenetic data (Fig. 4.1). Interestingly, the members of Rab32/38 subfamily are exceptionally conserved in particular if we concentrate our

attention on deuterostome clade. I focused on molecular peculiarities of the subgroup useful for evolutionary and, maybe, functional analyses.

Figure 4.3. Analysis of main functional domains of Rab32/38 subfamily. Here it is shown an analysis of three Rab domains from protostomes to vertebrates, hinting at an exceptional conservation of P-Loop (green), Switch I (turquoise) and Switch II (magenta). Using yellow, it has been evidenced a short ultra-conserved stretch (FALK) that is diagnostic for Rab32/38 subgroup members. To distinguish it from the rest of family, it has been added a human member for each Rab group.

4.2.3 - Rab32/38 conserved gene structure

With the aim to gain insights into the evolution of Rab32/38 subfamily members, I checked the splicing site conservation of genes belonging to this subfamily in distantly-related species. This type of information could be important for genome evolution investigations because the intron gain/loss is a rare and really slow phenomenon, if confronted with sequence protein modification that usually can affect phylogenetic reconstructions (Irimia and Roy, 2008). Using intron positions and phases represents a way for giving accuracy to evolutionary studies: it is an important instrument to evaluate common origin of genes, in order to surmount problems deriving from the signal-to-noise ratios of genomic and bioinformatics data (Irimia and Roy, 2008). For gene structure comparison, we selected genes from key species such as *L. gigantea*, *B. floridae*, *C. robusta* and *H. sapiens* whence came out a conservation of some splicing sites within subgroup genes (Rab32/38, Rab32LO, Rab7L1). In particular, observing the structure of invertebrate Rab32/38 genes and human Rab32 and Rab38 is clear the preservation of one intron in the Switch II domain: a possible evolutionary signature for the common origin for the whole protein class (Figure 4.4). Collectively, the analysis of intron/exon structures corroborates the hypotheses suggested by phylogeny and alignment on the evolution of vertebrate Rab32 and Rab38.

```
                                  Ancestral Intron
                                     phase 1
Lottia Rab32/38      VDFALKVLNWDSDTLIRLQLWDIA 1 GQERFGNMTRVYYKEAVGAFVVFDVTRA
Amphioxus Rab32/38   VDFALKVINWDADTLIRLQLWDIA 1 GQERFGNMTRVYYKEAVGAFVVFDVTRA
Ciona Rab32/38       VDFALKVVHWDGETLIRLQLWDIA 1 GQERFGNMTRVYYREAVGAFIVFDATRA
Human Rab32          VDFALKVLNWDSRTLVRLQLWDIA 1 GQERFGNMTRVYYKEAVGAFVVFDISRS
Human Rab38          VDFALKVLHWDPETVVRLQLWDIA 1 GQERFGNMTRVYYREAMGAFIVFDVTRP
```

Figure 4.4. Intron conservation inside Rab32/38 subfamily. Recostruction inferring the existence of a conserved intron (yellow) amongst Rab32/38, Rab32 and Rab38 genes retained after a vertebrate duplication. Switch I (partial) and Switch II domains are underlined.

4.2.4 - Rab32/38 conserved synteny in Gnathostomata

For better understanding the evolution of Rab32/38 members, I searched the degree of conservation surrounding these genes in the available deuterostome genomes. It has been performed a detailed search in four invertebrate genomes (*S. kowalevskii*, *S. purpuratus*, *B. floridae*, *C. robusta*) and, amongst vertebrates, in lamprey *P. marinus* for the agnathans, in elephant shark *C. milii* and spotted gar *L. oculatus* as non-teleost fish representatives (Venkatesh et al., 2014; Amores et al., 2011), *D. rerio* for teleosts, the lizard *A. carolinensis* in the Sauropsida clade, and *H. sapiens* and *M. musculus* as mammals. Concerning protostomes and non-vertebrate deuterostomes, there was no synteny in the *Rab32/38* genomic *locus* from mollusks to tunicates while, limited to sea urchin and amphioxus scaffolds, there was a microsyntenic preservation involving *Rab32LO* and *Tim9*, a widespread transporter known for its role in mitochondria traffic of mammals (Muhlenbein et al., 2004). Moreover, the chromosomal organization of genes belonging to invertebrates and vertebrates was not conserved. On the other hand, the situation in gnathostomes was totally different: in fact, both *Rab32* and *Rab38* neighbouring genes, respectively, presented a very high syntenic degree from fishes to human (Figure 4.5). The unique lamprey gene included in our analysis did not show any synteny. Employing ML phylogenies has indicated the orthology in vertebrates of genes flanking *Rab32/38 loci* that belong to big families as *Tab*, *Nox*, *Fzd* and *Stxbp* (data not shown), apart the conservation in all the chromosomes of different single-copy genes. The conserved triplet formed by *Rab38*, *Tyr* and *Grm5* was already registered in teleosts and human (Braasch et al., 2007) but this survey represents undoubtedly an improvement of the knowledge about this genomic region of vertebrates. In fact, it covers more species encompassing the reptile anole lizard, the rodent house mouse and key

representatives of non-teleost fish which are the holocephalan *C. milii* and the gar *L. oculatus*, showing the preservation of chromosomal order in gnathostome clade.
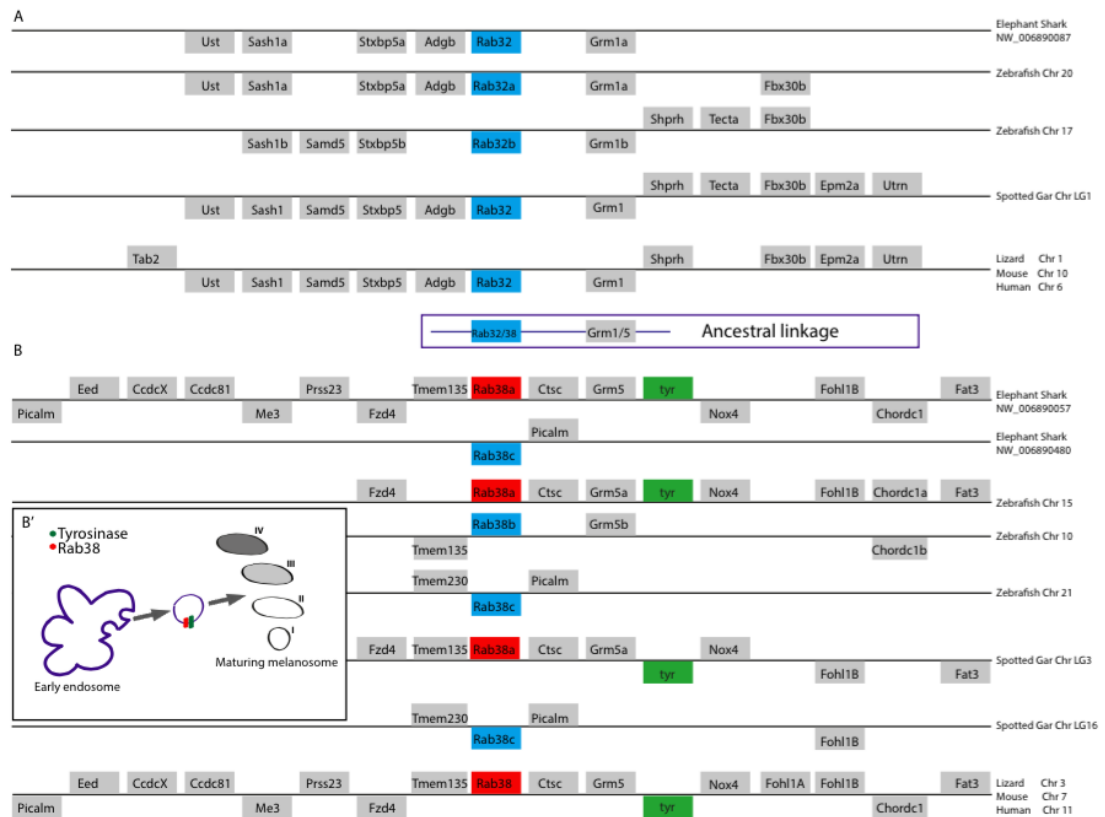
Figure 4.5. Paralogon conservation in gnathostome's Rab32/38 subfamily. The Rab32 (A) and Rab38 (B) loci harbour several conserved genes (grey boxes) across evolution; in blue boxes Rab genes we analyzed, in red boxes Rab38 genes that are physically linked to tyrosinase (green). The Rab32 is always linked to Grm1, while Rab38 is linked to Grm5. The scheme 3B$^{'}$ shows the functional relationship between Rab38 and Tyr during mammalian melanosome biogenesis (adapted from Bultema and Di Pietro, 2013). Genes represented above or below chromosomes (horizontal line) indicate their transcriptional orientation on positive or negative strand, respectively.

Additionally, I unraveled the presence in all the surveyed vertebrates of a physical linkage between *Rab32* and *Grm1* genes, similar to the retained couple *Rab38-Grm5*. The Glutamate metabotropic receptors (Grm) belong to C family of G-protein-coupled receptors (GPCRs) and are implicated in several processes and pathologies, in fact *Grm1* is a melanoma oncogene (Namkoong et al., 2007; Shin et al., 2008) whereas *Grm5* is involved in many diseases such as autism and schizophrenia

(Skafidas et al., 2014; Fatemi et al., 2013). These findings support the existence of an ancient chromosomal linkage composed by *Rab32/38* and *Grm1/5* genes in the ancestor of vertebrates, as suggested by a dedicated phylogenetic tree of *Grm* family where is clear the orthology between *Grm1* and *Grm5* vertebrate genes (Figure 4.6). Focusing on zebrafish *loci*, I noticed an interesting situation for Rab38 paralogues: there is more preservation in terms of gene number and organization around *Rab38a* than in the loci of *Rab38b* and *Rab38c*; coherently, a major conservation affects just one of two *Rab38* paralogons of elephant shark and spotted gar (Fig. 4.5B). The same paralogon, curiously, harbors not only *Rab38/38a* genes but also the unique *tyrosinase* copy present in vertebrate genomes.
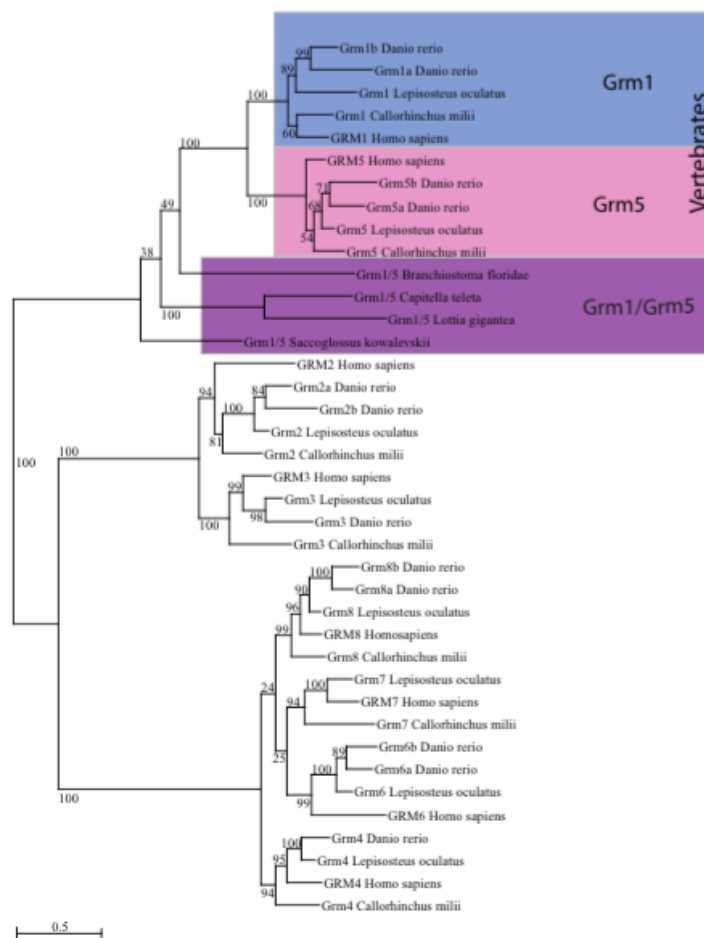
Figure 4.6. Phylogeny of Grm family. ML phylogenetic tree evidences three related well-supported classes inside Grm family: the two vertebrate-specific Grm1 (blue) and Grm5 (pink) that derive from invertebrate ancestor Grm1/5 (violet).

Moreover, the tetrapod's chromosomes show tandem-duplications of folate hydrolase 1 (Fohl1) and Coiled-coil domain containing protein (Ccdc): in particular the second one involves members of a large family whose function is completely obscure. In the *Rab38 loci* of mammals, I recognized a peculiar mass of specific receptors inserted between Fohl1 duplicates, probably originated by distinct repeated duplicative events in tandem. The mouse chromosome 7 presents a series of fifteen *Vomeronasal 2 receptors* (*Vmn2r*) belonging to a family whose members are central to mouse ultrasensitive chemodetection, a decisive skill for rodents (Leinders-Zufall et al., 2014). Nearby lie fourteen olfactory receptors (*OR*), which are comprised into one of the largest family in the mouse genome that have been linked to its exceptionally well-developed capability to discern odours (Godfrey et al., 2004). The orthologous region of human chromosome 11 is characterized by seven tripartite motif proteins (*TRIM*): associated to a myriad of mechanisms, their most studied role is the response to interferons during immunity (Carthagena et al., 2009). All the sequences employed for phylogenetics are listed in Supplementary Table 4.1. Syntenic data not inserted in Fig. 4.5 are shown in Supplementary Table 4.2.

In synthesis, synteny data hint at very high degree of chromosomal conservation in Gnathostomata and are consistent with my supposition regarding a common evolutionary origin for Rab32 and Rab38 genes which probably have been originated through WGDs involving vertebrates.

4.2.5 – *Rab32/38* expression pattern in amphioxus and zebrafish

For adding information to knowledge about the role during development of *Rab32/38* genes in chordates, we studied the expression profile of subfamily members present in amphioxus and zebrafish genomes. The first step was to clone

Rab32/38 and *Rab32LO* of Mediterranean amphioxus and test their expression pattern during embryogenesis through whole mount *in situ* hybridization (WISH) using riboprobes on embryos at different developmental stages. Unfortunately, *Rab32LO* transcript was not detectable by WISH experiments and, it has been confirmed also by its extremely low expression levels came out from RT-PCR experiments (Supplementary Table 4.3). By contrast, the ortholog to *Rab32/38* gene, expressed specifically in *C. robusta* pigment cells (Racioppi et al., 2014), is present along whole *B. lanceolatum* development in distinct territories (Figure 4.7). The presumptive notochord territories of the gastrula stage show *Rab32/38* localization: a signal that becomes stronger in formed notochord during neurula stage and is present alongside the anterior part of the embryo, without marking the caudal region (Fig. 4.7A, B, C). Additionally, transverse vibratome sections endorsed Rab32/38 presence in amphioxus notochord (Fig. 4.7D). Indeed, in the pre-mouth larvae the signal in notochord is absent whereas is clearly marked a territory comprised in the pharynx region (Fig. 4.7E). The gene expression seems to be absent from amphioxus pigmented territories as dorsal ocelli or frontal eye (Fig. 4.7). Moreover, RT-PCR demonstrated high expression of Rab32/38, particularly at gastrula stage (Suppl. Table 4.3).
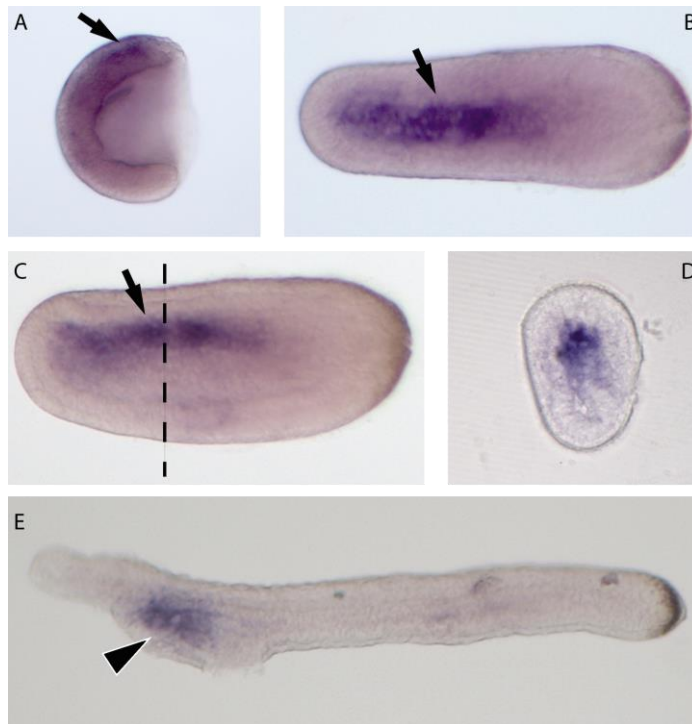
Figure 4.7. Expression pattern of *Rab32/38* during amphioxus embryogenesis. The gene is present in notochord presumptive territories at gastrula stage (A, black arrow) persisting at the neurula, mainly in the rostral part (B-C, black arrow). D represents a vibratome section (15 μm) of the neurula specimen shown in B-C, at the level of the vertical dashed line. In pre-mouth larvae, there is only a positive signal in the pharynx region (E, arrowhead).

Then, I applied the same approach to the *Rab32* and *Rab38* genes of zebrafish (Figure 4.8, 4.9), amplifying them in order to prepare riboprobes for WISH experiments. I was not able to amplify *Rab32b* gene starting from cDNA from several developmental stages and adult tissues such as eye and brain probably because its expression is very low or depends on peculiar physiological or environmental conditions. *Rab32a* transcript is present from early developmental stage of shield (6 hours post-fertilization, hpf) in the presumptive posterior axial mesoderm with a strong signal (Fig. 4.8A: as already described in the ZFIN database by Thisse et al., 2001). When embryo elongation occurs (tailbud stage, 8hpf), gene expression was detected in a region in the proximity of the animal pole constituting a longitudinal band in the dorsal midline, that represents the forming notochord and

comprises also the tail bud (Fig. 4.8B). In addition, 8hpf embryos show a strong signal in a structure located at the back of the yolk, named Kupffer's vesicle (Fig. 4.8B), a small epithelial sac belonging to phylotipic yolk extension (YE), which works as a transient embryonic "organ of asymmetry" regulating left-right development through a directional fluid flow (Virta and Cooper, 2011). During the segmentation process (24 hpf), *Rab32a* expression decreases in the notochord whilst becomes to be visible in the developing retinal pigmented epithelium (RPE) eye and in the neural crest-deriving melanoblasts which are migrating to their definitive position (Fig. 4.8C-F). At the long-pec stage (48 hpf), signal in melanoblasts results to be absent, persisting in the RPE and notochord, whereas it appears clearly in the swim bladder (Fig. 4.8G, H); this territory is marked up to 72 hpf , the protruding-mouth larva stage (Fig. 4.8I, J). This structure is an ultra-specialized teleost gas-filled organ employed for important functions as buoyancy, sound perception and, in some lungfishes, this organ is evolved in a sort of tetrapod-like lung.
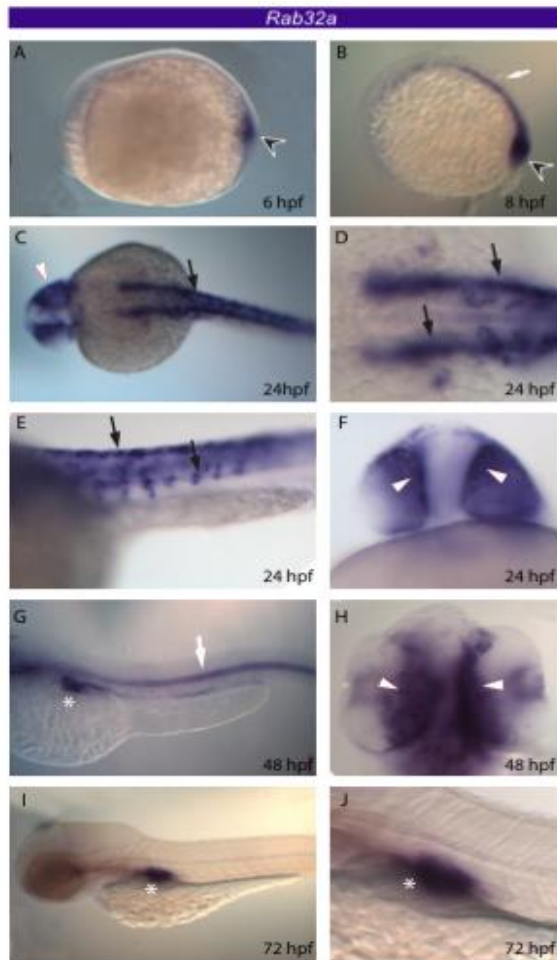
Figure 4.8. Expression pattern of zebrafish *Rab32a* during embryogenesis. The gene marks the posterior axial mesoderm (arrowhead) at 6 hpf (A), the developing notochord (white arrow) and Kupffer's vesicle (arrowhead) at 8 hpf (B). At 24 hpf, it has been observed in RPE (white arrowhead), notochord and migrating melanoblasts (black arrows) (C-F). At 48 hpf the signal persists in RPE and notochord (white arrows) (G-H) and appears in the swim bladder (G, white asterisk) up to 72 hpf (I-J, white asterisk).

The *in situ* hybridization experiments allow to me localize each *Rab38* during zebrafish embryogenesis (Fig. 4.9). *Rab38a* is present across the entire pharyngula embryo period, i.e. from 24 to 48 hours post-fertilization. Throughout segmentation, the embryos show a weak signal in RPE cells while migrating neural crest cells (probably melanoblasts) are strongly labeled and, a faint expression has been detected in the mid-ventral brain region. Successively, among pigmented territories only the RPE keeps a clear signal at 48 hpf (Fig. 4.9 A-D). The other two *Rab38* paralogues were not expressed in precursors of pigment cells. *Rab38b* was expressed

only in late embryogenesis: at 48 hpf close to pharyngeal arch and mark the natatory

vesicle whereas at 72 hpf exclusively in the buoyancy organ (Fig. 4.9 E-H). *Rab38c*

is characterized by a strong expression in the head region lasting from 6 to 72 hour

post-fertilization (Fig. 4.9 I, J).
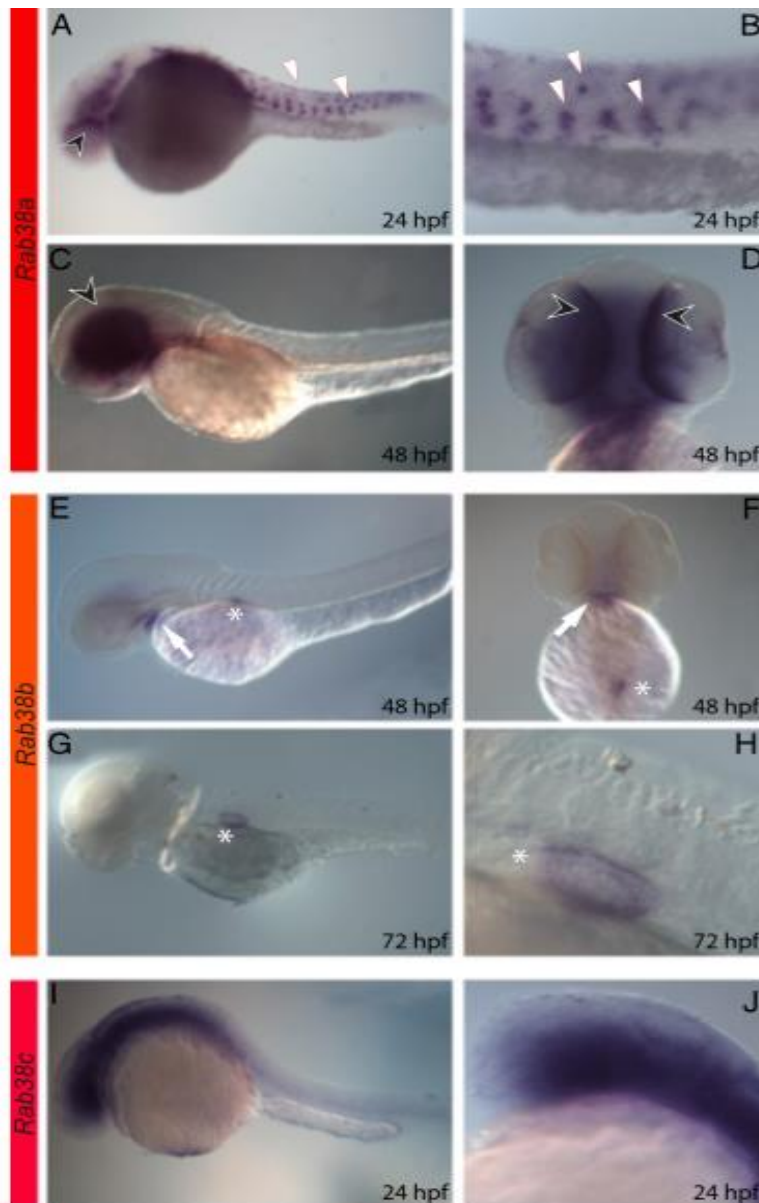
Figure 4.9. Expression profile of zebrafish *Rab38* genes during embryogenesis. *Rab38a* is present from 24 to 48 hpf stages, faintly in RPE and strongly in migrating neural crest cells (A-D); *Rab38b* is expressed in pharyngeal arches and natatory vesicle at 48 hpf stage with the latter persisting up to larva stage (E-H); *Rab38c* transcript has been observed with a signal in cephalic region (here shown at 24 hpf stage, I-J).

In short, from this study on the expression profile of *Rab32/38* genes in amphioxus and zebrafish come out scenario characterized by the presence of them in different embryo territories: it can represent an occasion for numerous evolutionary considerations.

4.3 - Discussion

4.3.1 – Rab32/38: a complex evolutionary scenario

Using different tools, we have contributed to the knowledge of *Rab32/38* genes history of within the group III, considered as a population of Rabs specialized in lysosomal and late-endosomal trafficking (Klopper et al., 2012). The ML phylogenetic tree clarifies the evolution of Rab group III, indicating the presence of four phylogenetically robust classes, with the existence of one (here called only "Rab32/38") composed by Rab32/38, Rab32LO and Rab7L1 subfamilies which shows a different molecular history respect Rab23, Rab7 and Rab9 protein classes. Moreover, this survey puts in order several nomenclature cases due to patchy nomenclature present in current literature (Elias et al., 2012; Klopper et al., 2012).

Phylogenetic analysis highlights the common origin of invertebrate's Rab32/38 and Rab32LO, already named Rab32A and Rab32B (Fig. 4.1). They are considered as fundamental genes for eukaryotic cell, in fact they represent an ancient couple of paralogues that emerged in the LECA ancestor where they were already connected with the improvement of post-Golgi trafficking (Elias et al., 2012). Particularly interesting is the case of Rab32LO protein, whose name derives from its evolutionary loss in all the Olfactores, the clade combining tunicates (larvaceans, appendicularians, ascidians) and vertebrates (Delsuc et al., 2006). This protein class has been identified in several species from unicellular eukaryotes to deuterostomes

(Elias et al., 2012) and, in particular, the genome search highlighted its presence in early-divergent animals like sponges (*A. queenslandica*), cnidarians (*N. vectensis*) and also other invertebrates. Curiously, in deuterostomes Rab32LO has been maintained only by sea urchin and by amphioxus, the unique chordate possessing this LECA gene; the reasons of this presence/absence should be investigated. In fact, WISH and RT-PCR experiments do not shed light on its developmental localization, leaving open questions about its functioning (Fig. 4.7, Suppl. Table 4.3). Describing its expression in other invertebrates would be very important, mainly if we consider its absence in all the Olfactores that could be related to the loss of peculiar biological functions alongside chordate evolution. However, phylogenetic reconstruction places definitively Rab7L1 (7-like-1) in the Rab32/38 subgroup. Sometimes wrongly named as Rab29 (Elias et al., 2012), an ancient group III member lost during metazoan evolution, Rab7L1 is a protein responsible for specific steps of post-Golgi transportation dynamics. In cohabitation with LRRK2 (Leucine-rich repeat kinase 2), it acts as a key regulator of retrograde trafficking for recycling different proteins on the route between lysosomes and Golgi apparatus in a process crucial for axonal morphology maintenance (Kuwahara et al., 2016). Besides, Rab7L1 is implicated in many human pathologies and it is thought to be a marker for Parkinson's disease (MacLeod et al., 2013; Khaligh et al., 2017).

To provide information about the evolution of Rab32/38 subgroup, the key Rab domains have been mapped, comparing them also with human representatives of members belonging to same group (Rab7, Rab9, Rab23). The most important result that emerges is represented by the presence of ultra-conserved FALK in each branch of the subgroup, enforcing the concept of a common origin for *Rab32/38*, *Rab32LO* and *Rab7L1* genes. This stretch, located downstream of Switch I domain, has been

retained by all the members after the separation from Rab7, Rab9 and Rab23 subfamilies. Then, its existence in other invertebrates sequences allows to hypothesize that FALK confers to these Rabs specific functional capabilities that should be understood (Fig. 4.1; Fig. 4.3).

A further point is the presence in the functional domains of some key residues considered as "diagnostic" to recognize some proteins. For instance, two conserved Histidines (H) within Switch II functional domain are present in all the Rab32LO here shown (Fig. 2.3). Indeed, the alternation between glutamic acid (E) and aspartic acid (D) at the second element of P-Loop led to distinguish between Rab32 and Rab38 of vertebrates. The domain survey evidences the number of changes of zebrafish Rab32b that is consistent with its tree position, demonstrating its fast evolutionary rate. Interestingly, a preliminary genome search in many fish genomes has unraveled that Rab32b fast evolutionary rate characterizes the entire teleost clade, even if this gene has been retained in a restricted number of species; similarly, Rab7L1 is present only in few teleost species and is absent in *D. rerio*. On the other hand, the remaining classes (Rab32a, Rab38b, Rab38c) are present in all the teleosts surveyed (data not shown).

Phylogeny and domain alignment partially solved the question about the origins of Rab32 and Rab38, probably due to heterogeneous evolutionary rate of the subfamily. Although a weak phylogenetic signal, the most parsimonious hypothesis emerged is that Rab32 and Rab38 separated at the root of vertebrates, by a whole-genome duplication event (Dehal and Boore, 2005). A manual evaluation of subfamily intron/exon structure supports this concept: comparing Rab32/38 of some invertebrates and human Rab32 and Rab38 is visible the presence of an ancestral "phase 1 intron" inside Switch II domain, evidence for of common origin for these

genes (Fig. 4.4). Moreover, investigating Rab7L1 and Rab32LO splicing site conservation, we identified other introns shared with Rab32/38, Rab32 and Rab38 genes, suggesting the existence of a common intron code for the entire subgroup (Fig. 3.3)

A further relevant element to evaluate subfamily evolution is the analysis of Rab32/38 *loci* alongside deuterostomes. I did not find any synteny between vertebrates and invertebrates chromosomes harbouring Rabs; indeed, there is a preserved gene couple formed by Rab32LO and the mithochondrial transporter Tim9 that is visible in sea urchin and amphioxus (Supplementary Table 4.2). Apart proving definitely the homology among Rab32LO of invertebrates, the Rab32LO-Tim9 gene pair could represent an evolutionary signature of an ancient microsynteny possibly due to the existence of a coordinated transcription or of a putative genomic regulatory block (GRB) between them (Irimia et al., 2012). By contrast, I discovered exceptional syntenic conservation in gnathostomes for genes surrounding both Rab32 and Rab38, respectively (Fig. 4.5). Orthology among neighbouring genes has been shown using dedicated phylogenetic trees (data not shown). This paralogon's preservation of such diverse genes evokes the presence of a specific genomic element which could act as enhancer in the vertebrates. The great conservation among vertebrates is emphasised by *C.milii Rab38a* and tetrapod *Rab38* loci, confirming the extraordinary similarity between the Chondrichthyes and tetrapod genomes (Ravi et al., 2009). Nevertheless, the *Rab38a* locus of *L. oculatus* (chr LG16) and *D. rerio* (chr 15) totally lacks synteny on just one side indicating clearly a genomic rearrangement event in the Actinopterygyans, with the replacement of genes like *Prss23*, *Eed*, *Ccd81* and *Me3* on LG17 chromosome of spotted gar and their scrambling in zebrafish genome.

Interestingly, the presence in all the surveyed gnathostomes of two ultra-conserved couples, Rab32-Grm1 and Rab38-Grm5, speaks in favor of an ancestral duplication of a chromosomal region. The most parsimonious explanation consists of a parallel history for two ancestral genes *Rab32/38* and *Grm1/5* pre-dating the last common ancestor of jawed vertebrates, coherently with a whole-genome duplication in the clade (Dehal and Boore, 2005) which have formed two ohnologues for both the ancestors: a result corroborated by a phylogeny of the *Grm* genes (Fig. 4.6). This microsynteny conserved from elephant shark to mammals could reflect functional correlation in the cell, but this needs to be investigated. Synteny, together with phylogeny and intron organization, hints at 1R or 2R as large-scale duplicative events originating the ohnologues *Rab32* and *Rab38* found in all the vertebrates. More in depth, it is evident that duplication events have influenced the Rab32/38 subfamily member number in zebrafish, with two Rabs32 and three Rabs38, probably impacting on the acquisition of new roles during development by these genes as suggested by WISH experiments. Compared to tetrapods, teleosts show more duplicates as consequence of TSGD (Taylor et al., 2001; Taylor et al., 2003; Hoegg et al., 2004; Kuraku et al., 2009) but this justifies the presence of just one additional Rab32 and Rab38: whereas three paralogues have been detected in zebrafish (*Rab38a*, *Rab38b*, *Rab38c*). The first and the third ones are present in the genomes of each analyzed fish, while *Rab38b* is possessed solely by teleosts. Interestingly, the presence in early-branching fishes (elephant shark, spotted gar), in coelacanth (*Latimeria chalumnae*) and amphibians (*Xenopus tropicalis*) of the *Rab38c* with conserved neighbouring genes (*Tmem*, *Picalm*) proposes questions about its origin. It represents a product of a gene duplication occurred at the stem of sarcopterygian lineage subsequently lost in "upper" vertebrates, otherwise, the result

of a genome duplication more ancient than TSGD, i.e. the 2R event. This concept is enforced also by the presence, on both spotted gar Rab38 spotted gar loci of Fohl1 duplicates. Then, it has been established the rising of Rab32, Rab38 (1R) and Rab38 (2R) and this suggests the existence, in the vertebrate ancestor, of a fourth Rab member originated during 2R event, now lost in vertebrate's lineage. Moreover, in the same place of mammalian Rab38 genomic *loci* there are large insertions with diverse genes between human and mouse, it would be interesting to analyze this region in other mammals.

Additionally, an evolutionary survey performed using Rab32/38 proteins belonging to several teleosts highlighted the retention of *Rab32a*, *Rab38a*, *Rab38b* and *Rab38c* in all the selected species, whereas Rab32b has been lost by several teleosts (Supplementary Table 4.4). This information helps to establish their WGD/TSGD-origin because is diffused the assumption according to which occurs a maintenance of whole-genome duplicates in multicellular organisms while are easily lost genes produced through more local duplications (Putnam et al., 2008; Braasch et al., 2009) Here we showed for the first time the expression in developing pigment cells of the genes *Rab32a* and *Rab38a*, already hypothesized to be part of the "vertebrate pigmentation genes" list (Braasch et al., 2009). It is thought that duplications intervened at different levels (gene network, tissue, cell type) represent a platform for the origin of evolutionary novelties (West-Eberhard, 2003) and it has been suggested there is a tight relationship between vertebrate's genomic duplications and their pigmentation genetic repertoire, with an increase of this connection in teleosts (Braasch et al., 2009). Therefore high rate of retention involving "pigmentation genes" after small-scale and extensive genome events is considered as one of the most influencing factors in the evolution of extraordinary variety of teleost's body

coloration (Braasch et al., 2009). In fact, the big teleost repertoire of genes involved in pigmentation has been phylogenetically connected to "colour innovations" dating back in the teleost lineage, as in the case of leucophores (Braasch et al., 2008). These data fit perfectly on scenario already hypothesized (Braasch et al., 2009), because *Rab32* and *Rab38* belong to "melanosome biogenesis class" of genes involved in pigmentation and their duplicates follow the retention scheme observed in other teleost's genes, for this grouping, the sixty percent. In particular, *Rab32* and *Rab38* are encompassed in the "TSGD-Duplicated Teleost Pigmentation Genes", which totally are 30 % more than those present in classical tetrapod models as mouse and chicken (Braasch et al., 2009). Interestingly, the Rab32/38 subfamily expansion is consistent with the duplication of several genes fundamental for pigmentation *Mitf*, *Kitl* and *Tyrp*, registered in teleosts (Braasch et al., 2007; Braasch et al., 2009). For instance, another "pigmentary expansion" has been described in medaka (*Oryzias latipes*) opsins, proteins widespread in metazoans which are fundamental for vision (Matsumoto et al., 2006; Trezise and Collin, 2005). This survey about two Rabs implied in melanosome formation, supports the effects of TSGD and gene duplications on main pigmentation pathways active in the pigment cells (Braasch et al., 2007). Hence, it seems clear a decisive role in "pigmentation expansion" not only for "classical" genes (enzymes, transcription factors) but also those involved in trafficking phenomena as Rabs. Finally, my reconstruction pinpoints the Rab32 and Rab38 duplications in a complex scenario of genomic events through teleosts have implemented their pigmentary capabilities even if, the different embryonic localization of *Rab38b* and *Rab38c* prompted me to conjecture a neofunctionalization process.

In light of this, the ultra-conserved physical linkage existing between a couple of genes involved in pigmentary dynamics (*Rab38* and *tyrosinase*) it is noteworthy (Fig. 4.5B[I]). For melanogenesis, the delivery of tyrosinase family members (Tyr, Tyrp1, Tyrp2) is pivotal, i.e. their proper transportation to melanosomes during their maturation represents a mandatory step. The ohnologues Rab32 and Rab38 are considered as vital players in the Tyr and Tyrp transport to LROs by specialized vesicles, modifying the ubiquitous "classical" lysosomal machinery (Bultema and Di Pietro, 2013). Interestingly, *Rab32* and *Rab38* are partially redundant in terms of function, with the latter that seems primarily implicated in Tyr transport in melanocytes (Bultema et al., 2012). This, together with retained chromosomal proximity and the fact that zebrafish *Rab38a* is the unique *Rab38* paralogue expressed in pigment cells, leads me to propose a model for which the genetic linkage is linked with the co-working of Rab38 and Tyrosinase in the pigment cells based on a common transcription during development. It means the possibility of bystander gene regulation (Cajiao et al., 2004) in all gnathostomes with functional consequences related to pigmentation process: taking into consideration the hundreds of microsyntenies conserved in metazoans regarding unrelated genes (Irimia et al., 2012), is not trivial the speculation of a bystander modality control of transportation concerning melanosome biogenesis pivotal players.

4.3.2 – *Rab32/38* subfamily expression: evolutionary implications

These data can represent a tool for understanding the impact of evolutionary events as gene and genome duplications on the role of *Rab32/38* subfamily members during development, with a focus on pigment cells. In mammals, the involvement of these genes in melanogenic dynamics is reflected by their expression profile, in fact *Rab32*

and *Rab38* are expressed in mouse melanocytes (Cohen-Sohal et al., 2003; Osanai et al., 2005). By contrast, Rab32 is present also in platelets and mast cells and Rab38 in the epithelial cells of lung (Cohen-Sohal et al., 2003; Zhang et al., 2011). In *D. rerio*, we identified transcript localization in developing pigment cells for *Rab32a* and for *Rab38a* paralogues. Both are expressed in ocular RPE cells of the eye and in the skin melanocytes deriving from neural crest, even if they seem to mark distinct populations of migrating melanoblasts (Fig. 4.8, 4.9). Their presence in embryonic precursors of pigment cells is consistent with other vertebrates, as mouse and frog (Osanai et al., 2005; Park et al., 2007). Extending preliminary data (Thisse et al., 2001), we shed light on *Rab32a* expression in notochord from 6 to 48 hpf (Fig. 4.8) with a signal that probably represents a zebrafish peculiarity, inside vertebrates. In support of this, Rab32a together with H(+)-ATPase has been shown to be fundamental for the proper biogenesis of zebrafish notochord vacuoles described as ultra-specialized LROs (Ellis et al., 2013). During late embryogenesis this gene is present in swim bladder or natatory vesicle, an organ evolved by teleosts for buoyancy regulation and characterized by many differences across species. This kind of expression is very interesting, mainly taking into account that in lungfishes this organ has been modified probably to become similar to lungs of tetrapods (Torday and Rehan, 2004), where *Rab32* expression is known (Cohen-Sohal et al., 2003). As aforementioned, zebrafish shows highly diversified spatio-temporal scenario for *Rab32* and *Rab38s* that is related to distinct genomic events that occurred during vertebrate evolution, particularly in the teleost clade. Three Rab38 paralogues are a good example of divergent expression profiles: while *Rab38a* is expressed chiefly in pigment cells, *Rab38b* marks at late developmental stages the pharyngeal arches and swim bladder and *Rab38c* in the head region from early embryogenesis (Fig. 4.9).

This represents an interesting case of functional differentiation driven by the formation of new paralogues through genome-wide changes. The presence of a sole member in pigmented territories mimics the pattern of other genes implicated in pigmentation dynamics, with the evolutionary specialization of a single representative for this kind of function (Braasch et al., 2009). Considering the whole-genome events as TSGD as a source of new genetic equipment exploitable for evolution, my work places Rab32/38 subfamily expansion in a scenario of increased pigmentary capabilities in teleost (Braasch et al., 2007; Braasch et al., 2009). Rab38c appears very interesting because it represents a 2R-gene lost in terrestrial tetrapods whose expression is in the central nervous system. Surprisingly, here it is reported the probable ancient vertebrate expression that suggests an involvement in nervous system development. It would be interesting to shed light on the functional impact of this gene loss in mammals and what could have captured its function: for instance, related Rabs as 32 and 38.

 It is possible to predict a sub-functionalization event for Rab38 paralogues (Force et al., 1999), with the subdivision of ancestral function among duplicates. For instance, the *Rab38b* expression in zebrafish pharyngeal arches can be compared to expression of *Rab32/38* gene in amphioxus pharynx unveils a possible ancient function which tetrapods have lost (Fig. 4.9 E, F; Fig. 4.7). Surprisingly, amphioxus Rab32/38 is not expressed in precursors of pigment cells (Fig. 4.7), differently from its invertebrate orthologues of nematodes, flies and tunicates: this allows to hypothesize the loss of pigmentation function for amphioxus. Another Rab could do the pigment function in place of Rab32/38, maybe Rab32LO and Rab7L1 or other Rabs belonging to same group. Given its low expression level, Rab32LO is not a good candidate but expression data from other invertebrate's Rab32LO could gain insights in its role. In

this way it will be possible to shed light on the functionality lost by Olfactores and on the amphioxus pigmentation dynamics. The conserved expression of *Rab32/38* genes in pigment cells of many invertebrate and vertebrate representatives indicates clearly a preservation of central role in melanogenesis. Collectively, functional experiments performed in protostomes and in the one of nearest living relatives of vertebrates, the ascidian *C. robusta* (Racioppi et al., 2014) and my data on zebrafish Rab32a and Rab38a evoke Rab32/38's ancestral implication in melanogenic dynamics retained in vertebrate's ohnologues, with potential "deviations" due to genomic events in other ohnologues.

CHAPTER 5

Cr-Klhl21: a new player in pigmentation from ascidian *Ciona robusta*

5.1 - Background

Pigmentation in animals depends on a plethora of pigment cell types and represents a fascinating theme to investigate. The majority of information regarding pigmented cells has been collected in vertebrates, partly driven by the relationship existing between melanogenic genes and human diseases (Goding, 2007). However, more recently some effort has been dedicated to study Rab family in protostomes and non-vertebrate deuterostomes. As aforementioned, the most widespread pigment in animal kingdom is melanin and some invertebrates present melanized cells containing melanosomes, lysosome-related organelles (LROs) responsible for pigmentation dynamics, as shown by rudimentary melanosomes observed in cuttlefish (Fiore et al., 2004). Although showing a highly divergent body plan, tunicates are the closest living vertebrate relatives and, therefore, the paraphyletic group of ascidians, such as *Ciona,* are powerful models (Delsuc et al., 2004). The sea squirt *Ciona robusta* is characterized by two melanin-containing sensory organs, the otolith and ocellus (Dilly, 1969; Eakin and Kuda, 1971). They are located in the sensory vesicle, a structure suggested by some authors to be homologue to the forebrain present in vertebrates (Moret et al., 2005; Dufour et al., 2006; Ikuta and Saiga, 2007). The otolith, sited in the anterior region of the sensory vesicle, is formed by a single specialized cell whose body is the statocyte, containing a large melanin granule. The statocyte is connected to the sensory vesicle ventral floor by a clenched stalk. The otolith body is connected to the sensory vesicle by two dendrites able to sense pigment granule movements through their deformation (Otsuki, 1991); these

features enable larvae to perceive gravity (Tsuda et al., 2003). Conversely, the ocellus is a more complex structure: it is formed by three lens cells, about thirty photoreceptors and one cup-shaped melanized cell (Horie et al., 2005). The photoreceptor cells are localized in the right side of sensory vesicle, their axons cross the midline of the larval sensory cavity whereas photoreceptor external segments cross the entire pigmented cell (Horie et al., 2005). Three lens cells are present in the ocellus although their homology with vertebrate lens cells is not demonstrated (Shimeld et al., 2005). Despite the exact role of the melanized cell in the ocellus has not been well studied the pigment granules are possibly involved in two pivotal functions for larvae, i.e. light filtration and the protection of the posterior photoreceptors (Tsuda et al., 2003). Researchers have found many molecular similarities between vertebrates eyes and ascidians ocellus, with a high degree of conservation in terms of genetic machinery. For instance, the *Rx* gene, whose mutation in mouse produces total eye absence (Bailey et al., 2004), has a pivotal role for ocellus development and function in *C. robusta* (D'Aniello et al., 2006). Another example is given by the *Pax6* gene, indispensable for pigment cell development both in tunicates and vertebrates (Callaerts et al., 1997). Moreover, mediators of vertebrate photo-transduction (Arshavsky, 2002; Blomhoff and Blomhoff, 2006), i.e. visual Opsins (G-protein coupled receptors) and visual Arrestins (opsin regulators), have been found to be expressed mainly in photoreceptors of ocellus. They show degree of sequence conservation with vertebrate counterparts (Kusakabe et al., 2001; Nakagawa et al., 2002; Nakashima et al., 2003). Regarding melanogenesis, the expression and regulation of tyrosinase family members during *Ciona* embryogenesis (Sato et al. 1997; Esposito et al., 2012) have been clarified, as well as their role in evolutionary loss of pigmentation in two distantly-related species of

Molgulids (Racioppi et al., 2017). The presence of six FGFs and only one FGF receptor in the *Ciona* genome (Satou et al., 2002) has encouraged the analysis of their role in tunicate ontogenesis. Recently, it has been elucidated the FGF role in the pigment cell determination of *C. robusta* (Squarzoni et al., 2011): its signaling governs pigment cell identity in the a9.49 lineage influencing the specific expression of some pigmentation markers and several factors never associated to pigmentation (Figure 5.1, Racioppi et al., 2014), as *Cr-Klhl21*.
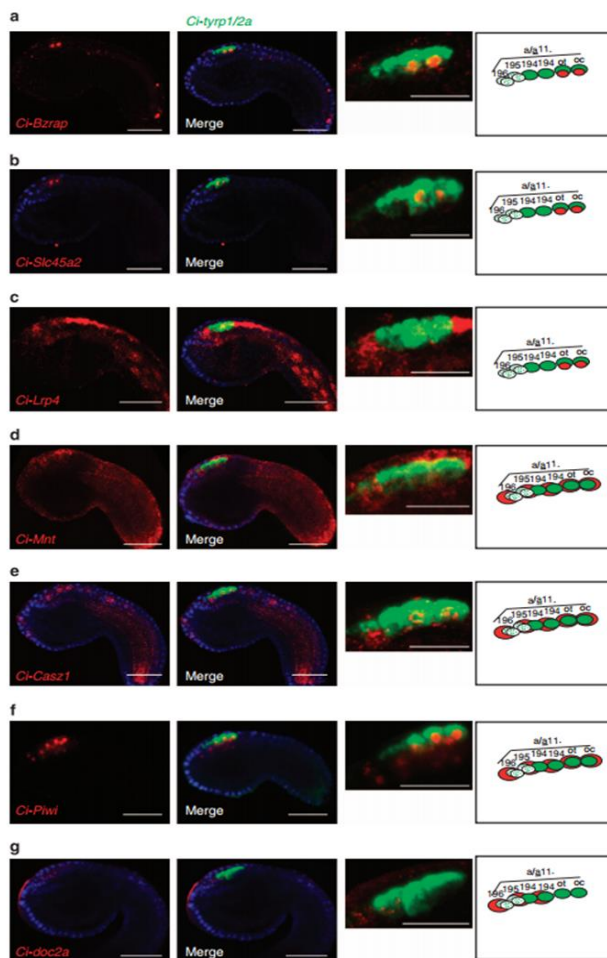
Figure 5.1. FGF-dependent candidate genes for pigmentation. Double whole-mount in situ hybridization experiments demonstrating co-localization of genes down-regulated by block of *FGF* (red) with *Tyrp1/2a* (green) in pigment cell lineage at tailbud stage (adapted from Racioppi et al., 2014).

This member of Kelch-like family is strongly repressed when FGF is inhibited in pigment cell precursors and encodes a poorly studied protein. It belongs to a family of proteins whose function has been associated to protein-protein interaction and ubiquitination. *Cr-Klhl21* belongs to a poorly studied family that in human encompasses 42 members, encoding proteins usually characterized by BTB/POZ domain, a BACK domain, and five to six Kelch motifs (Dhanoa et al., 2013). They belong to a family whose members facilitate protein-protein interactions and many of them are implicated in human pathologies such as cancer (Dhanoa et al., 2013). A subgroup of Kelch-like proteins involved in ubiquitination has been identified, as widely demonstrated for Keap1 (Klhl19) during oxidative stress (Ito et al., 1999).

Employing a combination of phylogeny, expression profiles and mutational analysis I discovered a dynamic expression pattern for this gene in ocellus and otolith, directed by regulatory genetic machinery organized in modules. This survey opens new perspectives in the knowledge of Kelch family member and in the otolith determination in ascidians.

5.2 - Results

5.2.1 - *Klhl21* molecular evolution

In order to find new genes specific to *Ciona robusta* pigment cell precursors (PCPs), FGF microarray data have been explored in depth. Among genes down-regulated by FGF signaling, the *Cr-Klhl21* transcript, belonging to Kelch-like family, results to be strongly down regulated in FGF block conditions and up regulated when *Ets* is constitutively activated. According to information present on Aniseed database, the transcript corresponds to the KH2012:KH.L84.23 gene model and its possible names are KLHL21, KLHL24, KLHL29. To assign it to a specific subfamily I performed a phylogenetic analysis of the *Ciona* predicted protein (590 aa) and using available

sequences of Klhl21, Klhl24, Klhl29 plus related Klhl6 and Klhl30 (Figure 5.2) from evolutionarily significant chordate genomes (Supplementary Table 5.1): amphioxus *Branchiostoma floridae*, ascidians *Ciona robusta* and *Ciona savignyi*, cartilagineous fish *Callorhinchus milii*, teleost fish *Danio rerio*, human *Homo sapiens*.
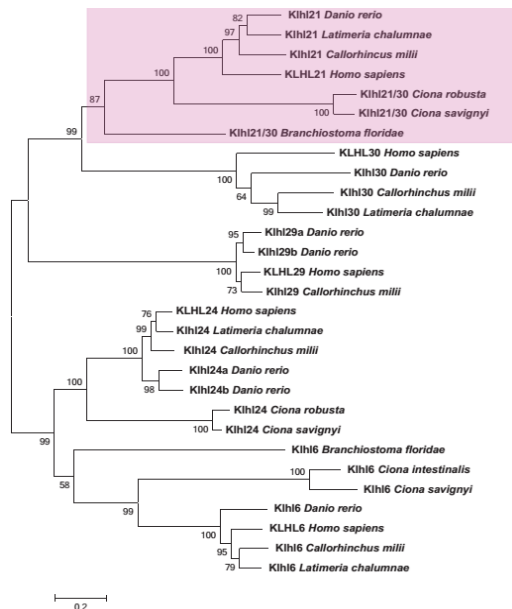
Figure 5.2. Phylogenetic tree of some Kelch-like chordate subfamilies. The Maximum Likelihood reconstruction shows the existence of five well-supported subfamilies: in particular, it focuses on the Klhl21 class in chordates (pink box).

The ML survey supports five distinct phylogenetically robust subfamilies (Klhl6, Klhl21, Klhl24, Klhl29, Klhl30) with Klhl21 connected to Klhl29 and Klhl30 proteins. Phylogenesis suggests orthology between the *Ciona* gene of interest and vertebrate Klhl21 genes (Fig. 5.2, pink box), with vertebrate Klhl29 and Klhl30 as extra-copy originated by duplicative events. For this reason, I named the protein present in amphioxus and ascidians *Klhl21*. The synteny analysis of human chomosomes (1, 2) harbouring Klhl21 and Klhl30 unveils the presence of common neighbouring genes, *Espn* and *Hes*, (Figure 5.3); this could trace back an ancient common origin for these two Klhl family member.
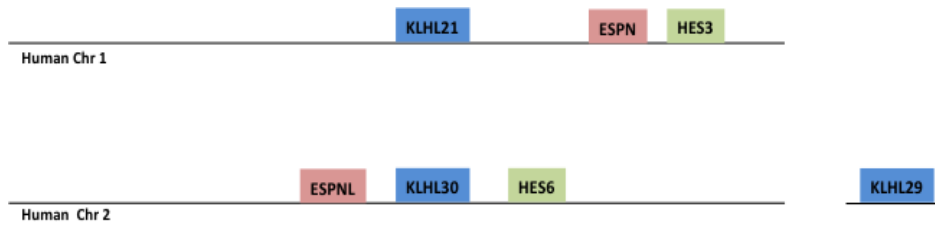
Figure 5.3. Synteny between *Klhl* genes in human. Schematic representation of human genomic *loci* (Chr 1, 2) harbouring *Klhl* genes (blue) included in phylogeny of Figure 4.2; on chromosomes 1 and 2 are shown genes syntenic with Klhl family members, that are Espn (light red) and Hes (green).

5.2.2 – *Cr-Klhl21* expression pattern

Given its phylogenetic position in chordates, *Ciona* may be useful to study *Cr-Klhl21* during embryogenesis. Whole-mount *in situ* hybridization experiments (WISH) using NBT-BCIP unravel the specific localization of *Cr-Klhl21* in two of four cells corresponding to pigment cell precursors (PCPs) from initial to early tailbud stage (Fig. 5.4A-B). Starting from middle tailbud, the expression seems to be restricted just to one cell (Fig. 5.4C-D). In order to assess the identity of cells expressing *Cr-Klhl21*, a double fluorescent WISH at middle tailbud stage with well-known melanogenic marker *Cr-Tyrp1/2* was performed (Fig. 5.4E): the co-localization between the two genes testifies *Cr-Klhl21* presence only in the otolith precursor. The expression profile of this gene is interesting for its a clear localization in otolith and ocellus precursors, with differences during embryogenesis in terms of labeled pigment cells.
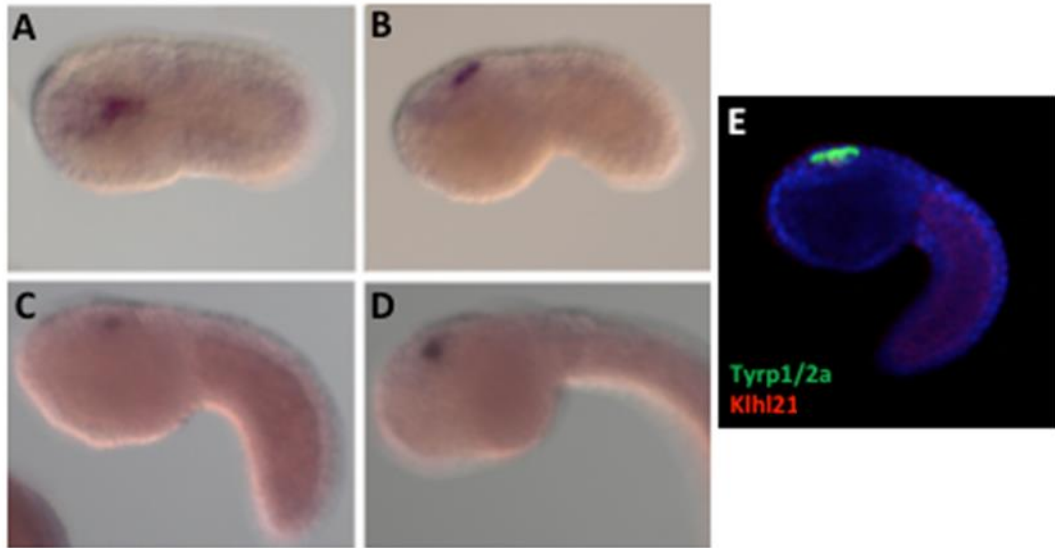
Figure 5.4. *Klhl21* **expression profile in** *Ciona robusta***.** A,B) The scheme demonstrates the *Cr-Klhl21* presence in two cells belonging to pigment cell lineage from initial to early tailbud stage; C,D) from middle tailbud the expression becomes restricted to one cell; E) Co-localization between *Cr-Klhl21* and *Cr-Tyrp1/2a* unveils that unique marked cell is the otolith precursor.

To further comprehend the evolutionary developmental scenario of this subfamily, I cloned the zebrafish *Klhl21* gene for studying its expression during vertebrate embryogenesis (Figure 5.5). WISH experiments demonstrated its transcription from 22 to 48 hours post-fertilization in the cephalic nervous system. The gene expression is absent from territories typically pigmented as retinal pigmented epithelium (RPE) or migrating melanoblast deriving from neural crest cell populations (Fig. 5.5), which are considered similar to ascidian pigment cells. Since ESTs reveal the presence of *Zf-Klhl30* only in heart, I did not perform WISH experiments.
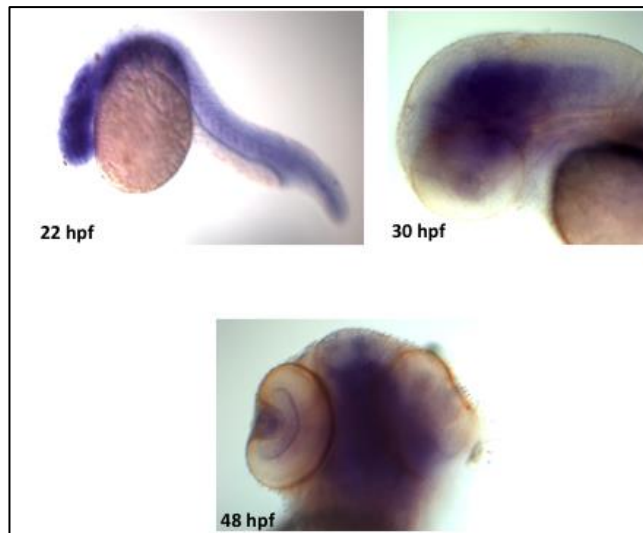
Figure 5.5. *Klhl21* **zebrafish expression pattern**. The image shows the expression of *Klhl21* from 22 to 48 hours post fertilization (hpf) in cephalic nervous system.

For the first time, I have collected in two key chordate species data regarding expression of *Klhl21* subfamily members: there is a clear difference between orthologues in sea squirt and zebrafish, in terms of expression pattern. In particular, the profile exhibited by *Ciona* is interesting because it is specific for pigmented cells with changes during embryogenesis.

5.2.3 - *Cr-Klhl21*: the regulatory scenario

In light of *Cr-Klhl21* dynamic expression, understanding its regulation in pigment cells can give insights on the molecular network responsible for differentiation between otolith and ocellus. To find the putative regulatory region for *Klhl21* activation, I selected from a public ascidian database (Aniseed) a 949 bp fragment (-1044 to -95 from the Transcription Start Site, TSS) highly conserved between genomic regions of *C. robusta* and *C. savignyi* (Figure 5.6A). This region has been PCR-amplified and cloned into the vector pSP72 upstream the beta Globin minimal promoter for driving the expression of GFP. The prepared construct (*klA>GFP*) has been electroporated in fertilized *Ciona* eggs and the GFP signal has been assessed

observing embryos from neurula to larva stage under fluorescent light microscopy. *klA>GFP* is able to recapitulate partially the endogenous expression in larvae with a strong signal restricted to otolith, present in the majority of them (70 %, Fig. 5.6B). Because GFP is not visible in the stages prior to the larva, I performed WISH on embryos (from early to late tailbud) electroporated with *klA>GFP* using a GFP probe. From preliminary experiments, I found the examined region was transcriptionally active from middle tailbud in the otolith (Fig. 5.6C), suggesting that the absence of GFP fluorescence before the larval stage is due to a delay in the accumulation of GFP protein (Fig. 5.6B).
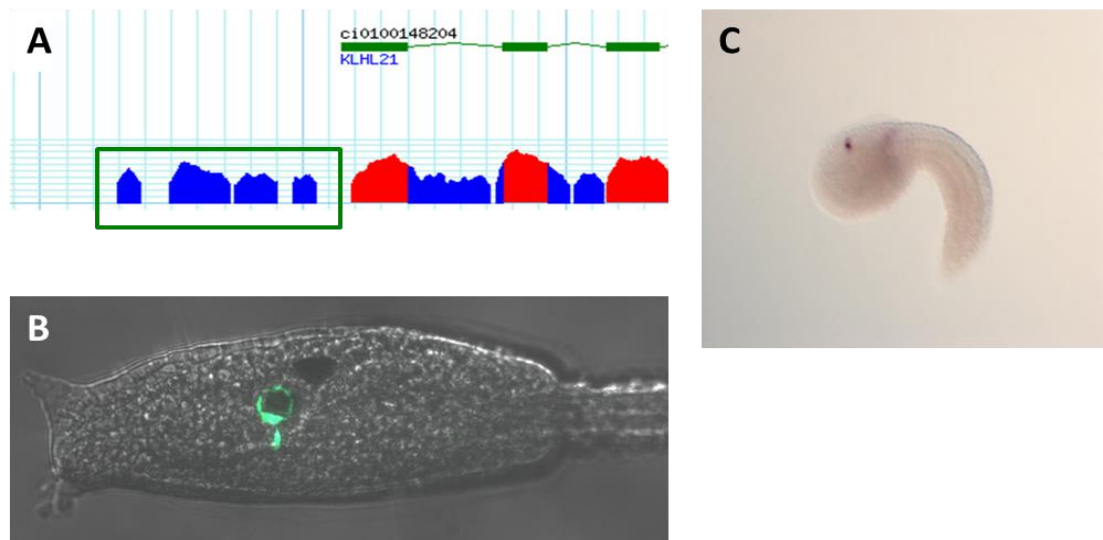
Figure 5.6. Putative regulatory region of *Cr-Klhl21*. A) The figure evidences the genomic region (green box) cloned upstream GFP; B) transgenesis via electroporation (*klA>GFP*) causes GFP specific expression in otolith of larvae (70 %); C) WISH using GFP riboprobe on embryos electroporated with *klA>GFP* shows transcriptional activity at middle tailbud stage.

To test the presence of potential transcription factor binding sites (TFBs) implicated in early activation, I enlarged the klA fragment by including the first intron sequence; unfortunately, the klA[I] region (1634 bp) is characterized by strong ectopic GFP expression in the mesenchyme (Figure 5.7)
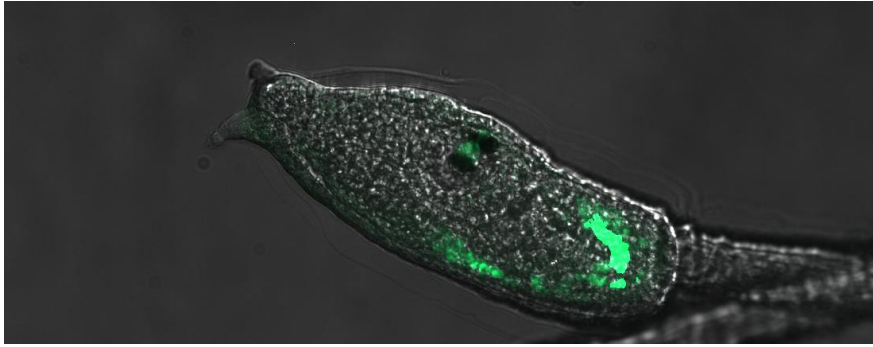
Figure 5.7. Ectopic expression driven by klA^I region. The figure evidences how *klA^I>GFP* (1634 bp) drives strong expression in the mesenchyme of *C. robusta* larva; this region comprises the first intron of *Cr-Klhl21* gene.

Subsequently, I decided to define the putative regulatory region inside klA fragment, through a deletion analysis in accordance to genomic conservation with the sister species *Ciona savignyi*. All the smaller fragments have been cloned in the same vector containing GFP. The first step has consisted of cutting the klA (949 bp) in two shorter fragments characterized by high genomic conservation, named klB (382 bp, -882 to -500) and klC (400 bp, -500 to − 95): *klB>GFP* is able to recapitulate *klA>GFP* expression (45 %), whereas *klC>GFP* does not drive expression in pigment cell precursors (Figure 5.8). It means that, despite a high degree of genomic conservation, no positive regulatory elements are present in the peaks near to TSS (klC).
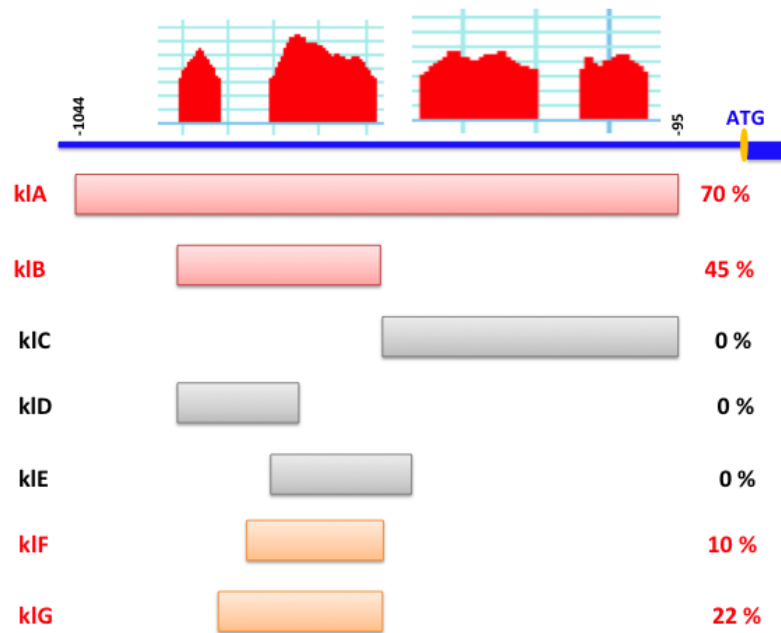
Figure 5.8. Deletion analysis of putative promoter of *Cr-Klhl21*. The figure describes the genomic fragments cloned upstream GFP employed for identification of *Cr-Klhl21* regulatory region. It has been used a color code to distinguish amongst distinct regions: positive with high penetrance (klA, klB; red), negative (klC, klD, klE; grey), positive with low penetrance (klF, klG; orange). The names and the corresponding percentage of regions are listed on the left and the right of the fragments, respectively.

To narrow the region comprising putative enhancer elements responsible for *Cr-Klhl21* expression, I focused my attention on klB fragment subdividing it in klD (-882 to -606) and klE (-606 to -500). Cloned upstream GFP, both of them were not able to guide reporter expression in the otolith. To understand why klD and klE do not drive GFP expression, I selected two new fragments enlarging from klE region. I called these fragments klF (-650 to -500) and klG (-700 to -500) and electroporations showed they are able to drive GFP in otolith, albeit with low percentage, 10 % and 22 %, respectively. All the chosen fragments have been tested four times; for each experiment, I have identified the positives observing a total of 100 embryos by using light fluorescence microscopy and I listed the results in a graph (Figure 5.9).

Results indicate klB (382 bp) as the shortest fragment capable to guide GFP expression in the otolith in a high percentage of animals, meaning it includes all the information necessary to activate transcriptional regulation of *Cr-Klhl21*.
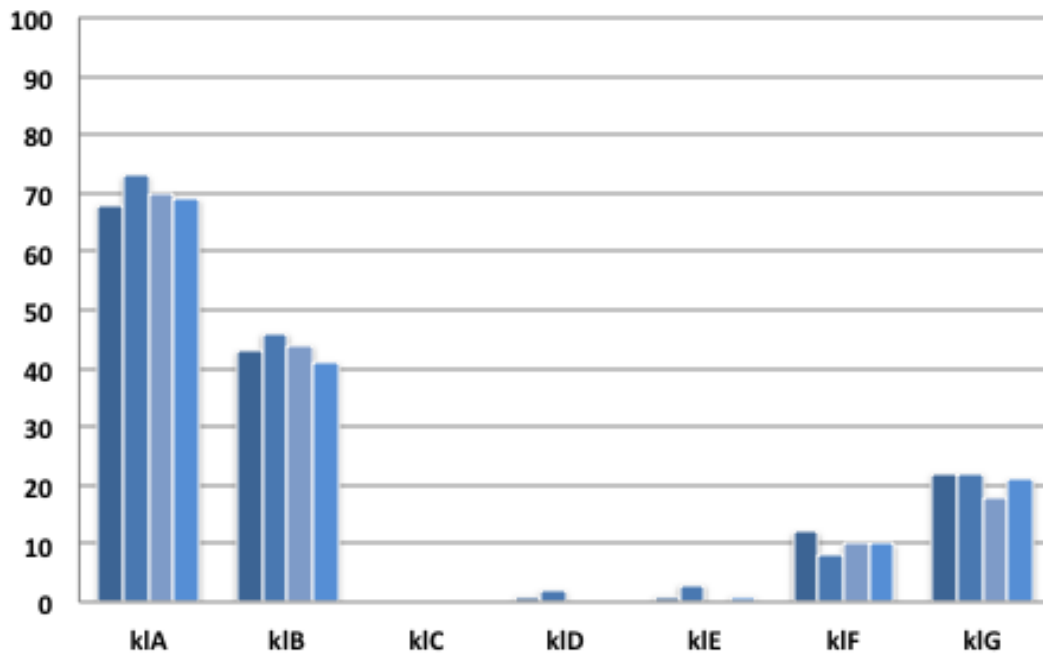
Figure 5.9. Statistics regarding *Cr-Klhl21* delection analysis. The graph reports the percentage about the seven genomic fragments used to study regulation of *Cr-Klhl21*; each fragment has been cloned in a vector containing GFP and tested four times. Each experiment has been performed counting the percentage of GFP-expressing animals on a total of 100.

In order to shed light on the basis of gene regulatory network for such specific expression, the klB fragment has been chosen for a bioinformatic analysis to find relevant transcription factor binding sites (TFBs), through MatInspector function of Genomatix software (Figure 5.10). Among a plethora of TFBs coming out from this *in silico* survey, according to high matrix similarity parameter and possible involvement in pigmentation dynamics, the most supported seem to be two Mitf, two Msx and one Dmrt sites; they have been selected for a mutational analysis (Figure 5.11). All the fragments mutated have been tested via electroporation (using GFP) and embryos have been observed by light fluorescence microscopy.

GCGCACTTATAACATGCA`ATTA`TATTCTAACGTTTCTTCTTTCTGTGATCAGTTCGACTATACTTT`TACA`TTTATTTCTC
AGTCCGTATAATACGAAGTGTACAGTGCCTAATTTAGTGAGTTAACATTTGTGCGTTTGGTCTGTTGCGA`ATTA`ACTGAT
TGTCAAGTTCTAAATCGTTTCGCTTTCTTTCTGCCCTGGTGCCTAGTCTTGTCA`CGTG`AAAAACACTCAGGGATTATAAA
TAACCACCCACGATTACTTACGTAATAGCTGAAATGATTCCCA`CGTG`ATGCGAAGTCATTAAACAAAGAAACAACGTCA
CGCAAGAACTTTACATGACTAGCTGAAGCAAGCGATGGATTTGTATGAGGTTACTAGAACGT

Figure 5.10. Genomic sequence used for TFBs analysis. Here is shown the regulatory region (klB, 382 bp) employed for Genomatix analysis and are highlighted potentially interesting binding sites: MITF (yellow), MSX (blue), DMRT (green).

Family	Matrix sim.	Sequence
Family	1	gttagaataTAATtgcatg
V$DLXF	1	tcttgtcaCGTGaaaaa
V$HIFF	1	cgtgaaaAACActcagg
V$FKHD	0.995	gaataTAATtgcatgttataa
V$CART	0.994	attaaACAAagaaacaacgtcac
V$SORY	0.993	gcgcACTTata
V$RUSH	0.993	ctatACTTtta
V$RUSH	0.992	cacgTGGaatca
V$RBPF	0.992	attccCACGtgatgcga
V$EBOX	0.990	atcccTGAGtgtttttcac
V$NKXH	0.987	tttttCACGtgacaaga
V$EBOX	0.986	ttttcACGTgacaag
V$HESF	0.986	cgcatCACGtgggaatc
V$EBOX	0.985	cttgtCACGtgaaaaac
V$EBOX	0.985	gctgaaGCAAgcg
V$BZIP	0.983	ATCAcgtgggaatca
V$LTSM	0.98	taACATttgtg
V$HOMF	0.977	ggcagaaagaaagcGAAAcgatttta
V$IRFF	0.975	cttgTCACgtgaaaa
V$MITF	0.974	ttgtcaCGTGaaaaa
V$HESF	0.973	tagaataTAATtgcatgtt
V$HOMF	0.973	aacatgcaATTAtattcta
V$RUSH	0.973	gtttttcaCGTGacaag
V$HIFF	0.972	gcatcaCGTGggaat
V$HESF	0.972	gtttctttgttTAATgact
V$HOMF	0.972	cttgcgTGACgttgtttcttt
V$HOMF	0.968	ctgttgcgaATTAactgat
V$HBOX	0.967	gttgcgaatTAACtgattgtc
V$MYBL	0.967	gattcccaCGTGatgcg
V$HIFF	0.966	agtgccTAATttagtgagt
V$HBOX	0.964	ttcccaCGTGatgcg
V$HESF	0.964	cgaagtcaTTAAacaaa
V$ABDB	0.962	ggatTATAaataacc
O$PTBP	0.962	attacttacGTAAtagc
V$PARF	0.961	ttttTCACgtgacaa
V$BCDF	0.959	agctattacGTAAgtaa
V$PARF	0.959	taaagttcttgCGTGacgttgtttc
V$MITF	0.958	ttcccaCGTGatgcg

V$BRNF	0.958	tcgcatCACGtgggaat
V$HIFF	0.954	tcTCAGtccgt
O$INRE	0.953	gcaTCACgtgggaat
V$SREB	0.948	gattaTAAAtaaccacc
O$VTBP	0.948	agtcattaAACAaagaa
V$FKHD	0.947	cagctattacGTAAgtaatcg
V$CREB	0.946	gattacttacGTAAtagctga
V$CREB	0.946	ttcgcatCACGtgggaatcat
V$HAND	0.945	tataacatgcAATTatatt
V$DLXF	0.943	ctaGTCTtgtc
V$SMAD	0.941	gttaattcgCAACagaccaaa
V$MYBL	0.940	gaTCAGttcga
O$INRE	0.939	actgatcacAGAAagaaga
V$STAT	0.936	tttagtgaGTTAacatt
V$HNF1	0.935	tttgtATGAggttactagaac
V$CREB	0.934	ttgtTTAAtgacttc
V$NKX6	0.933	tgacaatcagTTAAttcgc
V$DMRT	0.933	tactttTACAtttatt
V$CEBP	0.933	acgtGGGAatcat
V$IKRS	0.932	gttcttgcgTGACgttgtttc
V$CREB	0.93	gattacttacgTAATagct
V$BRNF	0.928	gcctaaTTTAgtgagttaaca
V$ARID	0.927	agaaagcgAAACgatttag
V$HOMF	0.927	atgTAAAgttcttgc
V$PLZF	0.921	gctagtcatGTAAagtt
V$PARF	0.92	ggattaTAAAtaaccac
V$FKHD	0.92	ataaccaCCCAcgatta
V$GLIF	0.918	gtggttaTTTAtaatcc
V$HOXC	0.916	gtgccTAATttagtgag
V$BCDF	0.914	aaCATGcaattatat
V$OCT1	0.914	tcagTTAAttcgcaa
V$NKX6	0.913	cgcaTCACgtgggaa
V$MITF	0.912	gaaagaagAAACgttagaa
V$HOMF	0.912	cttgacaatcaGTTAattcgcaa
V$LHXF	0.909	tctaaATCGtttcgc
V$HZIP	0.906	ttcgtATTAtacggactga
V$BRNF	0.904	tcagggattatAAATaaccaccc
V$MEF2	0.903	ttcgcatcACGTgggaatcat
V$CREB	0.901	atttataatccCTGAgtgtttttcacgtg

Figure 5.11. Predicted binding sites with MatInspector. The table resumes the characteristics of binding sites revealed from Genomatix with a matrix similarity > 0.900. Using the same colors of Figure 4.10, here are highlighted the sites selected for mutational survey.

The microphthalmia-associated transcription factor (Mitf) or bLHLe32 is involved in

many processes and, among them, it is fundamental for the expression of several key

genes involved in pigmentation (Levy et al., 2006). Moreover, Mitf is implicated in

diseases associated with pigmentation in humans. To find co-localization between *Cr-Klhl21* and *Cr-Mitf* (expressed in otolith and ocellus, Figure 5.12A), I carried out a double fluorescent WISH demonstrating their co-expression in otolith precursor at middle tailbud stage (Fig. 5.12B). Therefore, I have mutated the two Mitf sites (matrix similarity 0.975, 0.958) separately, changing the wild-type (*wt*) *core* sequence CGTG into CTCT. Each mutation caused almost an abolition of GFP signal (0-3 %) in larvae, suggesting a direct involvement for Mitf in transcriptional activation of *Cr-Klhl21*.
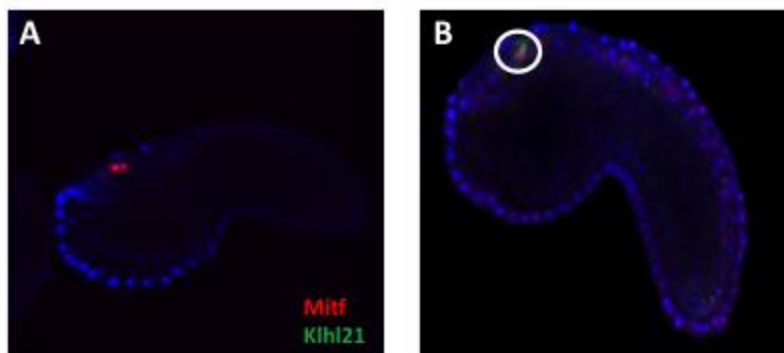
Figure 5.12. Co-localization between *Cr-Klhl21* and *Cr-Mitf*. A) Expression of *Cr-Mitf* in pigmented cells at middle tailbud stage; B) Co-expression of *Cr-Klhl21* and *Cr-Mitf* in the otolith precursor at middle tailbud.

Cr-Msxb is considered a marker of ascidian pigment cells up to early tailbud (Aniello et al., 1999) and a repressor in the ascidian nervous system (Roure and Darras, 2016; Esposito et al., 2017). As for *Cr-Mitf* , a double fluo-WISH has been used to study co-expression in pigmented cells of *Cr-Klhl21* and *Cr-Msxb* or their presence in cells that are adjacent but in territories mutually exclusive. I found the presence of both the genes in the otolith precursor at middle tailbud stage (Figure 5.13A), with absence of co-localization at late-tailbud (Fig. 4.13B). Their co-expression has encouraged me to mutate each robust putative Msx site (matrix similarity 0.973,

0.968). Substituting *wt* ATTA with AGGA, I observed in both cases approximately a strong decrease of GFP-positive larvae (20-25 %) with respect to the *wt* construct (Figure 5.14). Interestingly, coupling both the mutations in the same construct gave a nearly total lack of signal and this supports a role as activator for *Cr-msxb* in the transcriptional regulation of *Cr-Klhl21*.
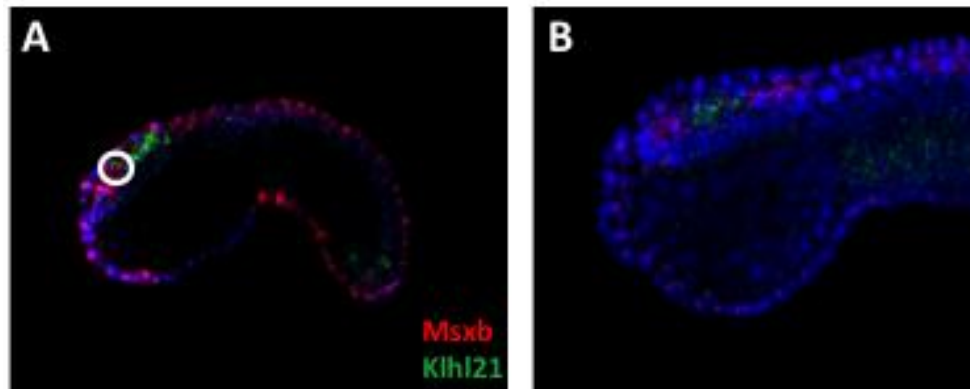
Figure 5.13. Co-localization between *Cr-Klhl21* and *Cr-msxb*. A) Co-Expression of *Cr-Mitf* in otolith precursor between two genes at middle tailbud stage; B) End of co-expression of *Cr-Klhl21* and *Cr-msxb* in the otolith precursor later in development.

Regarding the regulation of *Cr-Klhl21* through the Dmrt site, it is noteworthy that *Cr-Dmrt1* is also expressed in *C. robusta* sensory vesicle (Imai et al., 2004) and, moreover, in *Ciona savignyi* is crucial for proper development of pigment cells (Tresser et al., 2010). Therefore, I have mutated its binding site (matrix similarity = 0.933) changing the *wt* TACA in TGTA and I have observed that *Ciona* larvae exhibit a strong decrease of GFP expression (20%) respect to klB region (45 %), suggesting an important role for *Cr-Dmrt1* too, as shown in the scheme resuming the mutations performed on klB fragments (Fig. 5.14).
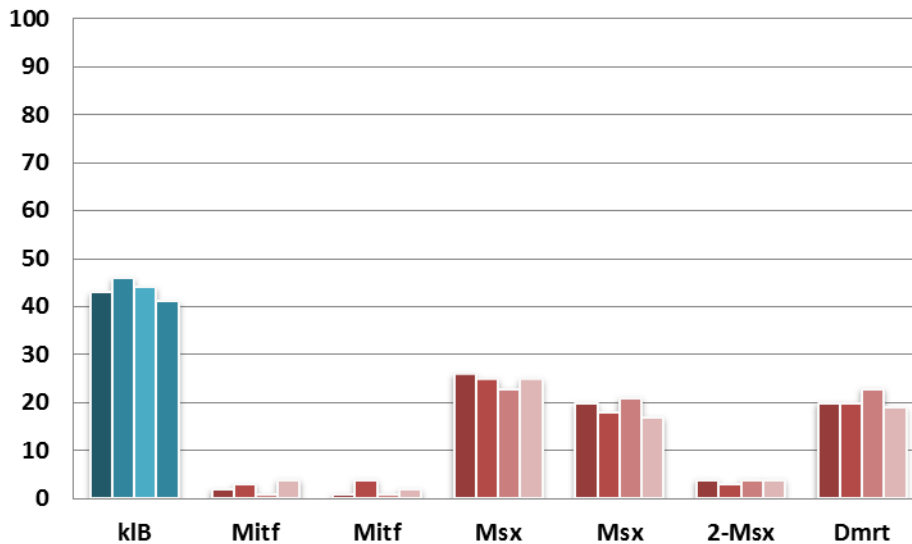
Figure 5.14. Statistics about *Cr-Klhl21* mutational survey. The figure summarizes the results obtained from electroporations of mutated klB fragments (here shown in blue) in fertilized eggs. Each experiment has been carried out four times and evaluated by observing the positives on a total of 100 animals.

If we consider these data, they suggest a role as key activator for *Cr-Mitf* and co-activators for *Cr-msxb* and *Cr-Dmrt1* of *Cr-Klhl21* gene in the pigment cell lineage. In summary, the transcriptional regulation of *Cr-Klhl21* appears as particularly interesting to investigate, with the possible intervention of (at least) five TFBs for its late specific expression in the otolith.

5.3 - Discussion

5.3.1 - *Cr-Klhl21*: the first otolith marker

Pigment cells are very important for larval behavior of ascidians because it can determine their ecological success, therefore it is relevant to understand which genes are decisive for pigment cell formation. It has been demonstrated that FGF pathway represents a key molecular inductor for proper development of pigment cells in *Ciona* (Squarzoni et al., 2011). Among FGF-dependent genes, new markers for the

pigment cell lineage have been found (Racioppi et al., 2014). Aside from well-known melanogenic actors as *Rab32/38* and *Slc45a2*, this kind of analysis has permitted to find potential new players in pigmentation as *Bzrap*, *Piwi*, *Lrp4* and *Doc2a*. Interestingly, they exhibit an extremely variable expression in the pigment cell lineage leading to us to hypothesize the existence of a distinct transcriptional code for each cell deriving from the a9.49 pair of blastomeres (Racioppi et al., 2014). As an example, *Tyr* and *Tyrps*, typical melanogenic markers, are present in all cells of the PCP lineage including those that will not become pigmented (Sato et al. 1997; Esposito et al., 2012) as well as *Rab32/38* (Racioppi et al., 2014), known as a transporter of tyrosinase family members (Bultema et al., 2012). None of the genes isolated in the screening exhibited specific expression in the otolith or ocellus. Finding genes specific of only one pigmented sensory organ could help to shed light on the molecular differences underlying their specification. My results unravel the first Kelch-like member expressed with a dynamic profile in the ascidian pigment cell precursors, and clarify the orthology of some Kelch-like genes.

An ML phylogeny with selected Kelch-like members placed the *Ciona* gene at the base of Klhl21 and close to Klhl30 vertebrate genes (Fig 4.2), distantly related to Klhl6 and Klhl24, which are probably ancient paralogues arisen in the ancestor of Olfactores. Although a common evolutionary origin for Klhl21 and Klhl30 was already suggested (Dhanoa et al., 2013), synteny analysis permits to hypothesize that vertebrate Klhl21 and Klhl30 derive from an ancient duplication occurred alongside metazoan evolution. In fact the presence of *Hes* (crucial for Notch signaling) and *Espn* orthologues on both human genomic *loci* (Chr 1 and 2, respectively) evokes the existence of conserved chromosomal region. Moreover, because also Klhl29 (maintained in all the analyzed vertebrates) lies on human chromosome 2, probably it

derives from a local-duplication at the base of vertebrates. Regarding ancient duplicates Klhl6 and Klhl24, their microsyntenic arrangement on human chromosome 3 could be linked to common regulation inside the cell (Fig. 4.3). This explanation about Klhl21 subfamily origins is the more parsimonious and suggest a massive loss of 1R, 2R and 3R (TSGD) duplicates (Abi-Rached et al., 2001; Dehal and Boore, 2005; Hoegg et al., 2004). Moreover, it could not easily explain the divergent expression observed in *Ciona* and *Danio* (Fig. 4.4; Fig. 4.6).

Cr-Klhl21 is the only gene belonging to Kelch-like family to so far be studied in ascidians. Expressed specifically in PCPs, for the first time its presence is described in pigmented cells and/or sensory organs. Despite scarcity of experimental data, it has been hypothesized that KLHL21 is able to bind Cullin 3 regulating, through ubiquitylation, cytokinesis and cell migration (Maerki et al., 2009; Courtheoux et al., 2016; Huang et al., 2017); moreover, KLHL21 is implicated in hepatocellular carcinoma (Shi et al., 2016). The expression pattern of *Cr-Klhl21* appears extremely interesting and dynamic. Down-regulated by FGF blocking conditions, it starts to be expressed in otolith and ocellus precursors at the initial tailbud stage and becomes specific to the otolith precursor from the middle tailbud stage, disappearing from the ocellus. Then, *Cr-Klhl21* is among the few genes discriminating between ascidian otolith and ocellus precursors together with *βγ-crystallin*, expressed in otolith of larvae (Shimeld et al., 2005). Interestingly, this Kelch-like member is the first gene distinguishing the otolith at middle tailbud stage (with shutdown in ocellus), differently from *βγ-crystallin*, which is able to mark the otolith only from larva stages. In light of its dynamic expression profile, *Cr-Klhl21* could be important for studying pigment cell determination (Fig. 4.4) as a primary otolith marker. Regarding *Cr-Klhl21* possible function, there is scarcity of information apart from

involvement of Kelch-like family members in protein-protein interactions linked to ubiquitination processes (Dhanoa et al., 2013). In vertebrates Klhl21 seems to be involved in cytokinesis regulation in HeLa cells (Maerki et al., 2009) and has been recognized as a candidate for hepatocellular carcinoma (Shi et al., 2016). *Cr-Klhl21* is not credible as mitotic regulator because PCPs do not divide at these stages. The ubiquitination of molecules typical of pigmentation could be a function to consider; a further possibility could be the involvement of ubiquitination in the regulation of genes necessary for otolith functioning. Alternatively, Cr-Klhl21 could mimic the function of a related protein present also in *Ciona*, Klhl24. This is involved in the replacement of intermediate filaments and its mutations are linked with human skin fragility (He et al., 2016; Has, 2017). It raises the possibility that *Cr-Klhl21* plays a role in the regulation of otolith cytoskeletal system.

Unfortunately, zebrafish genes related to *Cr-Klhl21* seem to be not involved in pigmentary dynamics, in fact *Zf-Klhl21* is present in unpigmented nervous territories (Fig. 4.5) while *Zf-Klhl30* is present only in the heart (as assessed by ESTs). These data evoke a scenario based on functional and developmental diversification across chordate evolution, which could be explained parsimoniously through loss of function (and expression) in pigmented cells at the base of vertebrates. On the other hand, a further possibility is the acquisition of an ultra-specialized function in ascidian pigmentation: this could be understood by studying it in other systems belonging to urochordates as *Halocynthia*, *Oikopleura* and *Molgula*. Expression data from other invertebrates as amphioxus and vertebrates as lamprey are needed for making more robust hypotheses.

In summary, *Cr-Klhl21* represents a fundamental rawplug to study pigment cell specification in the ascidian clade. Its dynamic expression profile, which becomes

otolith-specific from mid tailbud, leads me to hypothesize a new role for this gene because probably it is not involved in mitosis. Interestingly, the diversification in terms of role in nervous system during evolution is supported by different territories marked in ascidians and teleosts. Collectively, it is important understanding more about the function of this gene during evolution, with a special focus on ascidian's otolith.

5.3.2 - *Cr-Klhl21*: an intricate regulatory code

Cr-Klhl21 shows a dynamic expression profile, becoming restricted to the otolith from the middle tailbud stage (Fig. 4.4A), a pattern confirmed by a regulatory region active exclusively in the otolith from the middle tailbud stage (Fig. 4.6). After deletion analysis (Fig. 4.8; Fig. 4.9), I selected the klB region (382 bp, 45 % of GFP-expressing larva) to identify possible regulators of *Cr-Klhl21*, finding three putative actors: *Cr-Mitf*, *Cr-Msxb*, *Cr-Dmrt* (Fig. 4.10; Fig. 4.11). Considered fundamental for pigmentation (Levy et al., 2006) and dependent on the FGF pathway, *Cr-Mitf* is present exclusively in pigment cells and co-localizes with *Cr-Klhl21* in the otolith at middle tailbud (Fig. 4.12). Moreover, the specific expression of *Mitf* orthologues in pigment cells of other models as amphioxus and zebrafish (Yu et al., 2008; Lister et al., 2000) and its implication in pigmentation-related diseases such as melanoma and Tietz syndrome (Leclerc et al., 2017; Cortés-González et al., 2017) render this transcription factor a strong candidate to comprehend how *Cr-Klhl21* is regulated. Being a basic helix- loop-helix protein (bHLHe32), *Cr-Mitf* interacts with DNA through a leucine-zipper domain, with the presence of two near canonical E-boxes (CACGTG) which are separated by 66 nucleotides. In *Ciona*, each Mitf binding site mutation gave almost completely abolished the GFP otolith expression (2.5 %), suggesting that Mitf could work as dimer also in *Ciona,* and that is central to regulate

positively *Cr-Klhl21*. The Mitf gene is the master regulator of vertebrate pigmentation because it controls *Tyr* and *Tyrps* expression during commitment of pigment cells (Widlund and Fisher, 2003). However, have been reported many evidences about Mitf implication in regulating genes not directly connected to pigmentation, as *Oa1*. It demonstrated that factors involved in melanin production and melanosome formation are regulated similarly (Vetrini et al., 2004). My results suggest a possible activation from *Cr-Mitf* on *Cr-Klhl21* promoter. Although the presence of a putative Mitf binding site on Klhl21 promoter seems to be fundamental, the endogenous expression probably depends also on other activators: the region called klE, containing mostly two E-boxes, is not able to drive GFP signal in otolith possibly because is devoid of other signals (Fig. 4.5). Larger regions of promoter, containing TFBs for Msx and Dmrt, klF and klG are, albeit weakly, capable to guide gene expression in the otolith. Interestingly, I can define klG (325 bp) as the smaller region needed for *Cr-Klhl21* activation. This concept is strongly supported by mutational analysis performed on Msx and Dmrt sites, present in klB. The mutation of each Msx site caused a net decrease (20-25 %) of *Ciona* tadpoles expressing GFP, while their simultaneous mutation produce a result similar to Mitf mutations (4 %). These experiments and its early co-expression with *Cr-Klhl21* in pigment cells (Fig. 4.13), prompted me to consider *Cr-Msxb* as a fundamental co-activator for *Cr-Klhl21*. This finding is newsworthy because Msx proteins traditionally act as transcriptional repressors, as shown also in *Ciona robusta* CNS (Roure and Darras, 2016; Esposito et al., 2017). It is known as an early marker of pigment cell lineage (Aniello et al., 1999) and possibly activated by Tcf (Russo et al., 2004). *Cr-Msxb* (influenced by FGF) role as co-activator is consistent with some data from vertebrates however: in fact, the initiator of ovary meiosis *Stra8* is

activated by Msx1 and Msx2 (Le Bouffant et al., 2011) while *Atoh* expression in mouse spinal cord depends on activation operated by Msx1 and Msx2 (Duval et al., 2014). Curiously, I found that GFP-positive tadpoles diminish (20 %) when the unique site for Dmrt is mutated. Even if the members of this family have been classically associated to sex-specific traits (Kopp, 2012), Dmrt genes are connected with several aspects concerning vertebrate development (Hong et al., 2007). My results indicate doublesex/mab3 related-1 (Dmrt1) as positive regulator of *Cr-Klhl21* expression in the otolith, consistent with its presence in sensory vesicle (Imai et al., 2004). Moreover, functional experiments have shown that *Cr-Dmrt1* block causes the disruption of pigment cell development in sister species *C. savignyi* (Tresser et al., 2010). Ascidians possess a sole *Dmrt* copy and here is reported the first case of its implication in pigment cell development of chordates: this could represent a clade-specific innovation or a loss of function occurred in vertebrates. Comparing deletions and mutations, the expression of *Cr-Klhl21* is very complex with the intervention of three factors characterized by a different degree of relevance, resulting in a combinatorial code for transcription. The essential role of Mitf needs to be enhanced by co-activators *Cr-Msxb* and *Cr-Dmrt1*, here showing innovative functions. Their involvement in *Cr-Klhl21* activation is reflected by GFP expression obtained by using klF and klG with respect to the inactive klE fragment: the nucleotides comprised in these fragments correspond to the progressive inclusion of sites for Msx and Dmrt (concentrated in klD element). For this reason, I propose a cooperative model (Figure 4.15) for *Cr-Klhl21* expression with klE and klD thought of two distinct regulatory modules with quite diverse functions (both necessary), i.e. "regulatory" and "co-regulatory".
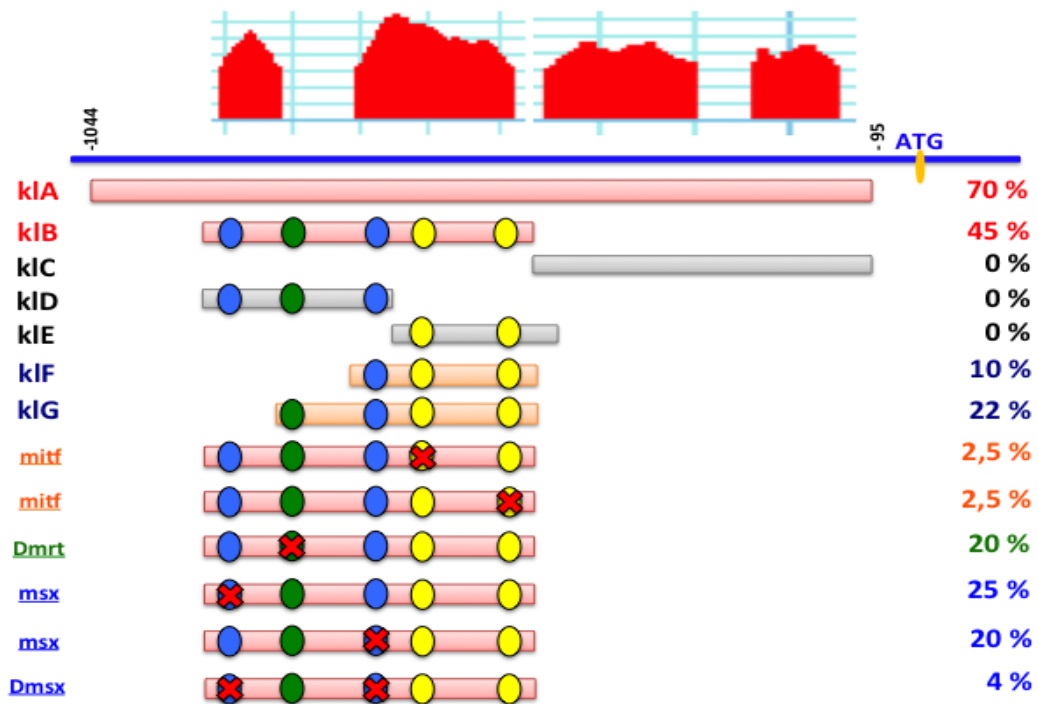
Figure 5.15. Model for *Cr-Klhl21* regulation. The figure summarizes the delection and mutational analyses performed to dissect promoter of *Cr-Klhl21*. Coloured ovals have been used to show studied TFBs: yellow (Mitf), blue (Msx), green (Dmrt). Red crosses indicate TFBs mutated on klB fragment.

Moreover, here is hypothesized the first case of activation operated by Msx in ascidians, influenced by the FGF pathway. It could substitute the "classical" role played by Msx gene as repressor. Then, there is an intricate regulatory pattern under the control of FGF signaling which, in light of *Cr-Klhl21* dynamic and unique expression profile, could be linked with otolith specification. Interestingly, it has been suggested that Wnt7/ β-catenin signaling has a key role in ocellus specification controlling a simple regulatory circuit (Wnt7→FoxD⊣Mitf) in which FoxD attenuates Mitf specifically in the ocellus precursor reducing its pigmentation (Abitua et al., 2012). This is coherent with *Cr-Mitf* expression that is stronger in otolith than ocellus (Fig. 4.11), and with the specific expression of *Cr-FoxD* in the

ocellus precursor (Abitua et al., 2012). Since *Cr-Klhl21* is characterized by otolith-specific expression from middle tailbud stage, it would be interesting to verify if FoxD transcription factor represses *Cr-Klhl21* in the ocellus. Although the search on klB fragment did not identify significant TFBs for FoxD, deeper investigation unraveled two sites for possible FoxD interaction (with low matrix similarity), which could enhance the attenuation of *Cr-Klhl21* expression in the ocellus. Further analyses will be needed to comprehend the involvement of FoxD in *Cr-Klhl21* regulation, as well as for *Cr-Mitf* (Abitua et al., 2012), in PCPs.

In order to better understand this, it will be important discovering the function of *Cr-Klhl21* through the CRISPR/Cas9 system (Stolfi et al., 2014), even if, its expression and putative regulators lead to hypothesize a strong relationship to pigmentation. Because of the importance of pigmented sensory organs for proper tadpole behavior (Jiang et al., 2005), it could be relevant to shed light on mechanisms at the base of otolith specification. In synthesis, *Cr-Klhl21* represents a new player in pigmentation, which depends on the lineage-specific regulatory network activated by FGF pathway through distinct activators (*Mitf*, *Msxb*, *Dmrt1*) interacting with diverse promoter regions.

CHAPTER 6

GENERAL DISCUSSION

Through this PhD thesis, it has been provided an example on how comparative genomics and developmental biology can produce significant results in the knowledge of a key process for animal life as pigmentation, straddling evolution and development.

Here is provided the most comprehensive study of eu-metazoan, chordate and vertebrate Rab toolkit to date, the principal intracellular transporter family in metazoans, which can constitute a platform for people interested in evolutionary biology and in cellular trafficking. Phylogeny, intron code and synteny helped to decipher the orthology of 486 Rabs and to depict a very intricate evolutionary scenario. Given that a plethora of Rabs is implicated in pigmentation, my survey represents the base for investigating the role of cellular traffic in pigmentation dynamics. Moreover, the knowledge of Rabs from an evolutionary perspective can be instrumental because they are involved in a multitude of diseases, with many pigmentation-related pathologies such as melanoma and albinism. An example is given by *Rab32/38* genes of two key chordate representatives, (amphioxus and zebrafish): in fact, also thanks to comparison with data in other model systems we evidenced a distribution of ancestral functions in chordates probably depending on genomic events. In teleosts this scenario is dramatically enhanced by genomic rearrangements, as shown by differences characterizing *Rab32* and *Rab38* paralogues in terms of distinct embryonic localization. The exceptional chromosomal conservation of gnathostome's paralogons is one of the most important results from an evolutionary perspective. Apart from being fundamental for understanding WGD-origin of vertebrate's Rab32 and Rab38, the chromosomal linkage existing between

Rab32/38 and Grm1/5 evokes the presence of a bystander regulation alongside vertebrate evolution or the "trapping" of an ultra-conserved enhancer. These hypotheses should be tested by using functional studies, together with the physical linkage between tyrosinase (Tyr) and Rab38 that are curiously functionally correlated during melanosome formation. A further case of FGF-dependent gene is represented by *Cr-Klhl21*, the first transcript exclusive to the otolith from middle tailbud stage. Because the zebrafish orthologue is expressed in nervous territories other than pigmented cells such as RPE or migrating melanoblasts, I hypothesize a functional diversification across chordate evolution. Its sustained expression in the otolith, coupled with a complex regulatory logic based on distinct modules, strongly indicated this gene as a new fundamental player for pigment cell development in ascidians, with a lineage-specific gene regulatory network.

In general, these data provided new information about the involvement of *Rab* and *Klhl* gene families in pigmentation, supporting new investigations regarding the members of these family also in other model systems, in order to elaborate a comprehensive evo-devo strategy for studying pigmentation dynamics in animals.

CHAPTER 7

METHODS AND MATERIALS

7.1 - Molecular evolution analyses

7.1.1 - Genome Database Searches and phylogenetic analyses

All the sequences used for the evolutionary analysis have been retrieved from the NCBI (https://www.ncbi.nlm.nih.gov) and Ensembl (http://www.ensembl.org/index.html) databases. Regarding analysis shown in Figure 3.2, protein sequences of vertebrate *Homo sapiens* Rab repertoire have been used as queries in BLASTp and tBLASTn searches in NCBI, Ensembl and Metazome genome databases of selected species. Orthologies of the Rab members have initially been assessed by reciprocal best blast hit (RBBH) approach and corroborated by phylogenetic analyses. Phylogenies have been based on ML inferences calculated with PhyML v3.0 and automatic selection mode of substitution model (Guindon et al., 2010) using protein alignments generated with MUSCLE (Edgar, 2004) and CLUSTALX (Larkin et al., 2007) programs and reviewed by hand to exclude too short or uninformative sequences. Only conserved parts of the proteins whose alignments were unambiguous among duplicates were included in the phylogenetic analysis, i.e. from codon D9 to G177 of human RAB1A. The Rab domains were mapped using ProSite (http://prosite.expasy.org) software (Sigrist et al., 2012) and drawn manually.

Ciona robusta Rab32/38 it has been employed as query sequence for Blastp and tBlastn (Gertz et al., 2006) in invertebrate genomes (Chapter 4), and reciprocal blasts were carried out on each selected genome. The sequences used in

evolutionary analyses of Chapter 4 are listed in Supplementary Table 4.1. The proteins have been aligned by ClustalW with default parameters (Thompson et al., 1994). The phylogenetic trees of Chapter 4 have been performed through Maximum Likelihood estimation (MLE) using MEGA7 with 1,000 replicates and the WAG+γ+I matrix (Kumar et al., 2016). The cladogram of evolutionary reconstructions have been obtained with Dendroscope (Huson and Scornavacca, 2012). Moreover, also the trees represented in Figures 3.6 and 5.2 have been constructed following the same procedure. The main Rab domains have been identified according to Park 2013 and aligned manually; it has been employed a domain-specific color code (Fig. 4.2).

7.1.2 - Intron survey

The splicing site conservation shown in Figures 3.3 and 4.3 has been evaluated using public genomic resources (NCBI, Ensembl) and mapped manually on alignment. Regarding intron analysis of Chapter 3, Rabs are represented using horizontal grey bars with three fundamental Rab domains represented by darker boxes: P-loop, Switch I, Switch II (Fig. 4.3). It has been uniformed the diversity of Rab proteins length considering 200 amino acid residues that corresponds to human RAB1A and manually mapped the conserved exon/intron structure with a color code. My reconstruction encompasses all the species selected for the phylogeny except *O. dioica* because few genomic information are available: i.e each single intron drawn in Fig. 3.3, represents the outcome of all selected species.

7.1.3 – Synteny analysis

The chromosomal conservation among Rab family metazoans (Chapter 3), it has been performed using synteny database of Oregon University (http://teleost.cs.uoregon.edu/synteny_db) (Catchen et al., 2009). Data shown in Figure 3.6 concerning Rab chimeras have been obtained by working manually on available genomic resources.

The synteny among Rab genomic *loci* of Fig. 4.3 and Suppl. Fig. 4.5 has been studied by manually mapping the genes on the scaffolds/chromosomes using available public resources (Ensembl, NCBI, Genomicus).

7.2 - Molecular biology approaches

7.2.1 - RNA extraction

For total RNA extraction, a mixture of amphioxus embryos from gastrula to 5 days-old larvae and susequently pelleted with a light centrifugation (1500-3000 rpm for 2-4 minutes); they have been kept at -20°C in Eurozol (EuroClone) until the RNA extraction. To obtain RNA from zebrafish embryos, a pool at the desired stage have been collected at -20°C in Eurozol (EuroClone) until the RNA extraction.

In order to avoid RNAase contaminations it is necessary to operate in sterile conditions. The samples conserved in Eurozol, have been homogenized with a pestle. After adding 0.1 volume of chloroform, the solution has been mixed and centrifuged at 14.000 rpm at 4°C. The aqueous phase has been collected and precipitated overnight with the same volume of isopropanol. Once precipitated, the sample has been centrifuged (14000 rpm) at 4°C for 30 minutes. The pellet has been washed with 70% ethanol, centrifuged, air-dried and resuspended in DEPC water. The sample's concentration has been measured with a "NanoDrop 1000"

spectrophotometer (Thermo, USA) while RNA integrity was evaluated on a 1% agarose gel. The obtained RNA has been stored at -80°C until use.

7.2.2 - cDNA preparation

cDNA has been prepared by *in vitro* reverse transcription using 0.5-1 μg of total RNA, drivingthe synthesis of DNA strand complementary to the RNA template with an RNA polymerase. It has been used the SuperScript VILO cDNA Synthesis kit (Invitrogen, India). 20 μl of reaction has been carried out in a thermocycling following this setting program: 25°C for 10 minutes, 42°C for 60 minutes, 85°C for 5 minutes. The cDNA has been mantained at -20°C until use.

7.2.3 - genomic DNA preparation

The spermduct has been cutted with a sharpen scalpel, to extract sperm from *Ciona robusta* adult specimens using a glass pipette. About 0.5 ml of fresh sperm has been mixed with 0.5 ml of RSB (10 mM NaCl, 10 mM Tris pH 7.5, 25mM EDTA pH 8.0). Subsequently, a concentration of 0.5 μg/ μl Proteinase K and 20X SDS have been added and the sample has been incubated into a water-bath for 1 hour at 45°C. After adding 1 volume of phenol:chloroform:isoamylic alcohol (25:24:1), the sample has been mixed and centrifuged for 20 minutes at 14000 rpm. The surnatant (containing genomic DNA) has been precipitated with ethanol 100 % and 1/10 volumes of ammonium acetate 2.5 M. After two washes with ethanol 80 %, genomic DNA has been dried at room temperature: then, I have diluted with 0.5 ml of sterile water; DNA quality has been assessed by gel electrophoresis. The sample has been stored at 4°C.

7.2.4 - Molecular cloning

Zebrafish Rab32 and Rab38 genes were cloned using the prediction available in the NCBI database: Rab32a (BC066502), Rab38a (XM_001342839.2), Rab38b (XM_003199354.1), Rab38c (XM_685900.3) and Klhl21 (NM_207081.1), while for mediterranean amphioxus have been used predicted sequences from the database of Amphioxus Genome Project Consortium. Regarding zebrafish, I have found expressed sequence tags (ESTs) in several developmental stages and body structures except for Rab38c. The cDNA sequences have been amplified through Polymerase Chain Reaction (Promega) using these oligo nucleotide pairs: BlRab32/38-F and BlRab32/38-R for amphioxus *Rab32/38*, BlRab32LO-F and BlRab32LO-R for amphioxus Rab32LO, DrRab32a-F and DrRab32a-R for zebrafish *Rab32a*, DrRab38a-F and DrRab38a-R for zebrafish *Rab38a*, DrRab38b-F and DrRab38b-R for zebrafish *Rab38b*, DrRab38c-F and DrRab38c-R for zebrafish *Rab38c*, DrKlhl21-F and DrKlhl21-R for zebrafish *Klhl21*. The amplification cycles have been conducted by means of Thermal Cycler Perkin-Elmer-Cetus. The gene fragments have been cloned using the TOPO-TA II Cloning Kit (Invitrogen). Regarding *Ciona robusta* genes, they have been prelevated from plasmids present in gene collection release I: tyrp1/2a (GC31h05), Msxb (GC42h24), Mitf (GC28k08), Klhl21(GC17e22). For putative regulatory region analysis, seven fragments have been cloned: CRCRklA-F and FCRklA-R for klA, CRklB-F and CRklB-R for klB, CRklC-F and CRklC-R for klC, CRklD-F and CRklD-R for klD, CRklE-F and CRklE-R for klE, CRklF-F and CRklF-R for klF, CRklG-F and CRklG-R for klG. All the oligos used in this thesis are listed in Supplementary Table 6.1.

7.2.5 - Constructs preparation for transgenesis *via* electroporation

Analytic and preparative plasmid DNA digestions have been performed using the appropriate restriction endonucleases in total volumes of 50 µl. The digestion reaction has been prepared as follows: 2,5 µg of DNA (GFP-SV40 vector and TOPO-TA vector in which *Ciona* genomi regions have been cloned; suitable restriction enzyme buffer (1/10. Roche; New England Biolabs; Amersham), XhoI and HindIII restriction enzymes (5 unites enzyme per 1 µg of DNA) and BSA (1/100, if required). Reaction has been performed at 37°C for three hours. To prevent self-ligation, a convenient amount of double strand linearized DNA has been incubated with 1U of Calf Intestinalis Alkaline Phosphatase enzyme (CIAP; Roche) per 1 pmol 5' ends of linearized DNA, in 1x CIP dephosphorylation buffer (Roche), at 37°C for 30'.

Each ligation reaction has been carried out in a final volume of 20 µl with a mix comprising 1x T4 Ligase buffer (50 mM Tris-HCl pH 7.5, 10 mM MgCl2, 10 mM dithiothreitol, 1 mM ATP, pH 7.5) and 1U of T4 DNA Ligase (New England Biolabs). The proportion of plasmid vector and insert DNA was tipically kept 1:3, and the total amount of DNA was kept within 50-100 ng. The reaction mix has been incubated at 16 °C overnight. The ligation products have been stored at 4°C.

7.2.6 - Isolation of plasmid DNA from *Escherichia coli*

Escherichia coli colonies have been picked from the plates and grown overnight at 37 °C by shaking in 4 ml of Luria-Bertani (LB) medium with 0,1 mg/ml of ampicillin. Mini-prep or Maxi-prep plasmide DNA isolations have been performed according to the protocols supplied of GenElute™ Plasmid Miniprep Kit (Sigma, USA) and GenElute™ Plasmid Maxiprep Kit (Sigma, USA). The eluted DNA has

been measured at the "NanoDrop 1000" spectrophotometer (Thermo, USA) as assorbance at 260 nm. For reducing the number of colonies to perform purification, PCR colony screening has been used to detect positive colonies. The colonies have been individually picked with a sterile plastic tip and dissolved into 12,5 µl of PCR reaction mix. M13 forward and M13 reverse primers corresponding to the insert sequence have been used for the amplification.

7.2.7 - DNA sequencing

Correct cloning was confirmed by sequencing of both DNA strands. It has been performed at the Molecular Biology Service of SZN employing Automated Capillary Electrophoresis Sequencer 3730 DNA Analyzer (Applied Biosystems, USA) with a BigDye® Terminator v3.1 Cycle Sequencing Kit (Life Technologies).

7.2.8 - Bacterial transformation and growth

The transformation of vectors with DNA of interest has been performed by electroporation in *E. coli* cells provided by the Molecular Biology Service of SZN and stored at -80°C. The cells have gently defrosted on ice for 10 minutes, and 40 µl are mixed with 4 µl of dialyzed vector, then the mix is transferred into electro-cuvette. The electric shock has been done by employing a "Bio-Rad Gene Pulser" with a constant voltage of 1.7 V. The transformed cells have been placed in 1 ml of Luria Bertani (LB) medium shaking at 270 rpm at 37 °C for 1 hour, then the cells have been plated on LB solid medium (NaCl 10g/l, tryptone 10 g/l, yeast extract 5 g/l, agar 15 g/l) (in volume of 200 and 600µl) in the presence of ampicillin (50 µg/ml) to which the plasmids are resistant. IPTG and

X-gal (4 µl + 40µl respectively) have added to perform the blue-white screening technique and grown overnight at 37°C.

7.2.9 - Site-directed mutagenesis

To perform diverse site-directed mutations in the putative regulatory region of Cr-Klhl21 gene, it has been used The QuikChange II Site-Directed Mutagenesis Kit (Agilent Technologies) directly on the construct to mutate (*klB>GFP*). The primers contain the desired mutation for annealing to the same sequence on opposite strands of the plasmid; the mutagenic primers have to be between 25 and 45 base pairs, with a melting temperature (Tm) of ≥78°C (longer oligos can increase the secondary structure formation, affecting efficiency of mutagenesis reaction). The most common formula for calculating melting temperature is: Tm =81.5+0.41(%GC)−(675/N)−% mismatch, where N is the primer length. The primers should have a minimum GC content of 40% and the selected mutation (deletion or insertion) should stay in the middle of the primer with ~10–15 bases of correct sequence on both sides (mutagenic oligos are listed in Suppl. Table 5.1). In a final volume of 50 µl, have been added 125 ng of both oligos and 1 µl of *PfuUltra* HF DNA polymerase (2.5 U/µl). Using thermal cycler, it has been employed this set of parameters, 30 seconds at 95°C followed by 16 cycles with 30 seconds at 95°C, 1 minute at 55°C, 1minute/kb of plasmid length (for instance, a plasmid of 3 kb needs 3 minutes). Immediately, the reaction mix must be placed on ice for 3 minutes, reaching ≥37°C. At this temperature, is performed a digestion with 1 µl of the Dpn I restriction enzyme (10 U/µl) at 37°C for one hour.

Then, it has been carried out chemical transformation using XL1-Blue Supercompetent Cells adding 1 µl of digestion product to 50 µl of cells. The reaction

has been incubated on ice for 30 minutes, 45 seconds at 42°C and placed on ice for 2 minutes. The transformation reaction has been mixed with 500 μl of LB medium and shaked at 37°C for one hour (225 rpm); subsequently, bacteria cells have been plated on LB solid medium with ampicillin, IPTG and X-gal (4 μl + 40μl respectively) have beenadded for the blue-white screening technique and grown overnight at 37°C.

7.2.10 - Riboprobe preparation

The DNA for riboprobe synthesis has been targeted by using M13fw and M13rev oligos, which are present in TOPO constructs. One μg of purified DNA has been used for *in vitro* transcription of the DIG- and FLUO labeled riboprobes, using SP6 and T7 RNA polymerases (Roche). The incubation consisted of two hours at 37°C with RNAse Inhibitor (Roche) and Transcription Buffer (Roche). The reaction has been blocked by using 0.25 M EDTA then the ribonucleic probes have been purified using 4 M lithium chloride (LiCl) transcripts. After adding cooled ethanol 100 %, they have been kept overnight at -20°C. Riboprobes have been washed with cooled ethanol 70 % and DEPC water; finally it has been added formammide and they have been stored at −80 °C until use.

7.2.11 - Quantitative real-time PCR (q PCR)

The expression of amphioxus mRNAs analyzed (Rab32/38, Rab32LO) has been studied through quantitative real time PCR (qPCR). Optimal cDNA concentration to use has been decided empirically, with serial dilutions. The qPCR has been performed in triplicate with a ViiATM 7 Real-Time PCR System (Applied Biosystems) in a 384-multi-well plate and each reaction has been carried out in a final volume of 10 μl with 0.7 pmol/μl of each primer, 5 μl of SYBR Green mix containing ROX (Applied Biosystems) and 1 μl of diluted cDNA. The parameters

selected for thermal cycling were: 95°C for 15 s, 40 cycles at 60°C for 1 min followed by a denaturation step from 60°C to 95°C with a continuous detection at 0.015°C/sec increment for 15 min to demonstrate the presence of a single product. The results have been analysed with the ViiA™ 7 Software and exported into Microsoft Excel for further analysis. Quantification results have been expressed in terms of cycle threshold (Ct). The Ct values were averaged for each triplicate. The ribosomal protein L32 (RPL32) gene was the endogenous control for the experiments. Differences between the mean RPL32 Ct value and those of the reference gene have been calculated as $\Delta Ctgene = Ctgene - Ctreference$. Relative expression has been analysed as $2-\Delta Ct$.

7.3 - Animal handling

7.3.1 - *Branchiostoma lanceolatum*

Adult amphioxus specimens (*Branchiostoma lanceolatum*) were collected from the Gulf of Naples (Italy) (40°48'33" N - 14°12'55" E) from a location that is not privately owned or protected. All procedures were in compliance with current available regulation for the experimental use of live animals in Italy. The animals were caught dragging on the soft bottom and collecting 5-10 cm of sand, with the support of the SZN vessel "Vettoria". After collecting sand at the depth of 5-12 meters, it was sifted on boat with a net characterized by a 1.25mm mesh (Fig.). Animal care is entrusted to "Aquaculture of Marine Organisms" facility at Zoological Station Anthon Dohrn of Naples. Animals were mantained in open circulating system reproducing natural thermal and ligh t conditions with continuous aeration and filtrated sea water. During the gonad maturation (April to July) temperature is maintained at 17°C, lower than the natural one, to avoid the natural emission of sperm and eggs in the tank. Animals were fed daily with a mix of three

unicellular microalgae: *Dunaliella tertiolecta*, *Isochrysis galbana* and *Tetraselmis suecica*. Gonads development starts in winter and arrives to maturation between spring and summer. In order to avoid the natural emission of sperm and eggs, the animals were mantaine at 17°C. Artificial spawning has been induced applying a heat shock to ripe animals. Animals with visible mature gonads were placed in a water bath settled at 5-6 degree of temperature higher respecto to the culturing system and the day after the animals have been divided one by one in glass beakers containing 100 ml filtered sea water for blocking uncontrolled fertilization. To obtain a spontaneous gonads release at the sunset, similar to natural spawning, the animals have been exposed to 36 hours temperature stress. Then, the adults are removed from beakers, the sperm from several males is mixed to increase the fertilization percentage and retained on ice. 200-300 eggs have been subdivided into petri dishes with scratched bottom because could attach there. Eggs have been fertilized with some drops of sperm mix. After approximately 10 minutes the percentage of fertilized eggs was checked by the elevation of the fertilization membrane. If less than 65% of fertilization, a further drop of sperm has been added. Subsequently, embryos have been rinsed two times using fresh sea water (FSW) so they can grow up to desired developmental stage in petri dishes at 18°C. Animals have been fixed at diverse developmental stages with 4 % paraformaldehyde (PFA) in MOPS overnight at 4 °C, and then stored at −20 °C in 70 % ethanol.

7.3.2 – *Ciona robusta*

C.robusta is a hermaphroditic broadcast spawner, present in Mediterranean Sea and in worldwide temperate costs. The animals used for experiments of this thesis, were fished by the crew of the SZN vessel "Vettoria" in the southern Italy, usually close to

Taranto in Puglia. At SZN, animals spent at least a week in an open circulating seawater tank at a temperature close to wild-type conditions to acclimate them. Animals were fed daily with *Spirulina platensis*. Animals care follows "Aquaculture of Marine Organisms" facility at Zoological Station Anthon Dohrn of Naples. The spawning period lasts from autumn to spring and to get gametes in laboratory, it is mandatory to sacrifice the animals. Using scalpel, tunic and muscles have been taken without damaging the gonaducts to do not cause premature mixing of. Sperm and eggs have been collected and kept separately until the fertilization that was carried out in 6cm petri dishes on agarose bottom.

7.3.3 – *Danio rerio*

Danio rerio

Wild-type AB zebrafish were mantained in a re-circulating water system at 28°C, on a 14 hours light/10 hours dark cycle. Embryos were staged in accordance to Kimmel et al. (1995) and all handling and breading protocols were performed in accordance to the GUIDELINES published in the Zebrafish Book (Nüsslein-Volhard and Dahm, 2012). The embryos up to 4 dpf have been obtained from natural spawning of wild-type animals and fixed overnight in 4 % PFA in PBS at 4 °C, then washed three times in PBS and stored at −20 °C in methanol. The protocols for handling of zebrafish and experiments involving not feeding larvae were approved by the ethical committee of the Stazione Zoologica Anton Dohrn of Napoli, Italy (Animal Welfare Body).

7.4 - Developmental biology approaches

7.4.1 - Whole-mount *in situ* hybridization

Branchiostoma lanceolatum

Whole-mount in situ hybridization (WISH) experiments in amphioxus have been performed following the protocol described in Irimia et al. (2010). Fixed embryos have re-hydrated digestion and rinsed in a phos- phate buffered saline solution containing Tween20 0.1 % (PBT). After that, it has been performed a treatment with Proteinase K (5 μg/ml) to facilitate the riboprobe penetration and the reaction has been blocked by washing with a solution of 2 mg/ml glycine in PBT. The embryos have been refixed in PBT containing 4 % PFA for 1 h at RT and then rinsed in 0.1 M triethanolamine with acetic anhydride to bleach the natural pigments of the embryos. After several washes in PBT, it has been carried out overnight hybridization at 65 °C in DEPC water hybridization buffer (50 % deionized formamide; 100 μg/ ml Heparin; 5× SSC; 0.1 % Tween20; 5 mM EDTA; 1× Denhardt's 1 mg/ml; 50 mg/ml yeast RNA). The day after embryos have been washed in HB and in solution containing HB plus decreasing concentrations of SSC. Embryos have been incubated overnight at 4°C with anti-DIG-AP (Roche) diluted 1:1000. After antibody incubation, embryos have been stained in BM Purple (Roche) at room temperature. Once reached desired signal expression, embryos have been washed in PBS and fixed for 1 h in 4 % PFA in PBT; they have been stored in glycerol/PBT (80-20 %). Embryo image capturing has been performed employing a Zeiss Axio Imager M1.

Ciona robusta

Embryos for single and double fluorescent WISH have been fixed at the different developmental stages for 2 h in 4% MEM-PFA (4% paraformaldehyde, 0.1 M MOPS pH 7.4, 0.5 M NaCl, 1 mM EGTA, 2 mM MgSO4, 0.05% Tween 20), then rinsed in

PBS and stored in 75% ethanol at -20 °C. Embryos have been treated with 2% H_2O_2 dissolved in methanol for 30 min at room temperature, and then washed in PBT.

They have been hybridized overnight at 60°C using hybridization buffer (HB) in DEPC water (50 % Formammide; 100 µg/ml Heparin; 1.3X SSC; 0.2 % Tween20; 5 mM EDTA pH 8,0; 50 µg/ml Yeast RNA). After two steps in HB, embryos have been washed with solutions with increasing concentrations of SSC. Then, embryos have been washed in PBT, equilibrated in TNT (100 mM Tris pH 7.5, 150 mM NaCl, 0.1% Tween 20) and blocked in TNB (0.5% Roche blocking reagent in 100 mM Tris pH 7.5, 150 mM NaCl) for 1–2 h. Anti-FLUO-POD and anti-DIG-POD (Roche) antibodies have diluted 1:1000 in TNB and the incubation has been carried out overnight at 4 °C. Embryos have been washed extensively in TNT. Concerning tyramide signal amplification, Cy3- and Cy5-coupled TSA Plus reagent (Perkin Elmer) has been diluted 1:400 in amplification buuffer and added to embryos for 5–10 min at room temperature. For 4,6- diamidino-2-phenylindole staining, DAPI (Sigma) has been dissolved 1:10000 in PBT, and embryos have been incubated overnight at 4 °C, subsequently washed three times in PBT. Finally, embryos have been stored in PBT at 4°C (Christiaen et al., 2009). Embryo imaging has been carried out using a Zeiss Axio Imager M1 and a Zeiss LSM 510 META confocal microscope.

Danio rerio

In zebrafish, whole-mount in situ hybridization (WISH) has been performed following Thisse and Thisse protocol (2008). After rehydration steps, embryos have been permeabilized employing Proteinase K (10 µg/ml), and the reaction has been stopped through fast washes in PBT. The embryos have been refixed in 4 % PFA in PBT for 1 h at RT and rinsed with PBT many times. They have been hybridized

overnight at 65 °C in hybridization buffer (HB) in DEPC water (50 % Formammide; 100 μg/ml Heparin; 1.3X SSC; 0.2 % Tween20; 5 mM EDTA pH 8,0; 50 μg/ml Yeast RNA; 0.5 % CHAPS). The day after embryos have been washed in HB and in solution containing HB plus decreasing concentrations of SSC. After fast washes in maleic acid buffer (MAB) in DEPC water, embryos have been incubated overnight at 4°C with anti-DIG-AP (Roche) diluted 1:400. After antibody incubation, embryos have been rinsed many times in MAB plus Tween 0,1 % and, subsequently, it has been been performed the coloration using BM-Purple (Roche) at room temperature. Embryos with desired signal have been washed several times with PBT and, to obtain a stronger signal visualization, put in methanol overnight at 4°C. After that, they have been stored in glycerol/PBT (70-30 %). Embryo image capturing has been performed with a Zeiss Axio Imager M1.

7.4.2 - *C. robusta* electroporation

Ripe oocytes and sperm have been collected and stored separately until *in vitro* fertilization. Chorion and follicular cells have been eliminated chemically by using a pH 10 solution of Thioglycolic acid (1%) and Proteinase E (0.05%) in Millipore-filtered sea water (MFSW). Embryos have been shaken with a glass pipette for 7-8 minutes and washed many times with fresh MSFW. Then, have been fertilized the eggs and subsequently washed three times in MFSW transferred in a solution with 0.77 M Mannitol and the DNA necessary for electroporation (usually 50–80 mg of each plasmid) (Christiaen et al., 2009). The electroporation experiments have been carried out in Bio-Rad Gene Pulser 0.4 cm cuvettes, employing Gene Pulser II (Bio-Rad) (Christiaen et al., 2009); each experiment has been performed at least three

times. Embryos were staged according to the developmental timeline established in Hotta et al. 2007. For embryo imaging it has been used a Zeiss Axio Imager M1.

APPENDIX

Supplementary Table 3.1. List of different kinds of duplication occurred inside Rab Family.

Chr = human chromosomes

Ohnologues:

- **Rab1A(chr2)-Rab1B(chr11)**
- **Rab2A(chr8)-Rab2B(chr14)**
- **Rab3A/D(chr19)-Rab3B(chr1)-Rab3C(chr5)**
- **Rab4A(chr1)-Rab4B(chr19)**
- **Rab5A(chr3)-Rab5B(chr12)-Rab5C(chr17)**
- **Rab6A(chr11)-Rab6B(chr3)-Rab6C(chr2)-Rab41(chrX)**
- **Rab8A(chr19)-Rab8B(chr15)-Rab13(chr1)**
- **Rab11(chr15)-Rab11B(chr19)-Rab25(chr1)**
- **Rab19(chr7)-Rab43(chr3)**
- **Rab22A(chr20)-Rab22B(chr18)**
- **Rab26(chr16)-Rab37(chr17)**
- **Rab27A(chr15)-Rab27B(chr18)**
- **Rab32(chr6)-Rab38(chr11)**
- **Rab33A(chrX)-Rab33B(chr4)**
- **Rab34(chr17)-Rab36(chr22)**
- **Rab39A(chr11)-Rab39B(chrX)**
- **EFcab4A(chr11)-EFcab4B(chr12)-Rab44(chr6)**

Vertebrate tandem-duplicates:

- **Rab3A-Rab3D   (chr19)**
- **Rab9A-Rab9B   (chrX)**
- **Rab40A-Rab40AL (chrX, primate-specific duplication)**

Vertebrate gene duplicates:

- **Rab7A (chr3)**
- **Rab7B (chr1)**
- **Rab17 (chr2)**
- **Rab21 (chr12)**
- **Rab40B (chr17)**
- **Rab40C (chr16)**
- **Rab42 (chr1)**

Reptile-specific duplicates:

- **Rab18a (chr5)**
- **Rab18b (chr6)**

Hemichordates tandem-duplicates:

- **Rab5a, Rab5b, Rab5c, Rab5d, Rab5e (NW_003141315.1)**

Supplementary Table 3.2. This figure shows conservation amongst genomic loci harbouring EFcab4/Rab44 subfamily members (blue). Syntenic genes belong to TSPAN (yellow), CDKN (green), KCNQ (orange); human chromosome 1 represents the site of fourth member of this subfamily and on the chromosome 11 there is a cluster of mucin (MUC, violet). Under the genes are drawn arrows symbolizing the transcription direction.
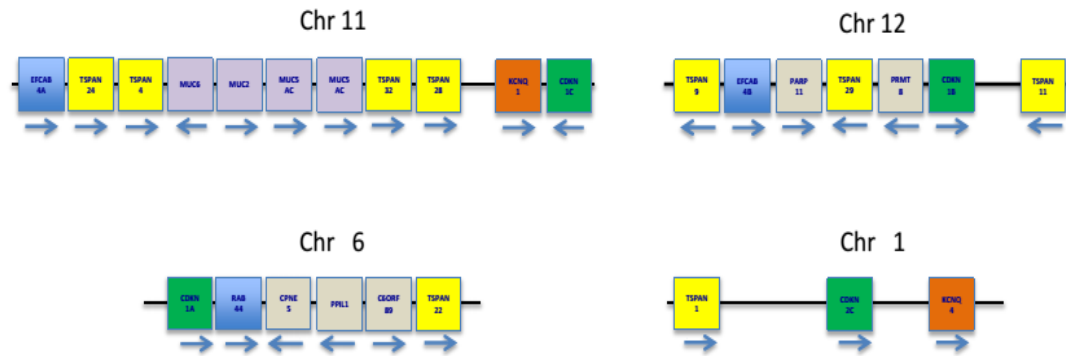
Supplementary Table 4.1. Table containing proteins used for all the evolutionary analyses of Chapter 4.

Species	Protein Name	Accession Number	Database
Capitella capitella	Rab23	ELT90055.1	NCBI
	Rab7	ELU11591.1	NCBI
	Rab9	ELU08962.1	NCBI
	Rab7L1	ELT94920.1	NCBI
	Rab32/38	ELU06149	NCBI
	Rab32LO	ELT98053	NCBI
Lottia gigantea	Rab23	LotgiP103096	Ensembl
	Rab7	LotgiP223383	Ensembl
	Rab32/38	LotgiP171871	Ensembl
	Rab32LO	LotgiP96617	Ensembl
Saccoglossus kowalevskii	Rab23	XP_002732916.1	NCBI
	Rab7	XP_006820804.1	NCBI
	Rab9	XP_002737937.1	NCBI
	Rab7L1	XP_006825119.1	NCBI
	Rab32/38	XP_002733795.1	NCBI
Strongylocentrotus purpuratus	Rab23	XP_003729499.1	NCBI
	Rab7	NP_001116983.1	NCBI
	Rab9	XP_791345.3	NCBI
	Rab7L1	XP_786497.2	NCBI
	Rab32/38	XP_782400.2	NCBI
	Rab32LO	XP_003731406.1	NCBI
Ciona intestinalis	Rab23	XP_002121180.1	NCBI

	Rab7	XP_002128753.1	NCBI
	Rab9	XP_002131619.1	NCBI
	Rab7L1	XP_002122178.2	NCBI
	Rab32/38	XP_002130668.1	NCBI
Petromyzon marinus	Rab32/38	ENSPMAP00000000405	Ensembl
Danio rerio	Rab23	ENSDARP00000002531	Ensembl
	Rab9a	ENSDARP00000136173	Ensembl
	Rab9b	ENSDARP00000140695	Ensembl
	Rab7a	AAI55203	NCBI
	Rab32a	AAH66502	NCBI
	Rab32b	XP_001340450.2	NCBI
	Rab38a	XP_001342875.2	NCBI
	Rab38b	XP_003199402	NCBI
	Rab38c	XP_690992	NCBI
Latimeria chalumnae	Rab32	ENSLACP00000023562	Ensembl
	Rab38a	ENSLACP00000000658	Ensembl
	Rab38c	ENSLACP00000012385	Ensembl
Callorinchus milii	Rab32	SINCAMP00000023543	Ensembl
	Rab38a	SINCAMP00000022146	Ensembl
	Rab38c	SINCAMP00000019284	Ensembl
Lepisosteus oculatus	Rab32	ENSLOCP00000019896	Ensembl
	Rab38a	ENSLOCP00000019896.2	Ensembl
	Rab38c	ENSLOCP00000019896.3	Ensembl
Anolis carolinensis	Rab23	ENSLOCP00000019896.4	NCBI
	Rab9A	ENSLOCP00000019896.5	NCBI
	Rab9B	ENSLOCP00000019896.6	NCBI
	Rab7	ENSLOCP00000019896.7	NCBI
	Rab7L1	ENSLOCP00000019896.8	NCBI
	Rab32	ENSLOCP00000019896.9	NCBI
	Rab38	ENSLOCP00000019896.10	NCBI
Xenopus tropicalis	Rab32	ENSLOCP00000019896.11	NCBI
	Rab38	ENSLOCP00000019896.12	NCBI
Gallus gallus	Rab32	ENSLOCP00000019896.13	Ensembl
	Rab38	ENSLOCP00000019896.14	Ensembl
Mus musculus	Rab32	ENSLOCP00000019896.15	NCBI
	Rab38	ENSLOCP00000019896.16	NCBI
Homo sapiens	RAB23	ENSLOCP00000019896.17	Ensembl
	RAB7A	ENSLOCP00000019896.18	Ensembl
	RAB9A	ENSLOCP00000019896.19	Ensembl
	RAB9B	ENSLOCP00000019896.20	Ensembl
	RAB7L1	ENSLOCP00000019896.21	NCBI
	RAB32	ENSLOCP00000019896.22	NCBI
	RAB38	ENSLOCP00000019896.23	NCBI
Capitella teleta	Grm1/5	ENSLOCP00000019896.24	NCBI
Lottia gigantea	Grm1/5	ENSLOCP00000019896.25	Ensembl

Saccoglossus kowalevskii	Grm1/5	ENSLOCP00000019896.26	NCBI
Branchiostoma floridae	Grm1/5	ENSLOCP00000019896.27	NCBI
Callorinchus milii	Grm1	ENSLOCP00000019896.28	NCBI
	Grm2	ENSLOCP00000019896.29	NCBI
	Grm3	ENSLOCP00000019896.30	NCBI
	Grm4	ENSLOCP00000019896.31	NCBI
	Grm5	ENSLOCP00000019896.32	NCBI
	Grm7	ENSLOCP00000019896.33	NCBI
	Grm8	ENSLOCP00000019896.34	NCBI
Lepisosteus oculatus	Grm1	ENSLOCP00000019896.35	Ensembl
	Grm2	ENSLOCP00000019896.36	Ensembl
	Grm3	ENSLOCP00000019896.37	Ensembl
	Grm4	ENSLOCP00000019896.38	Ensembl
	Grm5	ENSLOCP00000019896.39	Ensembl
	Grm6	ENSLOCP00000019896.40	Ensembl
	Grm7	ENSLOCP00000019896.41	Ensembl
	Grm8	ENSLOCP00000019896.42	Ensembl
Danio rerio	Grm1a	ENSLOCP00000019896.43	Ensembl
	Grm1b	ENSLOCP00000019896.44	Ensembl
	Grm2a	ENSLOCP00000019896.45	Ensembl
	Grm2b	ENSLOCP00000019896.46	Ensembl
	Grm3	ENSLOCP00000019896.47	Ensembl
	Grm4	ENSLOCP00000019896.48	Ensembl
	Grm5a	ENSLOCP00000019896.49	Ensembl
	Grm5b	ENSLOCP00000019896.50	Ensembl
	Grm6a	ENSLOCP00000019896.51	Ensembl
	Grm6b	ENSLOCP00000019896.52	Ensembl
	Grm8a	ENSLOCP00000019896.53	Ensembl
	Grm8b	ENSLOCP00000019896.54	Ensembl
Homo sapiens	GRM1	ENSLOCP00000019896.55	Ensembl
	GRM2	ENSLOCP00000019896.56	Ensembl
	GRM3	ENSLOCP00000019896.57	Ensembl
	GRM4	ENSLOCP00000019896.58	Ensembl
	GRM5	ENSLOCP00000019896.59	Ensembl
	GRM6	ENSLOCP00000019896.60	Ensembl
	GRM7	ENSLOCP00000019896.61	Ensembl
	GRM8	ENSLOCP00000019896.62	Ensembl
Callorinchus milii	Fzd1	ENSLOCP00000019896.63	NCBI
	Fzd2	ENSLOCP00000019896.64	NCBI
	Fzd3	ENSLOCP00000019896.65	NCBI
	Fzd4	ENSLOCP00000019896.66	NCBI
	Fzd5	ENSLOCP00000019896.67	NCBI
	Fzd6	ENSLOCP00000019896.68	NCBI
	Fzd7	ENSLOCP00000019896.69	NCBI
	Fzd8	ENSLOCP00000019896.70	NCBI

	Fzd9	ENSLOCP00000019896.71	NCBI
	Fzd10	ENSLOCP00000019896.72	NCBI
Lepisosteus oculatus	Fzd1	ENSLOCP00000019896.73	NCBI
	Fzd2	ENSLOCP00000019896.74	NCBI
	Fzd3	ENSLOCP00000019896.75	NCBI
	Fzd4	ENSLOCP00000019896.76	NCBI
	Fzd5	ENSLOCP00000019896.77	NCBI
	Fzd6	ENSLOCP00000019896.78	NCBI
	Fzd7	ENSLOCP00000019896.79	NCBI
	Fzd8	ENSLOCP00000019896.80	NCBI
	Fzd9	ENSLOCP00000019896.81	NCBI
	Fzd10	ENSLOCP00000019896.82	NCBI
Homo sapiens	FZD1	ENSLOCP00000019896.83	NCBI
	FZD2	ENSLOCP00000019896.84	NCBI
	FZD3	ENSLOCP00000019896.85	NCBI
	FZD4	ENSLOCP00000019896.86	NCBI
	FZD5	ENSLOCP00000019896.87	NCBI
	FZD6	ENSLOCP00000019896.88	NCBI
	FZD7	ENSLOCP00000019896.89	NCBI
	FZD8	ENSLOCP00000019896.90	NCBI
	FZD9	ENSLOCP00000019896.91	NCBI
	FZD10	ENSLOCP00000019896.92	NCBI
Callorhincus milii	Fat1	ENSLOCP00000019896.93	NCBI
	Fat2	ENSLOCP00000019896.94	NCBI
	Fat3	ENSLOCP00000019896.95	NCBI
	Fat4	ENSLOCP00000019896.96	NCBI
	Fat4like	ENSLOCP00000019896.97	NCBI
Lepisosteus oculatus	Fat1	ENSLOCP00000019896.98	NCBI
	Fat2	ENSLOCP00000019896.99	NCBI
	Fat3	ENSLOCP00000019896.100	NCBI
	Fat4	ENSLOCP00000019896.101	NCBI
Danio rerio	Fat1a	ENSLOCP00000019896.102	Ensembl
	Fat1b	ENSLOCP00000019896.103	Ensembl
	Fat2	ENSLOCP00000019896.104	Ensembl
	Fat3	ENSLOCP00000019896.105	Ensembl
	Fat4	ENSLOCP00000019896.106	Ensembl
Homo sapiens	FAT1	ENSLOCP00000019896.107	Ensembl
	FAT2	ENSLOCP00000019896.108	Ensembl
	FAT3	ENSLOCP00000019896.109	Ensembl
	FAT4	ENSLOCP00000019896.110	Ensembl
Mus musculus	Fat1	ENSLOCP00000019896.111	NCBI
	Fat2	ENSLOCP00000019896.112	NCBI
	Fat3	ENSLOCP00000019896.113	NCBI
	Fat4	ENSLOCP00000019896.114	NCBI
Callorhincus milii	Nox1	ENSLOCP00000019896.115	NCBI

	Nox3	ENSLOCP00000019896.116	NCBI
	Nox4	ENSLOCP00000019896.117	NCBI
	Nox5	ENSLOCP00000019896.118	NCBI
Lepisosteus oculatus	Nox1	ENSLOCP00000019896.119	Ensembl
	Nox3	ENSLOCP00000019896.120	Ensembl
	Nox4	ENSLOCP00000019896.121	Ensembl
	Nox5	ENSLOCP00000019896.122	Ensembl
Homo sapiens	NOX1	ENSLOCP00000019896.123	NCBI
	NOX3	ENSLOCP00000019896.124	NCBI
	NOX4	ENSLOCP00000019896.125	NCBI
	NOX5	ENSLOCP00000019896.126	NCBI
Mus musculus	Nox1	ENSLOCP00000019896.127	NCBI
	Nox3	ENSLOCP00000019896.128	NCBI
	Nox4	ENSLOCP00000019896.129	NCBI
Callorhincus milii	Tab1	ENSLOCP00000019896.130	NCBI
	Tab2	ENSLOCP00000019896.131	NCBI
	Tab3	ENSLOCP00000019896.132	NCBI
Lepisosteus oculatus	Tab2	ENSLOCP00000019896.133	Ensembl
	Tab3	ENSLOCP00000019896.134	Ensembl
Danio rerio	Tab1	ENSLOCP00000019896.135	Ensembl
	Tab2	ENSLOCP00000019896.136	Ensembl
	Tab3	ENSLOCP00000019896.137	Ensembl
Homo sapiens	TAB1	ENSLOCP00000019896.138	NCBI
	TAB2	ENSLOCP00000019896.139	NCBI
	TAB3	ENSLOCP00000019896.140	NCBI
Mus musculus	Tab1	ENSLOCP00000019896.141	NCBI
	Tab2	ENSLOCP00000019896.142	NCBI
	Tab3	ENSLOCP00000019896.143	NCBI
Callorinchus milii	Stxbp1	ENSLOCP00000019896.144	NCBI
	Stxbp2	ENSLOCP00000019896.145	NCBI
	Stxbp3	ENSLOCP00000019896.146	NCBI
	Stxbp4	ENSLOCP00000019896.147	NCBI
	Stxbp5	ENSLOCP00000019896.148	NCBI
	Stxbp5L	ENSLOCP00000019896.149	NCBI
	Stxbp6	ENSLOCP00000019896.150	NCBI
Lepisosteus oculatus	Stxbp1	ENSLOCP00000019896.151	Ensembl
	Stxbp2	ENSLOCP00000019896.152	Ensembl
	Stxbp3	ENSLOCP00000019896.153	Ensembl
	Stxbp4	ENSLOCP00000019896.154	Ensembl
	Stxbp5a	ENSLOCP00000019896.155	Ensembl
	Stxbp5L	ENSLOCP00000019896.156	Ensembl
	Stxbp6	ENSLOCP00000019896.157	Ensembl
Danio rerio	Stxbp1a	ENSLOCP00000019896.158	Ensembl
	Stxbp1b	ENSLOCP00000019896.159	Ensembl
	Stxbp2	ENSLOCP00000019896.160	Ensembl

	Stxbp3	ENSLOCP00000019896.161	Ensembl
	Stxbp4	ENSLOCP00000019896.162	Ensembl
	Stxbp5a	ENSLOCP00000019896.163	Ensembl
	Stxbp5b	ENSLOCP00000019896.164	Ensembl
	Stxbp5L	ENSLOCP00000019896.165	Ensembl
	Stxbp6	ENSLOCP00000019896.166	Ensembl
	Stxbp6L	ENSLOCP00000019896.167	Ensembl
Homo sapiens	STXBP1	ENSLOCP00000019896.168	Ensembl
	STXBP2	ENSLOCP00000019896.169	Ensembl
	STXBP3	ENSLOCP00000019896.170	Ensembl
	STXBP4	ENSLOCP00000019896.171	Ensembl
	STXBP5	ENSLOCP00000019896.172	Ensembl
	STXBP5L	ENSLOCP00000019896.173	Ensembl
	STXBP6	ENSLOCP00000019896.174	Ensembl
Mus musculus	Stxbp1	ENSLOCP00000019896.175	Ensembl
	Stxbp2	ENSLOCP00000019896.176	Ensembl
	Stxbp3a	ENSLOCP00000019896.177	Ensembl
	Stxbp3b	ENSLOCP00000019896.178	Ensembl
	Stxbp4	ENSLOCP00000019896.179	Ensembl
	Stxbp5	ENSLOCP00000019896.180	Ensembl
	Stxbp5L	ENSLOCP00000019896.181	Ensembl

Supplementary Table 4.2. A) The scheme represents insertions on Rab38 locus of human chromosome 11 (TRIMs, light blue) and f mouse chromosome 7 (OR, orange; Vmn2r, light blue). B) Conserved microsynteny of Rab32LO (blue) and Tim9 (grey) between sea urchin and amphioxus.
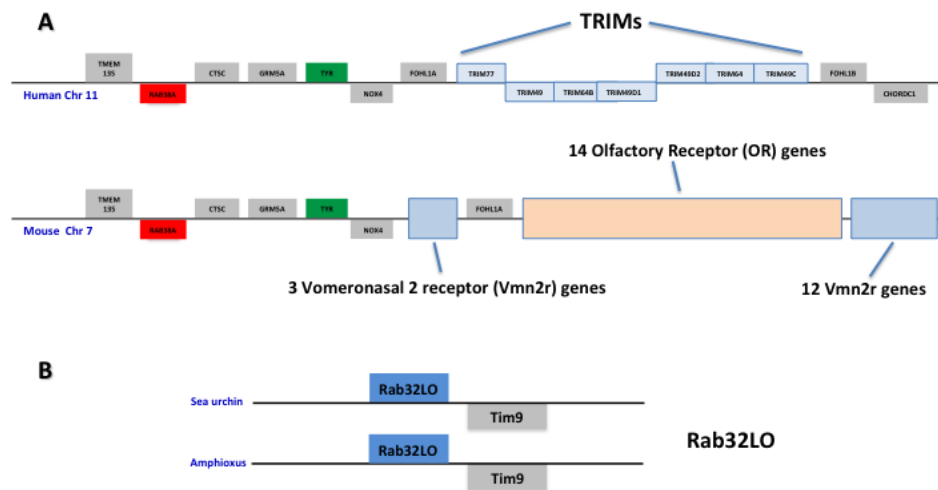
Supplementary Table 4.3. Here are shown expression levels obtained from RT-PCR experiments conducted on *Branchiostoma lanceolatum Rab32/38* (blue) and *Rab32LO* (yellow) genes. As control, it has been used *Rpl32* (Fw: GGCTTCAAGAAATTCCTCGTC, Rev: GATGAGTTTCCTCTTGCGTGA)
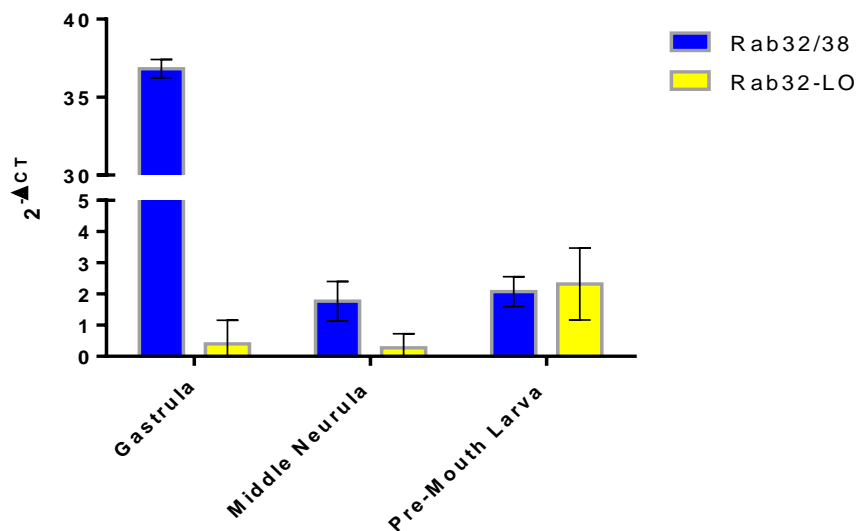
Supplementary Table 4.4. Alignment of main Rab domains of Rab32/38 members in teleosts, similarly to Figure 4.3.

```
Petromyzon marinus       Rab32    GELGVGKT  FSHGYRATIGVDFALK   DIAGQERFGNMTR
Callorhinchus milii      Rab32    GELGVGKT  FSQNYRATIGVDFALK   DIAGQERFGNMTR
Leucoraja erinacea       Rab32    GDLGVGKT  FSQNYRATIGVDFALK   DIAGQERFGNMTR
Lepisosteus oculatus     Rab32    GELGVGKT  FSQHYRATIGVDFALK   DIAGQERFGNMTR
Danio rerio              Rab32a   GELGVGKT  FSQHYRATIGVDFALK   DIAGQERFGNMTR
                         Rab32b   GDHKVGKS  FYEELKTSIGVDSMA    DIAGQERVRGLNR
Xiphophorus maculatus    Rab32    GELGVGKT  FSQHYRATIGVDFALK   DIAGQERFGNMTR
Tetraodon nigroviridis   Rab32    GELGVGKT  FSQHYRATIGVDFALK   DIAGQERFGNMTR
                         Rab32b   GDLGVGKS  FVEKYKASIGVDFALK   DIAGQERFRKMSR
Takifugu rubripes        Rab32    GELGVGKT  FSQHYRATIGVDFALK   DIAGQERFGNMTR
Gasterosteus aculeatus   Rab32a   GELGVGKT  FSQHYRATIGVDFALK   DIAGQERFGNMTR
                         Rab32b   GDVGVGKS  FNETYKASIGVDFALK   DIGGQERFRKMSR
Maylandia zebra          Rab32a   GELGVGKT  FSQHYRATIGVDFALK   DIAGQERFGNMTR
                         Rab32b   GDLGVGKS  FDETYKASIGVDFALK   DIGGQERFKNMSR
Oreochromis niloticus    Rab32a   GELGVGKT  FSQHYRATIGVDFALK   DIAGQERFGNMTR
                         Rab32b   GDLGVGKS  FDETYKASIGVDFALK   DTGGQERVKNMSR
Nothobranchius furzeri   Rab32a   GELGVGKT  FSQHYRATIGVDFALK   DIAGQERFGNMTR
Gadus morhua             Rab32a   GELGVGKT  FSQHYRATIGVDFALK   DIAGQERFGNMTR
Oryzias latipes          Rab32a   GELGVGKT  FSQHYRATIGVDFALK   DIAGQERFGNMTR
Salmo salar              Rab32a   GELGVGKT  FSQHYRATIGVDFALK   DIAGQERFGNMTR
                         Rab32b   GELGVGKT  FSQHYRATIGVDFALK   DIAGQERFGNMTR
                         Rab32c   GERGVGKT  FKEEYKASIGVDFALK   DIAGQERFGNMTR
Stegastes partitus       Rab32a   GDVKVGKS  FDENYKGTIGIDTL     DIAGQDRFCNMSR
Latimeria chalumnae      Rab32    GELGVGKT  FSQHYRATIGVDFALK   DIAGQERFGNMTR
Homo sapiens             RAB32    GELGVGKT  FSQHYRATIGVDFALK   DIAGQERFGNMTR


Callorhinchus milii      Rab38a   GDLGVGKT  FSQHYRATIGVDFALK   DIAGQERFGNMTR
                         Rab38c   GDLGVGKT  FSQHYRATIGVDFALK   DIAGQERFGNMTR
Leucoraja erinacea       Rab38    GDLGVGKT  FSQHYRATIGVDFALK   DIAGQERFGNMTR
Lepisosteus oculatus     Rab38b   GDLGVGKT  YSPNYRATIGVDFALK   DIAGQERFGNMTR
                         Rab38c   GDLGVGKT  FSQHYRATIGVDFALK   DIAGQERYGNMTR
Danio rerio              Rab38a   GDLGVGKT  FSPNYRATIGVDFALK   DIAGQERFGNMTR
                         Rab38b   GDLGVGKT  YSTNYRATIGVDFALK   DIAGQERFGNMTR
                         Rab38c   GDLGVGKT  FSQHYRATIGVDFALK   DIAGQERYGNMTR
Xiphophorus maculatus    Rab38a   GDLGVGKT  FSPNYRATIGVDFALK   DIAGQERFGNMTR
                         Rab38b   GDLGVGKT  FSSNYRATIGVDFALK   DIAGQERFGNMTR
                         Rab38c   GDLGVGKT  FSQHYRTTIGVDFALK   DIAGQERYGNMTR
Tetraodon nigroviridis   Rab38a   GDLGVGKT  FSPNYRATIGVDFALK   DIAGQERFGNMTR
                         Rab38b   GDLGVGKT  YSNNYRATIGVDFAMA   DIAGQERFGNMTR
                         Rab38c   GDLGVGKT  FSQHYRATIGVDFALR   DIAGQERYGHMTR
Takifigu rubripes        Rab38a   GDLGVGKT  FSPNYRATIGVDFALK   DIAGQERFGNMTR
                         Rab38b   GDLGVGKT  YSNNYRATIGVDFALK   DIAGQERFGNMTR
                         Rab38c   GDIGVGKT  FSQHYRATIGVDFALK   DIAEGQRYGNMTR
Gasterosteus aculeatus   Rab38a   GDLGVGKT  FSPNYRATIGVDFALK   DIAGQERFGNMTR
                         Rab38b   GDLGVGKT  YSTNYRATIGVDFALK   DIAGQERFGNMTR
                         Rab38c   GDLGVGKT  FSQHYRATIGVDFALK   DIAGQERYGNMTR
Maylandia zebra          Rab38a   GDLGVGKT  FSPNYRATIGVDFALK   DIAGQERFGNMTR
                         Rab38b   GDLGVGKT  YSTNYRATIGVDFALK   DIAGQERFGNMTR
                         Rab38c   GDLGVGKT  FSQHYRATIGVDFALK   DIAGQERYGNMTR
Oreochromis niloticus    Rab38a   GDLGVGKT  FSPNYRATIGVDFALK   DIAGQERFGNMTR
                         Rab38b   GDLGVGKT  YSTNYRATIGVDFALK   DIAGQERFGNMTR
                         Rab38c   GDHGVGKT  FSQHYRATIGVDFALK   DIAGQERYGNMTR
Notobranchius furzeri    Rab38a   GDLGVGKT  FSPNYRATIGVDFALK   DIAGQERFGNMTR
                         Rab38b   GDLGVGKT  YSSNYRATIGVDFALK   DIAGQERFGNMTR
                         Rab38c   GDIGVGKT  FSQHYRTTIGVDFALK   DIAGQERYGNMTR
Gadus morhua             Rab38a   GDLGVGKT  FSPNYRATIGVDFALK   DIAGQERFGNMTR
                         Rab38b   GDLGVGKT  YSANYRATIGVDFALK   DIAGQERFGNMTR
                         Rab38c   GDLGVGKT  FSQHYQATIGVDFALK   DIAGQERYGNMTR
Oryzias latipes          Rab38a   GDLGVGKT  FSPNYRATIGVDFALK   DIAGQERFGNMTR
                         Rab38b   GDLGVGKT  YSTNYRATIGVDFALK   DIAGQERFGNMTR
                         Rab38c   GDLGVGKT  FSQHYRATIGVDFVLK   DIAGQERYGNMTR
Salmo salar              Rab38a   GDLGVGKT  FSPNYRATIGVDFALK   DIAGQERFGNMTR
                         Rab38b   GDLGVGKT  YSTNYRATIGVDFALK   DIAGQERFGNMTR
                         Rab38c   GDLGVGKT  FSQHYRATIGVDFALK   DIAGQERYGNMTR
                         Rab38d   GDLGVGKT  FSQHYRATIGVDFALK   DIAGQERYGNMTR
                         Rab38e   GDLGVGKT  FSQHYRATIGVDFALK   DIAGQERYGNMTR
Astyanax mexicanus       Rab38a   GDLGVGKS  FSPNYRATIGVDFALK   DIAGQERFGNMTR
                         Rab38b   GDLGVGKT  YSTNYRATIGVDFALK   DIAGQERFGNMTR
                         Rab38c   GDLGVGKT  FSQHYRATIGVDFALK   DIAGQERYGNMTR
Latimeria chalumnae      Rab38a   GDLGVGKT  FSPHYRATIGVDFALK   DIAGQERFGNMTR
                         Rab38c   GEIGVGKT  FYHHYRATIGVDFALK   DIAGQERFGNMTR
Homo sapiens             RAB38    GDLGVGKT  FSPHYRATIGVDFALK   DIAGQERFGNMTR
```

Supplementary Table 5.1. Table comprising proteins used for phylogenetic tree of Figure 4.2.

Species	Protein Name	Accession Number	Database
Branchiostoma floridae	Klhl21	XP_002602326.1	NCBI
	Klhl6/24	XP_0026o5784.1	NCBI
Ciona robusta	Klhl21	XP_002128060.2	NCBI
	Klhl6	XP_018670466.1	NCBI
	Klhl24	XP_002129210.1	NCBI
Ciona savignyi	Klhl21	ENSCSAVP00000018227.1	Ensembl
	Klhl6	ENSCSAVP00000007741.1	Ensembl
	Klhl24	ENSCSAVP00000009638.1	Ensembl
Callorhinchus milii	Klhl21	XP_007900314.1	NCBI
	Klhl6	XP_007903332.1	NCBI
	Klhl24	XP_007903188.1	NCBI
	Klhl29	XP_007895224.1	NCBI
	Klhl30	XP_007905024.1	NCBI
Latimeria chalumnae	Klhl21	ENSLACP00000017967.2	Ensembl
	Klhl6	ENSLACP00000019231.2	Ensembl
	Klhl24	ENSLACP00000019062.2	Ensembl
	Klhl30	ENSLACP00000012967.2	Ensembl
Danio rerio	Klhl21	NP_001307336.1	NCBI
	Klhl6	NP_001005316.2	NCBI
	Klhl24a	NP_001070808.1	NCBI
	Klhl24b	NP_956734.1	NCBI
	Klhl29a	XP_009291058.1	NCBI
	Klhl29b	XP_003200801.2	NCBI
	Klhl30	XP_688150.4	NCBI
Homo sapiens	KLHL21	NP_055666.2	NCBI
	KLHL6	AAL35594.1	NCBI
	KLHL24	NP_060114.2	NCBI
	KLHL29	NP_443152.1	NCBI
	KLHL30	NP_980984.3	NCBI

Supplementary Table 7.1. Oligonucleotides employed in thesis.

Species	Oligo Name	Sequence
Danio rerio	DrRab32a-F	GTTGCACAGAGTTGCCAAAA
	DrRab32a-R	GTGTCTGTCAACCCCTGGAT
	DrRab38a-F	TGGGGAAAACCAGCATTATC
	DrRab38a-R	TGCTGCGGTGAAATAGTGTC
	DrRab38b-F	CATGACGCGGGTTTATTACA
	DrRab38b-R	TGGGTCCTTATCGGTGACTT
	DrRab38c-F	GCATCTGTTCAAAGTTCTGG
	DrRab38c-R	TGACTTGGAACACGTCATGC
	DrRabKlhl21-F	CGCTGGTCACTTCTCAACAG
	DrRabKlhl21-R	TCGCTGAAAATCTAAGTCACCT
Branchiostoma lanceolatum	Bl-Rab32/38-F	CACAAACCTCACACCTTCCA
	Bl-Rab32/38-R	TGGTTCATCTGTGCTCGTTC
	Bl-Rab32LO-F	TCGGACAGCAGAAACAACAC
	Bl-Rab32LO-R	CTGCTCAGCTTCAGGATGTG
Ciona robusta	CRklA-F	CCTAAGGTGATCTCACAACG
	CRklA-R	GGTTAAGTATACCATTACCG
	CRklB-F	GCGCACTTATAACATGCAAT
	CRklB-R	ACGTTCTAGTAACCTCATAC
	CRklC-F	GTATGAGGTTACTAGAACGT
	CRklC-R	GGTTAAGTATACCATTACCG
	CRklD-F	GACAGTCGTGATCTAGTCTT
	CRklD-R	GGCAGAAAGAAAGCGAAACG
	CRklE-F	TTTCTTTCTGCCCTGGTGCCTA
	CRklE-R	GTAGGCTATGTGCCATAAATTG
	CRklF-F	ACATTTGTGCGTTTGGTCTG
	CRklF-R	ACGTTCTAGTAACCTCATAC
	CRklG-F	CTTCTTTCTGTGATCAGTTC
	CRklG-R	ACGTTCTAGTAACCTCATAC
	mutMITF1-F	CCCTGGTGCCTAGTCTTGTCACTCTAAAAACACTCAGGGATTATAAATAACC
	mutMITF1-R	GGTTATTTATAATCCCTGAGTGTTTTTAGAGTGACAAGACTAGGCACCAGGG
	mutMITF2-F	GCTGAAAATGATTCCCACTCTATGCGAAGTCATTAAACAAAGAAACAACG
	mutMITF2-R	CGTTGTTTCTTTGTTTAATGACTTCGCATAGAGTGGGAATCATTTTCAGC
	mutMSX1-F	GCGCACTTATAACATGCAAGCATATTCTAACGTTTCTTC
	mutMSX1-R	GAAGAAACGTTAGAATATGCTTGCATGTTATAAGTGCGC
	mutMSX2-F	GTGCGTTTGGTCTGTTGCGAAGGAACTGATTGTCAAGTTCTAAATCG
	mutMSX2-R	CGATTTAGAACTTGACAATCAGTTCCTTCGCAACAGACCAAACGCAC
	mutDMRT-F	GTGATCAGTTCGACTATACTTTGGCATTTATTTCTCAGTCCG
	mutDMRT-R	CGGACTGAGAAATAAATGCCAAAGTATAGTCGAACTGATCAC

BIBLIOGRAPHY

Abi-Rached L, Gilles A, Shiina T, Pontarotti P, Inoko H. Evidence of en bloc duplication in vertebrate genomes. Nat Genet. 2002;31(1):100–5.

Abitua PB, Wagner E, Navarrete IA, Levine M. Identification of a rudimentary neural crest in a non-vertebrate chordate. Nature. 2012 Dec 6;492(7427):104-7. doi: 10.1038/nature11589.

Albalat R, Cañestro C. Evolution by gene loss. Nat Rev Genet. 2016 Jul;17(7):379-91. doi: 10.1038/nrg.2016.39.

Alexandrov K, Horiuchi H, Steele-Mortimer O, Seabra MC, Zerial M. Rab escort protein-1 is a multifunctional protein that accompanies newly prenylated rab proteins to their target membranes. EMBO J. 1994 Nov 15;13(22):5262-73.

Alto NM, Soderling J, Scott JD. Rab32 is an A-kinase anchoring protein and participates in mitochondrial dynamics. J Cell Biol. 2002 Aug 19;158(4):659-68. Epub 2002 Aug 19.

Amores A, Catchen J, Ferrara A, Fontenot Q, Postlethwait JH. Genome evolution and meiotic maps by massively parallel DNA sequencing: spotted gar, an outgroup for the teleost genome duplication. Genetics. 2011;188(4): 799–808.

Anant JS, Desnoyers L, Machius M, Demeler B, Hansen JC, Westover KD, Deisenhofer J, Seabra MC. Mechanism of Rab geranylgeranylation: formation of the catalytic ternary complex. Biochemistry. 1998 Sep 8;37(36):12559-68.

Aniello F, Locascio A, Villani MG, Di Gregorio A, Fucci L, Branno M. Identification and developmental expression of Ci-msxb: a novel homologue of Drosophila msh gene in Ciona intestinalis. Mech Dev. 1999 Oct;88(1):123-6.

Arshavsky VY. Rhodopsin phosphorylation: from terminating single photon responses to photoreceptor dark adaptation. Trends Neurosci. 2002 Mar;25(3):124-6.

Bagnara JT. Comparative anatomy and physiology of pigment cells in nonmammalian tissues. In: Nordlund JJ, Boissy RE, Hearing VJ, King RA, Ortonne JP, editor. The Pigmentary System: Physiology and Pathophysiology 1998. New York: Oxford University Press; pp. 9–40

Barr FA. Review series: Rab GTPases and membrane identity: causal or inconsequential? J Cell Biol. 2013 Jul 22;202(2):191-9. doi: 10.1083/jcb.201306010.

Barr FA, Lambright DG. Rab GEFs and GAPs. Curr Opin Cell Biol. 2010 Aug;22(4):461-70. doi: 10.1016/j.ceb.2010.04.007.

Battistoni A, Guarguaglini G, Degrassi F, Pittoggi C, Palena A, Di Matteo G, Pisano C, Cundari E, Lavia P. Deregulatedexpression of the RanBP1 gene alterscellcycleprogression in murine fibroblasts. J Cell Sci. 1997 110, 2345-2357.

Beaumont KA, Hamilton NA, Moores MT, Brown DL, Ohbayashi N, Cairncross O, Cook AL, Smith AG, Misaki R, Fukuda M, Taguchi T, Sturm RA, Stow JL. The recycling

endosome protein Rab17 regulates melanocytic filopodia formation and melanosome trafficking. Traffic. 2011 May;12(5):627-43. doi: 10.1111/j.1600-0854.2011.01172.x. Epub 2011 Feb 25.Bennett DC, Lamoreux ML. The color loci of mice—A genetic century. Pigment Cell Res. 2003; 16:333–344.

Berná L, Alvarez-Valin F. Evolutionary genomics of fast evolving tunicates. Genome Biol Evol. 2014 Jul 8;6(7):1724-38. doi: 10.1093/gbe/evu122.

Bertrand V, Hudson C, Caillol D, Popovici C, Lemaire P. Neural tissue in ascidian embryos is induced by FGF9/16/20, acting via a combination of maternal GATA and Ets transcription factors. Cell. 2003 Nov 26;115(5):615-27.

Bharti K, Nguyen MT, Skuntz S, Bertuzzi S, Arnheiter H. The other pigment cell: specification and development of the pigmented epithelium of the vertebrate eye. Pigment Cell Res. 2006 Oct;19(5):380-94.

Bin BH, Bhin J, Yang SH, Shin M, Nam YJ, Choi DH, Shin DW, Lee AY, Hwang D, Cho EG, Lee TR..Membrane-Associated Transporter Protein (MATP) Regulates Melanosomal pH and Influences Tyrosinase Activity. PLoS One 2015 Jun 9;10(6):e0129273.

Bock JB, Matern HT, Peden AA, Scheller RH. A genomic perspective on membrane compartment organization. Nature. 2001 Feb 15;409(6822):839-41.

Borovanský J, Wiley I. Melanins and Melanosomes Biosynthesis, Biogenesis, Physiological, and Pathological Functions John Wiley Distributor 2011: Weinheim, Baden-Wurttemberg, Germany..

Braasch I, Schartl M, Volff JN. Evolution of pigment synthesis pathways by gene and genome duplication in fish. BMC Evol Biol. 2007; 7:74.

Braasch I, Volff JN, Schartl M.. The evolution of teleost pigmentation and the fish-specific genome duplication. J Fish Biol. 2008; 73:1891–1918.

Braasch I, Brunet F, Volff JN, Schartl M.Pigmentation pathway evolution after whole-genome duplication in fish. Genome Biol Evol. 2009; Nov 25;1:479-93.

Brighouse A, Dacks JB, Field MC. Rab protein evolution and the history of the eukaryotic endomembrane system. Cell Mol Life Sci. 2010 Oct;67(20):3449-65. doi: 10.1007/s00018-010-0436-1.

Bright, LJ, Kambesis N, Nelson SB, Jeong B, Turkewitz AP. Comprehensive analysis reveals dynamic and evolutionary plasticity of Rab GTPases and membrane traffic in Tetrahymena thermophila. PLoS Genet. 2010 6, e1001155.

Brunetti R, Gissi C, Pennati R, Caicci F, Gasparini F, Manni L: Morphological evidence that the molecularly determined Ciona intestinalis type A and type B are different species: Ciona robusta and Ciona intestinalis. J Zool Syst Evol Res. 2015, 53(3):186-193

Bultema JJ, Ambrosio AL, Burek CL, Di Pietro SM. BLOC-2, AP-3, and AP-1 proteins function in concert with Rab38 and Rab32 proteins to mediate protein trafficking to lysosome-related organelles. J Biol Chem. 2012; 287(23):19550–63.

Bultema JJ, Di Pietro SM. Cell type-specific Rab32 and Rab38 cooperate with the ubiquitous lysosome biogenesis machinery to synthesize specialized lysosome-related organelles. Small GTPases. 2013 Jan-Mar;4(1):16-21. doi: 10.4161/sgtp.22349.

Bultema JJ, Boyle JA, Malenke PB, Martin FE, Dell'Angelica EC, Cheney RE, Di Pietro SM. Myosin vc interacts with Rab32 and Rab38 proteins and works in the biogenesis and secretion of melanosomes. J Biol Chem. 2014 Nov 28;289(48):33513-28. doi: 10.1074/jbc.M114.578948. Epub 2014 Oct 16.

Bustamante J, Bredeston L, Malanga G, Mordoh J. Role of melanin as a scavenger of active oxygen species. Pigment Cell Res. 1993, 6(5): 348-53.

Cai H, Reinisch K and Ferro-Novick S. (2007). Coats, tethers, Rabs, and SNAREs work together to mediate the intracellular destination of a transport vesicle. Dev. Cell 12, 671-682.

Cajiao I, Zhang A, Yoo EJ, Cooke NE, Liebhaber SA. Bystander gene activation by a locus control region.EMBO J. 2004, Oct 1;23(19):3854-63. Epub 2004 Sep 9.

Callaerts P, Halder G, Gehring WJ. PAX-6 in development and evolution. Annu Rev Neurosci. 1997;20:483-532.

Camp E, Lardelli M. Tyrosinase gene expression in zebrafish embryos. Dev Genes Evol. 2001 Mar;211(3):150-3.

Carlton JM, Hirt RP, Silva JC, Delcher AL, Schatz M, Zhao Q, Wortman JR, Bidwell SL, Alsmark UC, Besteiro S. et al. (2007). Draft genome sequence of the sexually transmitted pathogen Trichomonas vaginalis. Science 315, 207-212.

Carthagena L, Bergamaschi A, Luna JM, David A, Uchil PD, Margottin-Goguet F, et al. Human TRIM gene expression in response to interferons. PLoS One. 2009; 4(3), e4894.

Catchen JM, Conery JS, Postlethwait JH. Automated identification of conserved synteny after whole-genome duplication. Genome Res. 2009 Aug;19(8):1497-505. doi: 10.1101/gr.090480.108. Epub 2009 May 22.

Cavalier-Smith T. (2002). The phagotrophic origin of eukaryotes and phylogenetic classification of Protozoa. Int. J. Syst. Evol. Microbiol. 52, 297-354.

Chen L, Hu J, Yun Y, Wang T. Rab36 regulates the spatial distribution of late endosomes and lysosomes through a similar mechanism to Rab34. Mol Membr Biol. 2010 Jan;27(1):23-30. doi: 10.3109/09687680903417470.

Claus H, Decker H. Bacterial tyrosinases. Syst Appl Microbiol. 2006 Jan;29(1):3-14.

Cohen-Solal KA, Sood R, Marin Y, Crespo-Carbone SM, Sinsimer D, Martino JJ, et al. Identification and characterization of mouse Rab32 by mRNA and protein expression analysis. Biochim Biophys Acta. 2003;1651(1-2):68–75.

Coppola U, Annona G, D'Aniello S, Ristoratore F. Rab32 and Rab38 genes in chordate pigmentation: an evolutionary perspective. BMC Evol Biol 2016 DOI: 10.1186/s12862-016-0596-1.

Cortés-González V, Zenteno JC, Guzmán-Sánchez M, Giordano-Herrera V, Guadarrama-Vallejo D, Ruíz-Quintero N, Villanueva-Mendoza C. Tietz/Waardenburg type 2A syndrome associated with posterior microphthalmos in two unrelated patients with novel MITF gene mutations. Am J Med Genet A. 2016 Dec;170(12):3294-3297.

Courtheoux T, Enchev RI, Lampert F, Gerez J, Beck J, Picotti P, Sumara I, Peter M. Cortical dynamics during cell motility are regulated by CRL3(KLHL21) E3 ubiquitin ligase. Nat Commun. 2016 Sep 19;7:12810. doi: 10.1038/ncomms12810.

Christiaen, L., Wagner, E., Shi, W. & Levine, M. Isolation of sea squirt (Ciona) gametes, fertilization, dechorionation, and development. Cold Spring Harb. Protoc. 2009. doi:10.1101/pdb.prot5344.

Christiaen, L., Wagner, E., Shi, W. & Levine, M. Electroporation of transgenic DNAs in thesea squirt Ciona. Cold Spring Harb. Protoc. 2009. doi:10.1101/pdb.prot5345.

Christiaen, L., Wagner, E., Shi, W. & Levine, M. Whole-mount in situ hybridization on sea squirt (Ciona intestinalis) embryos. Cold Spring Harb. Protoc. 2009. doi:10.1101/pdb.prot5348.

Colicelli J. Human RAS superfamily proteins and related GTPases. Sci STKE. 2004 Sep 7;2004(250).

Darras S, Nishida H. The BMP signaling pathway is required together with the FGF pathway for notochord induction in the ascidian embryo. Development. 2001 Jul;128(14):2629-38.

Davidson B, Shi W, Beh J, Christiaen L, Levine M. FGF signaling delineates the cardiac progenitor field in the simple chordate, Ciona intestinalis. Genes Dev. 2006 Oct 1;20(19):2728-38.

Dehal, P, Satou Y, Campbell RK, Chapman J, Degnan B, De Tomaso A, Davidson B, Di Gregorio A, Gelpke M, Goodstein DM, Harafuji N, Hastings KE, et al. The draft genome of Ciona intestinalis: insight into chordate and vertebrate origins. Science 2000; 298, 2157–2167.

Delahaye JL, Foster OK, Vine A, Saxton DS, Curtin TP, Somhegyi H, Salesky R, Hermann GJ. Caenorhabditis elegans HOPS and CCZ-1 mediate trafficking to lysosome-related organelles independently of RAB-7 and SAND-1. Mol Biol Cell. 2014 Apr;25(7):1073-96. doi: 10.1091/mbc.E13-09-0521.

Dehal P, Boore JL. Two rounds of whole genome duplication in the ancestral vertebrate. PLoS Biol. 2005;3(10), e314.

del Marmol V, Beermann F. Tyrosinase and related proteins in mammalian pigmentation. FEBS Lett. 1996, 381, 165-168.

Delsuc F, Brinkmann H, Chourrout D, Philippe H. Tunicates and not cephalochordates are the closest living relatives of vertebrates. Nature 2006; 439(7079):965–8.

Dhanoa BS, Cogliati T, Satish AG, Bruford EA, Friedman JS. Update on the Kelch-like (KLHL) gene family. Human Genomics 2013, 7:13

Diekmann Y, Seixas E, Gouw M, Tavares-Cadete F, Seabra MC, Pereira-Leal JB. Thousands of rab GTPases for the cell biologist. PLoS Comput Biol. 2011; 7(10), e1002217.

Dilly PN. Studies on the receptors in Ciona intestinalis. 3. A second type of photoreceptor in the tadpole larva of Ciona intestinalis. Z Zellforsch Mikrosk Anat. 1969; 96(1):63-5.

D'Mello SA, Finlay GJ, Baguley BC, Askarian-Amiri ME. Signaling Pathways in Melanogenesis. Int J Mol Sci. 2016 15;17 (7).

Dorsky RI, Moon RT, Raible DW. (1998). Control of neural crest cell fate by the Wnt signalling pathway. Nature 1998; 396, 370-373.

Dufour HD, Chettouh Z, Deyts C, de Rosa R, Goridis C, Joly JS, Brunet JF. Precraniate origin of cranial motoneurons. Proc Natl Acad Sci USA. 2006 Jun 6;103(23):8727-32.

Dunst S, Kazimiers T, von Zadow F, Jambor H, Sagner A, Brankatschk B, Mahmoud A, Spannl S, Tomancak P, Eaton S, Brankatschk M. Endogenously tagged rab proteins: a resource to study membrane trafficking in Drosophila. Dev Cell. 2015 May 4;33(3):351-65. doi: 10.1016/j.devcel.2015.03.022.

Duval N, Daubas P, Bourcier de Carbon C, St Cloment C, Tinevez JY, Lopes M, Ribes V, Robert B. Msx1 and Msx2 act as essential activators of Atoh1 expression in the murine spinal cord. Development. 2014 Apr;141(8):1726-36.

Eakin RM, Kuda A. Ultrastructure of sensory receptors in Ascidian tadpoles. Z Zellforsch Mikrosk Anat. 1971;112(3):287-312.

Edelman A.M., Blumenthal D.K., Krebs E.G. Protein serine threonine kinases. Annu. Rev. Biochem. 1987; 56:567–613.

Edgar RC. MUSCLE: a multiple sequence alignment method with reduced time and space complexity. BMC Bioinformatics. 2004 Aug 19;5:113.

Eisenman HC and Casadevall A. Synthesis and assembly of fungal melanin. Appl Microbiol Biotechnol. 2012; 93(3), 931–940.

Elias, M. (2010). Patterns and processes in the evolution of the eukaryotic endomembrane system. Mol. Membr. Biol. 27, 469-489.

Elias M, Brighouse A, Gabernet-Castello C, Field MC, Dacks JB. Sculpting the endomembrane system in deep time: high resolution phylogenetics of Rab GTPases. J Cell Sci. 2012;125(Pt 10):2500–8.

Ellis K, Bagwell J, Bagnat M. Notochord vacuoles are lysosome-related organelles that function in axis and spine morphogenesis. J Cell Biol. 2013;200(5):667–79.

Embley TM and Martin W.. Eukaryotic evolution, changes and challenges. Nature 2006; 440, 623-630.

Esteves FF, Springhorn A, Kague E, Taylor E, Pyrowolakis G, Fisher S, Bier E.BMPs regulate msx gene expression in the dorsal neuroectoderm of Drosophila and vertebrates by distinct mechanisms. PLoS Genet. 2014 Sep 11;10(9):e1004625. doi:

Esposito R, D'Aniello S, Squarzoni P, Pezzotti MR, Ristoratore F, Spagnuolo A. New insights into the evolution of metazoan tyrosinase gene family. PLoS One (2012) 7(4), e35731

Esposito R, Yasuo H, Sirour C, Palladino A, Spagnuolo A, Hudson C. Patterning of brain precursors in ascidian embryos. Development. 2017 Jan 15;144(2):258-264. doi: 10.1242/dev.142307. Epub 2016 Dec 19.

Fatemi SH, Folsom TD, Rooney RJ, Thuras PD. mRNA and protein expression for novel GABAA receptors theta and rho2 are altered in schizophrenia and mood disorders; relevance to FMRP-mGluR5 signaling pathway. Transl Psychiatry. 2013;3, e271.

Fedorow H, Tribl F, Halliday G, Gerlach M, Riederer P, Double KL. Neuromelanin in human dopamine neurons: comparison with peripheral melanins and relevance to Parkinson's disease. Prog Neurobiol 2005; 75(2):109-24.

Fiore G, Poli A, Di Cosmo A, d'Ischia M, Palumbo A. Dopamine in the ink defence system of Sepia officinalis: biosynthesis, vesicular compartmentation in mature ink gland cells, nitric oxide (NO)/cGMP-induced depletion and fate in secreted ink. Biochem J. 2004; 15;378(Pt 3):785-91

Force A, Lynch M, Pickett FB, Amores A, Yan YL, Postlethwait J. Preservation of duplicate genes by complementary, degenerative mutations. Genetics. 1999 Apr;151(4):1531-45.
Goding CR. Melanocytes: the new Black. Int J Biochem Cell Biol. 2007, 39(2): 275-9.

Fujii R. Coloration and chromatophores. In: Evans DH, editor. The Physiology of Fishes. Boca Raton, Florida: CRC Press; 1993. pp. 535–562.

Gallegos ME, Balakrishnan S, Chandramouli P, Arora S, Azameera A et al. The C. elegans rab family: identification, classification and toolkit construction. PLoS One. 2012;7(11):e49387. doi: 10.1371/journal.pone.0049387.

Gertz EM, Yu YK, Agarwala R, Schaffer AA, Altschul SF. Composition-based statistics and translated nucleotide searches: improving the TBLASTN module of BLAST. BMC Biol. 2006; 4:41.

Gillbro JM, Olsson MJ. The melanogenesis and mechanisms of skin-lightening agents--existing and new approaches. Int J Cosmet Sci. 2011 Jun;33(3):210-21. doi: 10.1111/j.1468-2494.2010.00616.x.

Gillingham AK, Sinka R, Torres IL, Lilley KS, Munro S. Toward a comprehensive map of the effectors of rab GTPases. Dev Cell. 2014 Nov 10;31(3):358-73. doi: 10.1016/j.devcel.2014.10.007.

Godfrey PA, Malnic B, Buck LB. The mouse olfactory receptor gene family. Proc Natl Acad Sci USA. 2004;101(7):2156–61.

Goding CR. Melanocytes: the new Black. Int J Biochem Cell Biol. 2007 39(2): 275-9.

Gorman AL, McReynolds JS, Barnes SN. Photoreceptors in primitive chordates: fine structure, hyperpolarizing receptor potentials, and evolution. Science. 1971 Jun 4;172(3987):1052-4.

Guindon S, Dufayard JF, Lefort V, Anisimova M, Hordijk W, Gascuel O. New algorithms and methods to estimate maximum-likelihood phylogenies: assessing the performance of PhyML 3.0. Syst Biol. 2010 May;59(3):307-21. doi: 10.1093/sysbio/syq010.

Has C. The "Kelch" Surprise: KLHL24, a New Player in the Pathogenesis of Skin Fragility. J Invest Dermatol. 2017 Jun;137(6):1211-1212. doi: 10.1016/j.jid.2017.02.011.

He Y, Maier K, Leppert J, Hausser I, Schwieger-Briel A, Weibel L, Theiler M, Kiritsi D, Busch H4, Boerries M, Hannula-Jouppi K, Heikkilä H, Tasanen K, Castiglia D, Zambruno G, Has C. Monoallelic Mutations in the Translation Initiation Codon of KLHL24 Cause Skin Fragility. Am J Hum Genet. 2016 Dec 1;99(6):1395-1404. doi: 10.1016/j.ajhg.2016.11.005. Epub 2016 Nov 23.

Hermansky F, Pudlak P. Albinism associated with hemorrhagic diathesis and unusual pigmented reticular cells in the bone marrow: report of two cases with histochemical studies. Blood. 1959;14(2):162–9.

Hoegg S, Brinkmann H, Taylor JS, Meyer A. Phylogenetic timing of the fish-specific genome duplication correlates with the diversification of teleost fish. J Mol Evol. 2004;59(2):190–203.

Hong CS, Park BY, Saint-Jeannet JP. The function of Dmrt genes in vertebrate development: it is not just about sex. Dev Biol. 2007 Oct 1;310(1):1-9. Epub 2007 Aug 3.

Hongo I, Kengaku M, Okamoto H. FGF signaling and the anterior neural induction in Xenopus. Dev Biol. 1999 Dec 15;216(2):561-81.

Hotta, K. et al. A web-based interactive developmental table for the ascidian Ciona intestinalis, including 3D real-image embryo reconstructions: I. From fertilized egg to hatching larva. Dev. Dyn. 2007; 236, 1790–1805.

Horie T, Orii H, Nakagawa M. Structure of ocellus photoreceptors in the ascidian Ciona intestinalis larva as revealed by an anti-arrestin antibody. J Neurobiol. 2005 Dec;65(3):241-50

Huang G, Kaufman AJ, Xu K, Manova K, Singh B. SCCRO neddylates Cul3 to selectively promote midbody localization and activity of Cul3KLHL21 during abscission. J Biol Chem. 2017 Jun 15. pii: jbc.M117.778530. doi: 10.1074/jbc.M117.778530

Hudson C, Lemaire P. Induction of anterior neural fates in the ascidian Ciona intestinalis. Mech Dev. 2001 Feb;100(2):189-203.

Hudson C, Darras S, Caillol D, Yasuo H, Lemaire P. A conserved role for the MEK signalling pathway in neural tissue specification and posteriorisation in the invertebrate chordate, the ascidian Ciona intestinalis. Development 2003 Jan;130(1):147-59.

Hudson C, Lotito S, Yasuo H. Sequential and combinatorial inputs from Nodal, Delta2/Notch and FGF/MEK/ERK signalling pathways establish a grid-like organisation of distinct cell identities in the ascidian neural plate. Development. 2007 Oct;134(19):3527-37. Epub 2007 Aug 29.

Huet D, Blisnick T, Perrot S, Bastin P. The GTPase IFT27 is involved in both anterograde and retrograde intraflagellar transport. eLife. 2014; 3: e02419. doi: 10.7554/eLife.02419

Huson DH, Scornavacca C. Dendroscope 3: an interactive tool for rooted phylogenetic trees and networks. Syst Biol. 2012; 61(6):1061–7.

Hutagalung AH, Novick PJ. Role of Rab GTPases in membrane traffic and cell physiology. Physiol Rev. 2011 Jan;91(1):119-49. doi: 10.1152/physrev.00059.2009.

Iida H, Noda M, Kaneko T, Doiguchi M, Mōri T. Identification of rab12 as a vesicle-associated small GTPase highly expressed in Sertoli cells of rat testis. Mol Reprod Dev. 2005 Jun;71(2):178-85.

Ikuta T, Saiga H. Dynamic change in the expression of developmental genes in the ascidian central nervous system: revisit to the tripartite model and the origin of the midbrain-hindbrain boundary region. Dev Biol 312, 2007, 7631-643 doi:S0012-1606(07)01425-X .

Imai KS, Hino K, Yagi K, Satoh N, Satou Y. Gene expression profiles of transcription factors and signaling molecules in the ascidian embryo: towards a comprehensive understanding of gene networks. Development. 2004 Aug;131(16):4047-58. Epub 2004 Jul 21.

Irimia M, Roy SW. Evolutionary convergence on highly-conserved 3' intron structures in intron-poor eukaryotes and insights into the ancestral eukaryotic genome. PLoS Genet. 2008 Aug 8;4(8):e1000148. doi: 10.1371/journal.pgen.1000148.

Irimia M, Pineiro C, Maeso I, Gomez-Skarmeta JL, Casares F, Garcia-Fernandez J. Conserved developmental expression of Fezf in chordates and Drosophila and the origin of the Zona Limitans Intrathalamica (ZLI) brain organizer. Evodevo. 2010;1(1):7.

Irimia M, Tena JJ, Alexis MS, Fernandez-Miñan A, Maeso I, Bogdanovic O, de la Calle-Mustienes E, Roy SW, Gómez-Skarmeta JL, Fraser HB. Extensive conservation of ancient microsynteny across metazoans due to cis-regulatory constraints. Genome Res. 2012 Dec;22(12):2356-67. doi: 10.1101/gr.139725.112. Epub 2012 Jun 21.

Ito S, Wakamatsu K. Chemistry of mixed melanogenesis--pivotal roles of dopaquinone. Photochem Photobiol. 2008; 84(3):582-92.

Itoh K, Wakabayashi N, Katoh Y, Ishii T, Igarashi K, Engel JD, Yamamoto M. Keap1 represses nuclear activation of antioxidant responsive elements by Nrf2 through binding to the amino-terminal Neh2 domain. Genes Dev. 1999 Jan 1;13(1):76-86.

Jaillon O, Aury JM, Brunet F, Petit JL, Stange-Thomann N, Mauceli E, et al. Genome duplication in the teleost fish Tetraodon nigroviridis reveals the early vertebrate proto-karyotype. Nature. 2004;431(7011):946–57.

Jeffery WR, Meier S. Ooplasmic segregation of the myoplasmic actin network in stratified ascidian eggs. Wilehm Roux Arch Dev Biol. 1984 Jul;193(4):257-262. doi: 10.1007/BF01260348.

Jensen VL, Carter S, Sanders AA, Li C, Kennedy J, Timbers TA, Cai J, Scheidel N, Kennedy BN, Morin RD, Leroux MR, Blacque OE. Whole-Organism Developmental Expression Profiling Identifies RAB-28 as a Novel Ciliary GTPase Associated with the

BBSome and Intraflagellar Transport. PLoS Genet. 2016 Dec 8;12(12):e1006469. doi: 10.1371/journal.pgen.1006469.

Jiang D, Tresser JW, Horie T, Tsuda M, Smith WC. Pigmentation in the sensory organs of the ascidian larva is essential for normal behavior. J Exp Biol. 2005 Feb;208(Pt 3):433-8.

Kalab P, Pu RT, Dasso. The Ran GTPase regulates mitotic spindle assembly. Curr. Biol. 1999. 9, 481-484.

Kamura T, Sato S, Haque D, Liu L, Kaelin WG Jr, Conaway RC, Conaway JW. The Elongin BC complex interacts with the conserved SOCS-box motif present in members of the SOCS, ras, WD-40 repeat, and ankyrin repeat families. Genes Dev. 1998 Dec 15;12(24):3872-81.

Kanie T, Abbott KL, Mooney NA, Plowey ED, Demeter J, Jackson PK.The CEP19-RABL2 GTPase Complex Binds IFT-B to Initiate Intraflagellar Transport at the Ciliary Base. Dev Cell. 2017 Jul 10;42(1):22-36.e12. doi: 10.1016/j.devcel.2017.05.016.

Kaplon J, Hömig-Hölzel C, Gao L, Meissl K, Verdegaal EM, van der Burg SH, van Doorn R, Peeper DS. Near-genomewide RNAi screening for regulators of BRAF(V600E) -induced senescence identifies RASEF, a gene epigenetically silenced in melanoma. Pigment Cell Melanoma Res. 2014 Jul;27(4):640-52. doi: 10.1111/pcmr.12248. Epub 2014 May 14.

Kawaminani S, Nishida H. Induction of trunk lateral cells, the blood cell precursors, during ascidian embryogenesis. Dev Biol. 1997 Jan 1;181(1):14-20.

Kawasaki H, Kretsinger RH. Calcium-binding proteins 1: EF-hands. Protein Profile. 1995;2(4):297-490.

Keeling, PJ. (2010). The endosymbiotic origin, diversification and fate of plastids. Philos. Trans. R. Soc. Lond. B Biol. Sci. 365, 729-748.

Kelsh RN, Brand M, Jiang YJ, Heisenberg CP, Lin S, Haffter P, Odenthal J, Mullins MC, van Eeden FJ, Furutani-Seiki M, Granato M, Hammerschmidt M, Kane DA, Warga RM, Beuchle D, Vogelsang L, Nüsslein-Volhard C. Zebrafish pigmentation mutations and the processes of neural crest development. Development 1996, Dec;123:369-89.

Kelsh RN, Schmid B, Eisen JS. Genetic analysis of melanophore development in zebrafish embryos. Dev Biol. 2000; Sep 15;225(2):277-93.

Khaligh A, Goudarzian M, Moslem A, Mehrtash A, Jamshidi J, Darvish H, Emamalizadeh B. RAB7L1 promoter polymorphism and risk of Parkinson's disease; a case-control study. Neurol Res. 2017 May;39(5):468-471. doi: 10.1080/01616412.2017.1297558. Epub 2017 Feb 28.

Kim GJ, Nishida H. Suppression of muscle fate by cellular interaction is required for mesenchyme formation during ascidian embryogenesis. Dev Biol. 1999 Oct 1;214(1):9-22.

Kimura T, Nagao Y, Hashimoto H, Yamamoto-Shiraishi Y, Yamamoto S, Yabe T, Takada S, Kinoshita M, Kuroiwa A, Naruse K. Leucophores are similar to xanthophores in their specification and differentiation processes in medaka. Proc Natl Acad Sci USA 2014 May 20; 111(20):7343-8. doi: 10.1073/pnas.1311254111..

Kimura T, Takehana Y, Naruse K. pnp4a Is the Causal Gene of the Medaka Iridophore Mutant guanineless. G3 (Bethesda). 2017 Apr 3;7(4):1357-1363. doi: 10.1534/g3.117.040675.

Kopp A. Dmrt genes in the development and evolution of sexual dimorphism. Trends Genet. 2012 Apr;28(4):175-84. doi: 10.1016/j.tig.2012.02.002. Epub 2012 Mar 14.

Klopper TH, Kienle N, Fasshauer D, Munro S. Untangling the evolution of Rab G proteins: implications of a comprehensive genomic analysis. BMC Biol. 2012;10:71.

Kumar S, Stecher G, Tamura K. MEGA7: Molecular Evolutionary Genetics Analysis Version 7.0 for Bigger Datasets. Mol Biol Evol. 2016 Jul;33(7):1870-4. doi:10.1093/molbev/msw054. Epub 2016 Mar 22.

Kuraku S, Meyer A. The evolution and maintenance of Hox gene clusters in vertebrates and the teleost-specific genome duplication. Int J Dev Biol. 2009;53(5-6):765–73.

Kusakabe T, Kusakabe R, Kawakami I, Satou Y, Satoh N, Tsuda M. Ci-opsin1, a vertebrate-type opsin gene, expressed in the larval ocellus of the ascidian Ciona intestinalis. FEBS Lett. 2001 Sep 28;506(1):69-72.

Kuwahara T, Inoue K, D'Agati VD, Fujimoto T, Eguchi T, Saha S, Wolozin B, Iwatsubo T, Abeliovich A. LRRK2 and RAB7L1 coordinately regulate axonal morphology and lysosome integrity in diverse cellular contexts. Sci Rep. 2016 Jul 18;6:29945. doi: 10.1038/srep29945.

Lacalli TC. Sensory systems in amphioxus: a window on the ancestral chordate condition. Brain Behav Evol. 2004;64(3):148–62

Lamb TD, Collin SP, Pugh EN Jr. Evolution of the vertebrate eye: opsins, photoreceptors, retina and eye cup. Nat Rev Neurosci. 2007 Dec;8(12):960-76.

Larkin MA, Blackshields G, Brown NP, Chenna R, McGettigan PA, McWilliam H, Valentin F, Wallace IM, Wilm A, Lopez R, Thompson JD, Gibson TJ, Higgins DG. Clustal W and Clustal X version 2.0. Bioinformatics. 2007 Nov 1;23(21):2947-8. Epub 2007 Sep 10.

Le Bouffant R, Souquet B, Duval N, Duquenne C, Hervé R, Frydman N, Robert B, Habert R, Livera G. Msx1 and Msx2 promote meiosis initiation. Development 2011 138: 5393-5402.

Leclerc J, Ballotti R, Bertolotto C. Pathways from senescence to melanoma: focus on MITF sumoylation. Oncogene. 2017 Aug 21. doi: 10.1038/onc.2017.292.

Leinders-Zufall T, Ishii T, Chamero P, Hendrix P, Oboti L, Schmid A, et al. A family of nonclassical class I MHC genes contributes to ultrasensitive chemodetection by mouse vomeronasal sensory neurons. J Neurosci. 2014;34(15):5121–33.

Lee RH, Iioka H, Ohashi M, Iemura S, Natsume T, Kinoshita N. XRab40 and XCullin5 form a ubiquitin ligase complex essential for the noncanonical Wnt pathway. EMBO J. 2007 Aug 8;26(15):3592-606.

Lee MT, Mishra A, Lambright DG. Structural mechanisms for regulation of membrane traffic by rab GTPases. Traffic. 2009 Oct;10(10):1377-89. doi: 10.1111/j.1600-0854.2009.00942.x

Levy C., Khaled M., Fisher D.E. MITF: Master regulator of melanocyte development and melanoma oncogene. Trends Mol. Med. 2006 12:406–414.

Li Z, Joseph NM, Easter SS Jr. The morphogenesis of the zebrafish eye, including a fate map of the optic vesicle. Dev Dyn. 2000; 218:175–188

Li F, Yi L, Zhao L, Itzen A, Goody RS, Wu Y. The role of the hypervariable C-terminal domain in Rab GTPases membrane targeting Proc Natl Acad Sci U S A. 2014 Feb 18; 111(7): 2572–2577. Published online 2014 Feb 3. doi: 10.1073/pnas.1313655111Lin JY, Fisher DE. Melanocyte biology and skin pigmentation. Nature 2007, 22;445(7130):843-50.

Lister JA, Robertson CP, Lepage T, Johnson SL, Raible DW. nacre encodes a zebrafish microphthalmia-related protein that regulates neural-crest-derived pigment cell fate. Development. 1999 Sep;126(17):3757-67.

Lister JA. Development of pigment cells in the zebrafish embryo. Microsc Res Tech. 2002 Sep 15;58(6):435-41.

Lopes, V. S., Wasmeier, C., Seabra, M. C. & Futter, C. E. Melanosome maturation defect in Rab38-deficient retinal pigment epithelium results in instability of immature melanosomes during transient melanogenesis. Mol. Biol. Cell. 2007, 18, 3914–3927.

Loftus SK, Larson DM, Baxter LL, Antonellis A, Chen Y, Wu X, Jiang Y, Bittner M, Hammer JA 3rd, Pavan WJ. Mutation of melanosome protein RAB38 in chocolate mice. Proc Natl Acad Sci U S A. 2002 Apr 2;99(7):4471-6.

Loftus SK, Larson DM, Baxter LL, Antonellis A, Chen Y, Wu X, et al. Mutation of melanosome protein RAB38 in chocolate mice. Proc Natl Acad Sci U S A. 2002; 99(7):4471–6.

Ma J, Plesken H, Treisman JE, Edelman-Novemsky I, Ren M. Lightoid and Claret: a rab GTPase and its putative guanine nucleotide exchange factor in biogenesis of Drosophila eye pigment granules. Proc Natl Acad Sci USA. 2004;101(32):11652–7.

Maat W, Beiboer SH, Jager MJ, Luyten GP, Gruis NA, van der Velden PA. Invest Ophthalmol Vis Sci. 2008 Apr;49(4):1291-8. doi: 10.1167/iovs.07-1135. Epigenetic regulation identifies RASEF as a tumor-suppressor gene in uveal melanoma.

MacLeod DA, Rhinn H, Kuwahara T, Zolin A, Di Paolo G, McCabe BD, Marder KS, Honig LS, Clark LN, Small SA, Abeliovich A. RAB7L1 interacts with LRRK2 to modify intraneuronal protein sorting and Parkinson's disease risk. Neuron. 2013 Feb 6;77(3):425-39. doi: 10.1016/j.neuron.2012.11.033

Maerki S, Olma MH, Staubli T, Steigemann P, Gerlich DW, Quadroni M, Sumara I, Peter M. The Cul3-KLHL21 E3 ubiquitin ligase targets aurora B to midzone microtubules in anaphase and is required for cytokinesis. J Cell Biol. 2009 Dec 14;187(6):791-800.

Mahanty S, Ravichandran K, Chitirala P, Prabha J, Jani RA, Setty SR. Rab9A is required for delivery of cargo from recycling endosomes to melanosomes. Pigment Cell Melanoma Res. 2016 Jan;29(1):43-59. doi: 10.1111/pcmr.12434.

Marks MS and Seabra MC. The melanosome: membrane dynamics in black and white. Nat Rev Mol Cell Biol. 2001; 2, 738-748.

Marubashi S, Shimada H, Fukuda M, Ohbayashi N. RUTBC1 Functions as a GTPase-activating Protein for Rab32/38 and Regulates Melanogenic Enzyme Trafficking in Melanocytes. J Biol Chem. 2016 Jan 15;291(3):1427-40. doi: 10.1074/jbc.M115.684043.

Matsui T, Fukuda M. Small GTPase Rab12 regulates transferrin receptor degradation: Implications for a novel membrane trafficking pathway from recycling endosomes to lysosomes. Cell Logist. 2011 Jul;1(4):155-158.

Melchior F, Paschal B, Evans J, Gerace J. Inhibition of nuclear protein import by non hydrolyzable analogues of GTP and identification of the small GTPase Ran/TC4 as an essential transport factor. J. Cell. Biol. 1993; 123, 1649-1659.

Mellgren EM, Johnson SL. 2005.kitb, a second zebrafish ortholog of mouseKit. Dev Genes Evol. 215:470–477.

Ménasché G, Pastural E, Feldmann J, Certain S, Ersoy F, Dupuis S, Wulffraat N, Bianchi D, Fischer A, Le Deist F, de Saint Basile G. Mutations in RAB27A cause Griscelli syndrome associated with haemophagocytic syndrome. Nat Genet. 2000 Jun;25(2):173-6.

Meredith P and Riesz J. Radiative relaxation quantum yields for synthetic eumelanin. Photochem Photobiol. 2004; 79(2): 211-6.

Meredith P and Sarna T. The physical and chemical properties of eumelanin. Pigment Cell Res. 2006; 19, 572-594.

Michiels NK, et al. 2008. Red fluorescence in reef fish: a novel signalling mechanism? BMC Ecol. 8:16.

Moore MS, Blobel G. The GTP-binding protein Ran/TC4 is required for protein import into the nucleus. Nature. 1993; 365, 661-663.

Moore I, Schell J, Palme K. Subclass-specific sequence motifs identified in Rab GTPases. Trends Biochem Sci. 1995 Jan; 20(1):10-2.

Moreira J, Deutsch A. Pigment pattern formation in zebrafish during late larval stages: a model based on local interactions. Dev Dyn. 2005 Jan;232(1):33-42.

Moret F, Christiaen L, Deyts C, Blin M, Vernier P, Joly JS. Regulatory gene expressions in the ascidian ventral sensory vesicle: evolutionary relationships with the vertebrate hypothalamus. Dev Biol. 2005 Jan 15;277(2):567-79.

Muhlenbein N, Hofmann S, Rothbauer U, Bauer MF. Organization and function of the small Tim complexes acting along the import pathway ofmetabolite carriers into mammalian mitochondria. J Biol Chem. 2004; 279(14):13540–6.

Nakagawa M, Orii H, Yoshida N, Jojima E, Horie T, Yoshida R, Haga T, Tsuda M. Ascidian arrestin (Ci-arr), the origin of the visual and nonvisual arrestins of vertebrate. Eur J Biochem. 2002 Nov;269(21):5112-8.

Nakamura Y, Mori K, Saitoh K, Oshima K, Mekuchi M, Sugaya T, Shigenobu Y, Ojima N, Muta S, Fujiwara A, Yasuike M, Oohara I, Hirakawa H, Chowdhury VS, Kobayashi T, Nakajima K, Sano M, Wada T, Tashiro K, Ikeo K, Hattori M, Kuhara S, Gojobori T, Inouye K. Evolutionary changes of multiple visual pigment genes in the complete genome of Pacific bluefin tuna. Proc Natl Acad Sci USA 2013 Jul 2;110(27):11061-6.

Nakashima Y, Kusakabe T, Kusakabe R, Terakita A, Shichida Y, Tsuda M. J Origin of the vertebrate visual cycle: genes encoding retinal photoisomerase and two putative visual cycle proteins are expressed in whole brain of a primitive chordate. Comp Neurol. 2003 May 26;460(2):180-90.

Namkoong J, Shin SS, Lee HJ, Marin YE, Wall BA, Goydos JS, et al. Metabotropic glutamate receptor 1 and glutamate signaling in human melanoma. Cancer Res. 2007;67(5):2298–305.

Nappi AJ, Christensen BM. Melanogenesis and associated cytotoxic reactions: applications to insect innate immunity. Insect Biochem Mol Biol. 2005, 35(5):443-59.

Nguyen VH, Schmid B, Trout J, Connors SA, Ekker M, Mullins MC. Ventral and lateral regions of the zebrafish gastrula, including the neural crest progenitors, are established by a bmp2b/swirl pathway of genes. Dev Biol. 1998Jul 1;199(1):93-110.

Nicol D, Meinertzhagen IA. Cell counts and maps in the larval central nervous system of the ascidian Ciona intestinalis (L.). J Comp Neurol. 1991 Jul 22;309(4):415-29.

Nilsson Skold H, Aspengren S, Wallin M. Rapid color change in fish and amphibians-function, regulation, and emerging applications. Pigment Cell Melanoma Res. 2013; 26(1):29–38.

Newton JM, Cohen-Barak O, Hagiwara N, Gardner JM, Davisson MT, King RA, Brilliant MH. Mutations in the human orthologue of the mouse underwhite gene (uw) underlie a new form of oculocutaneous albinism, OCA4. Am J Hum Genet. 2001 Nov;69(5):981-8. Epub 2001 Sep 26.

Nishida H. Patterning the marginal zone of early ascidian embryos: localized maternal mRNA and inductive interactions. Bioessays. 2002 Jul;24(7):613-24.

Nishida H. Cell lineage analysis in ascidian embryos by intracellular injection of a tracer enzyme. III. Up to the tissue restricted stage. Dev Biol. 1987 Jun;121(2):526-41.

Nishida H, Satoh N. Determination and regulation in the pigment cell lineage of the ascidian embryo. Dev Biol. 1989 Apr;132(2):355-67.

Nordlund JJ, Boissy RE, Hearing VJ, King RA, and Ortonne JP. The Pigmentary System. Physiology and Pathophysiology 1998. New York: Oxford Univ. Press. pp. 151–158.

Odenthal J, Nüsslein-Volhard C. Fork head domain genes in zebrafish. Dev Genes Evol. 1998 Jul;208(5):245-58.

Ohno S. Patterns in genome evolution. Curr Opin Genet Dev. 1993; 3(6):911–4.

Oiso N, Riddle SR, Serikawa T, Kuramoto T, Spritz RA. The rat Ruby (R) locus is Rab38: identical mutations in Fawn-hooded and Tester-Moriyama rats derived from an ancestral Long Evans rat sub-strain.. 2004;15(4):307–14.

Olkkonen VM, Ikonen E. When intracellular logistics fails--genetic defects in membrane trafficking. J Cell Sci. 2006 Dec 15;119(Pt 24):5031-45.

Omotezako T, Onuma T, Nishida H.DNA interference: DNA-induced gene silencing in the appendicularian Oikopleura dioica. Proc Biol Sci. 2015 May 22;282(1807):20150435. doi: 10.1098/rspb.2015.0435.

Osanai K, Iguchi M, Takahashi K, Nambu Y, Sakuma T, Toga H, Ohya N, Shimizu H, Fisher JH, Voelker DR. Expression and localization of a novel Rab small G protein (Rab38) in the rat lung. Am J Pathol. 2001 May;158(5):1665-75.

Osanai K, Takahashi K, Nakamura K, Takahashi M, Ishigaki M, Sakuma T, et al. Expression and characterization of Rab38, a new member of the Rab small G protein family. Biol Chem. 2005;386(2):143–53

Otsuki H. Sensory organs in the cerebral vesicle of the Ascidian larva, Aplidium sp.: an SEM study. Zoological Science 1991, 8 pp. 235–242.

Owen DJ, Collins BM, Evans PR. Adaptors for clathrin coats: structure and function. Annu Rev Cell Dev Biol 2004; 20:153-91; PMID:15473838.Otto SP. 2007. The evolutionary consequences of polyploidy. Cell. 131:452–462.

Palumbo A, Solano F, Misuraca G, Aroca P, Garcia Borron JC, Lozano JA, Prota G. Comparative action of dopachrome tautomerase and metal ions on the rearrangement of dopachrome. Biochim Biophys Acta (1991) 1115, 1-5.

Panzella L, Micillo R, Bentley WE, Napolitano A, Payne GF. Reverse Engineering Applied to Red Human Hair Pheomelanin Reveals Redox-Buffering as a Pro-Oxidant Mechanism. Sci Rep (2015) 16; 5:18447.

Parichy DM, Ransom DG, Paw B, Zon LI, Johnson SL. An orthologue of the kit-related gene fms is required for development of neural crest-derived xanthophores and a subpopulation of adult melanocytes in the zebrafish, Danio rerio. Development. (2000) Jul;127(14):3031-44.

Park M, Serpinskaya AS, Papalopulu N, Gelfand VI. Rab32 regulates melanosome transport in Xenopus melanophores by protein kinase a recruitment. Curr Biol. 2007;17(23):2030–4.

Park HH. Structural basis of membrane trafficking by Rab family small G protein. Int J Mol Sci. 2013 Apr 25;14(5):8912-23. doi: 10.3390/ijms14058912

Pereira-Leal JB, Seabra MC. Evolution of the Rab family of small GTP-binding proteins. J Mol Biol. 2001;313(4):889–901.

Pereira-Leal JB. (2008). The Ypt/Rab family and the evolution of trafficking in fungi. Traffic 9, 27-38.

Plonka PM, Grabacka M. Melanin synthesis in microorganisms-biotechnological and medical aspects. Acta Biochim Pol (2006) 53, 429-443.

Popovici C, Roubin R, Coulier F, Birnbaum D. An evolutionary history of the FGF superfamily. Bioessays. 2005 Aug;27(8):849-57.

Press CMcL, Evensen Ø. The morphology of the immune system in teleost fishes. Fish & Shellfish Immunology 1999 9, 309–318.

Putnam NH, Butts T, Ferrier DE, Furlong RF, Hellsten U, Kawashima T, et al. The amphioxus genome and the evolution of the chordate karyotype. Nature. 2008;453(7198):1064–71.

Quevedo WC, Fleischmann RD. Developmental biology of mammalian melanocytes. J. Invest. Dermatol. 1980 75, 116–120.

Racioppi C, Kamal AK, Razy-Krajka F, Gambardella G, Zanetti L, di Bernardo D, Sanges R, Christiaen LA, Ristoratore F. Fibroblast growth factor signalling controls nervous system patterning and pigment cell formation in Ciona intestinalis. Nat Commun. 2014 Sep 5;5:4830. doi: 10.1038/ncomms5830.

Racioppi C, Valoroso MC, Coppola U, Lowe EK, Brown CT, Swalla BJ, Christiaen L, Stolfi A, Ristoratore F. Evolutionary loss of melanogenesis in the tunicate Molgula occulta. Evodevo. 2017 Jul 18;8:11. doi: 10.1186/s13227-017-0074-x. eCollection 2017.

Raible DW, Wood A, Hodsdon W, Henion PD, Weston JA, Eisen JS. Segregation and early dispersal of neural crest cells in the embryonic zebrafish. Dev Dyn. 1992 Sep;195(1):29-42.

Ravi V, Lam K, Tay BH, Tay A, Brenner S, Venkatesh B. Elephant shark (Callorhinchus milii) provides insights into the evolution of Hox gene clusters in gnathostomes. Proc Natl Acad Sci U S A. 2009;106(38):16327–32.

Riley PA. Materia melanica: further dark thoughts. Pigment Cell Res 1992; 5, 101-106.

Riley PA. Melanin. Int J Biochem Cell Biol (1997) 29, 1235-1239.

Rojas AM, Fuentes G, Rausell A, Valencia A. The Ras protein superfamily: evolutionary tree and role of conserved amino acids. J Cell Biol. 2012 Jan 23;196(2):189-201.

Robinson ML. An essential role for FGF receptor signaling in lens development. Semin Cell Dev Biol. 2006 Dec;17(6):726-40. Epub 2006 Oct 27.

Roure A, Darras S. Msxb is a core component of the genetic circuitry specifying the dorsal and ventral neurogenic midlines in the ascidian embryo. Dev Biol. 2016 Jan 1;409(1):277-87. doi: 10.1016/j.ydbio.2015.11.009.

Russo MT, Donizetti A, Locascio A, D'Aniello S, Amoroso A, Aniello F, Fucci L, Branno M. Regulatory elements controlling Ci-msxb tissue-specific expression during Ciona intestinalis embryonic development. Dev Biol. 2004 Mar 15;267(2):517-28.

Rutherford S, Moore I. The Arabidopsis Rab GTPase family: another enigma variation. Curr Opin Plant Biol. 2002;5(6):518–28.

Sakurai D, Goda M, Kohmura Y, Horie T, Iwamoto H, Ohtsuki H, Tsuda M. The role of pigment cells in the brain of ascidian larva. J Comp Neurol. 2004 12;475(1):70-82.

Saito-Nakano Y, Nakahara T, Nakano K, Nozaki T, Numata O. Marked amplification and diversification of products of ras genes from rat brain, Rab GTPases, in the ciliates Tetrahymena thermophila and Paramecium tetraurelia. J Eukaryot Microbiol. 2010;57(5):389–99.

Sato S, Masuya H, Numakunai T, Satoh N, Ikeo K, Gojobori T, Tamura K, Ide H, Takeuchi T, Yamamoto H.Ascidian tyrosinase gene: its unique structure and expression in the developing brain. Dev Dyn. 1997 Mar;208(3):363-74.

Satoh N, Satou Y, Davidson B, Levine M.. Ciona intestinalis: an emerging model for whole-genome analyses. Trends Genet. 2003, 19, 376–381.

Satou Y, Imai KS, Satoh N. Fgf genes in the basal chordate Ciona intestinalis. Dev Genes Evol. 2002 Oct;212(9):432-8. Epub 2002 Sep 5.

Schartl M, Larue L, Goda M, Bosenberg MW, Hashimoto H, Kelsh RN. What is a vertebrate pigment cell? Pigment Cell Melanoma Res. 2014 Jan; 29(1):8-14.

Schlenstedt G. Protein import into the nucleus. FEBS Lett. 1996 Jun 24;389(1):75-9.
Schnetkamp PP. The SLC24 gene family of $Na^+/Ca^{2+}-K^+$ exchangers: from sight and smell to memory consolidation and skin pigmentation. Mol Aspects Med. 2013 Apr-Jun;34(2-3):455-64.

Seo HC, Saetre BO, Håvik B, Ellingsen S, Fjose A. The zebrafish Pax3 and Pax7 homologues are highly conserved, encode multiple isoforms and show dynamic segment-like expression in the developing brain. Mech Dev. (1998) Jan;70(1-2):49-63.

Shi L, Zhang W, Zou F, Mei L, Wu G, Teng Y. KLHL21, a novel gene that contributes to the progression of hepatocellular carcinoma. BMC Cancer. 2016 Oct 21;16(1):815.

Shintani M, Tada M, Kobayashi T, Kajiho H, Kontani K, Katada T. Characterization of Rab45/RASEF containing EF-hand domain and a coiled-coil motif as a self-associating GTPase. Biochem Biophys Res Commun. 2007 Jun 8;357(3):661-7.

Shimeld SM, Holland PW. Vertebrate innovations. Proc Natl Acad Sci USA 2000 Apr 25;97(9):4449-52.

Shimeld SM, Purkiss AG, Dirks RP, Bateman OA, Slingsby C, Lubsen NH. Urochordate betagamma-crystallin and the evolutionary origin of the vertebrate eye lens. Curr Biol. 2005 Sep 20;15(18):1684-9.

Shin SS, Namkoong J, Wall BA, Gleason R, Lee HJ, Chen S. Oncogenic activities of metabotropic glutamate receptor 1 (Grm1) in melanocyte transformation. Pigment Cell Melanoma Res. 2008;21(3):368–78.

Sigrist CJA, de Castro E, Cerutti L, Cuche BA, Hulo N, Bridge A, Bougueleret L, Xenarios I. News and continuing developments at PROSITE. Nucleic Acids Res. 2012; doi: 10.1093/nar/gks1067.

Silver DL, Hou L, Pavan WJ. The genetic Regulation of Pigment Cell Development. Austin (TX): Landes Bioscience; 2000-2013.

Sitaram A, Marks MS. Mechanisms of protein delivery to melanosomes in pigment cells. Physiology (Bethesda). 2012 Apr;27(2):85-99.

Skafidas E, Testa R, Zantomio D, Chana G, Everall IP, Pantelis C. Predicting the diagnosis of autism spectrum disorder using gene pathway analysis. Mol Psychiatry. 2014;19(4):504–10.

Slominski A, Tobin DJ, Shibahara S, Wortsman J. Melanin Pigmentation in Mammalian Skin and Its Hormonal Regulation. Physiol Rev. 2004; 84: 1155–1228.

Squarzoni P, Parveen F, Zanetti L, Ristoratore F, Spagnuolo A. FGF/MAPK/Ets signaling renders pigment cell precursors competent to respond to Wnt signal by directly controlling Ci-Tcf transcription. Development. 2011 Apr;138(7):1421-32. doi: 10.1242/dev.057323.

Srikanth S, Jung HJ, Kim KD, Souda P, Whitelegge J, Gwack Y.A novel EF-hand protein, CRACR2A, is a cytosolic Ca2+ sensor that stabilizes CRAC channels in T cells. Nat Cell Biol. 2010 May;12(5):436-46. doi: 10.1038/ncb2045.

Srikanth S, Kim KD, Gao Y, Woo JS, Ghosh S, Calmettes G, Paz A, Abramson J, Jiang M, Gwack Y. A large Rab GTPase encoded by CRACR2A is a component of subsynaptic vesicles that transmit T cell activation signals. Sci Signal. 2016 Mar 22;9(420):ra31. doi: 10.1126/scisignal.aac9171.

Srikanth S, Woo JS, Gwack Y. A large Rab GTPase family in a small GTPase world. Small GTPases. 2017 Jan 2;8(1):43-48. doi: 10.1080/21541248.2016.1192921. Steel KP, Barkway C. Another role for melanocytes: their importance for normal stria vascularis development in the mammalian inner ear. Development 1989 107(3):453-63.

Steingrímsson E. The basic helix-loop-helix leucine zipper transcription factor Mitf is conserved inDrosophila and functions in eye development. Genetics. 2004 May;167(1):233-41.

Stenmark H, Olkkonen VM. The Rab GTPase family. Genome Biol. 2001;2(5)

Stenmark H. Rab GTPases as coordinators of vesicle traffic. Nat Rev Mol Cell Biol. 2009;10(8):513–25.

Stenmark H. The Rabs: a family at the root of metazoan evolution. BMC Biol. 2012 Aug 8;10:68. doi: 10.1186/1741-7007-10-68.

Stolfi A, Gandhi S, Salek F, Christiaen L. Tissue-specific genome editing in Ciona embryos by CRISPR/Cas9. Development. 2014 Nov;141(21):4115-20.

Strauss O. The retinal pigment epithelium in visual function. Physiol Rev. 2005, 85:845–81

Streit A, Berliner AJ, Papanayotou C, Sirulnik A, Stern CD. Initiation of neural induction by FGF signalling before gastrulation. Nature. 2000 Jul 6;406(6791):74-8.

Sudhof TC, Rothman JE. (2009). Membrane fusion: grappling with SNARE and SM proteins. Science 323, 474-477.

Sugimoto M. Morphological color changes in fish: regulation of pigment cell density and morphology. Microsc Res Tech. 2002;58(6):496–503.

Sulaimon SS, Kitchell BE. The biology of melanocytes. Vet Dermatol. 2003, 4(2):57-65.

Surkont J, Pereira-Leal JB. Are There Rab GTPases in Archaea? Mol Biol Evol. 2016 Jul;33(7):1833-42. doi: 10.1093/molbev/msw061.

Takeda K, Yasumoto K, Takada R, Takada S, Watanabe K, Udono T, Saito H, Takahashi K, Shibahara S. Induction of melanocyte-specific microphthalmia-associated transcription factor by Wnt-3a. J Biol Chem. 2000 May 12;275(19):14013-6.

Tamura K, Ohbayashi N, Maruta Y, Kanno E, Itoh T, Fukuda M. Varp is a novel Rab32/38-binding protein that regulates Tyrp1 trafficking in melanocytes. Mol Biol Cell. 2009 Jun;20(12):2900-8. doi: 10.1091/mbc.E08-12-1161. Epub 2009 Apr 29.

Tan R, Wang W, Wang S, Wang Z, Sun L, et al. Small GTPase Rab40c Associates with Lipid Droplets and Modulates the Biogenesis of Lipid Droplets. PLoS ONE (2013) 8(4): e63213. doi:10.1371/journal.pone.0063213.

Tarafder AK, Bolasco G, Correia MS, Pereira FJ, Iannone L, Hume AN, Kirkpatrick N, Picardo M, Torrisi MR, Rodrigues IP, Ramalho JS, Futter CE, Barral DC, Seabra MC. Rab11b mediates melanin transfer between donor melanocytes and acceptor keratinocytes via coupled exo/endocytosis. J Invest Dermatol. 2014 Apr;134(4):1056-66. doi: 10.1038/jid.2013.432. Epub 2013 Oct 18.

Taylor JS, Van de Peer Y, Braasch I, Meyer A. Comparative genomics provides evidence for an ancient genome duplication event in fish. Philos Trans R Soc Lond B Biol Sci. 2001;356(1414):1661–79

Taylor JS, Braasch I, Frickey T, Meyer A,Van de Peer Y. Genome duplication, a trait shared by 22000 species of ray-finned fish. Genome Res. 2003;13(3):382–90.

Thisse B, Pflumio S, Fürthauer M, Loppin B, Heyer V, Degrave A, et al. Expression of the zebrafish genome during embryogenesis (NIH R01RR15402). ZFIN Direct Data Submission (http://zfinorg). 2001

Thisse B, Thisse C. Fast Release Clones: A High Throughput Expression Analysis. ZFIN Direct Data Submission 2004 (http://zfin.org).

Touchot N, Chardin P, Tavitian A. Four additional members of the ras gene superfamily isolated by an oligonucleotide strategy: molecular cloning of YPT-related cDNAs from a rat brain library. Proc Natl Acad Sci U S A. 1987 Dec;84(23):8210-4.

Vetrini F, Auricchio A, Du J, Angeletti B, Fisher DE, Ballabio A, Marigo V. The microphthalmia transcription factor (Mitf) controls expression of the ocular albinism type 1 gene: link between melanin synthesis and melanosome biogenesis. Mol Cell Biol. 2004 Aug;24(15):6550-9.

Thompson JD, Higgins DG, Gibson TJ. CLUSTAL W: improving the sensitivity of progressive multiple sequence alignment through sequence weighting, position-specific gap penalties and weight matrix choice. Nucleic Acids Res. 1994; 22(22):4673–80.

Torday JS, Rehan VK. Deconvoluting lung evolution using functional/comparative genomics. Am J Respir Cell Mol Biol. 2004;31(1):8–12.

Tresser J, Chiba S, Veeman M, El-Nachef D, Newman-Smith E, Horie T, Tsuda M, Smith WC. doublesex/mab3 related-1 (dmrt1) is essential for development of anterior neural plate derivatives in Ciona. Development. 2010 Jul;137(13):2197-203. doi: 10.1242/dev.045302

Trezise AE, Collin SP. Opsins: evolution in waiting. Curr Biol 2005, 15:R794-6.
Matsumoto Y, Fukamachi S, Mitani H, Kawamura S. Functional characterization of visual opsin repertoire in Medaka (Oryzias latipes). Gene 2006, 371:268-78.

Tsuda M, Sakurai D, Goda M. Direct evidence for the role of pigment cells in the brain of ascidian larvae by laser ablation. J Exp Biol. 2003, 206(Pt 8):1409–17.

Venkatesh B, Lee AP, Ravi V, Maurya AK, Lian MM, Swann JB, et al. Elephant shark genome provides unique insights into gnathostome evolution. Nature. 2014;505(7482):174–9.

Virta VC, Cooper MS. Structural components and morphogenetic mechanics of the zebrafish yolk extension, a developmental module. J Exp Zool B Mol Dev Evol. 2011;316(1):76–92

Vopalensky P, Pergner J, Liegertova M, Benito-Gutierrez E, Arendt D, Kozmik Z. Molecular analysis of the amphioxus frontal eye unravels the evolutionary origin of the retina and pigment cells of the vertebrate eye. Proc Natl Acad Sci USA 2012, 109(38):15383–8.

Wada H, Saiga H, Satoh N, Holland PW. Tripartite organization of the ancestral chordate brain and the antiquity of placodes: insights from ascidian Pax-2/5/8, Hox and Otx genes. Development. 1998 Mar;125(6):1113-22.

Wang C, Liu Z, Huang X. Rab32 is important for autophagy and lipid storage in Drosophila. PLoS One. 2012;7(2), e32086.

Wasmeier C, Romao M, Plowright L, Bennett DC, Raposo G, Seabra MC. Rab38 and Rab32 control post-Golgi trafficking of melanogenic enzymes. J Cell Biol. 2006;175(2):271–81.

Wei ML. Hermansky-Pudlak syndrome: a disease of protein trafficking and organelle function. Pigment Cell Res. 2006;19(1):19–42.
Widlund HR, Fisher DE. Microphthalamia-associated transcription factor: a critical regulator of pigment cell development and survival. Oncogene. 2003 May 19;22(20):3035-41.

West-Eberhard MJ. 2003. Developmental plasticity and evolution. New York: Oxford University Press.

Wittkopp PJ, True JR, Carroll SB. Reciprocal functions of the Drosophila yellow and ebony proteins in the development and evolution of pigment patterns. Development 2002 129, 1849-1858

Wasmeier C, Romao M, Plowright L, Bennett DC, Raposo G, Seabra MC. Rab38 and Rab32 control post-Golgi trafficking of melanogenic enzymes. J Cell Biol. 2006 175(2):271–81.

Wu X, Rao K, Bowers MB, Copeland NG, Jenkins NA, Hammer JA. Rab27a enables myosin Va-dependent melanosome capture by recruiting the myosin to the organelle. J Cell Sci. 2001, 114: 1091–1100.

Wu XS, Rao K, Zhang H, Wang F, Sellers JR, Matesic LE, Copeland NG, Jenkins NA, Hammer JA 3rd. Identification of an organelle receptor for myosin-Va. Nature Cell Biol. 2002, 4: 271–278.

Yajima I, Endo K, Sato S, Toyoda R, Wada H, Shibahara S, Numakunai T, Ikeo K, Gojobori T, Goding CR, Yamamoto H. Cloning and functional analysis of ascidian Mitf in vivo: insights into the origin of vertebrate pigment cells. Mech Dev. 2003 Dec;120(12):1489-504.

Yang XJ. Roles of cell-extrinsic growth factors in vertebrate eye pattern formation and retinogenesis. Semin Cell Dev Biol. 2004 Feb;15(1):91-103.

Yasumoto K., Yokoyama K., Shibata K., Tomita Y., Shibahara S. Microphthalmia-associated transcription factor as a regulator for melanocyte-specific transcription of the human tyrosinase gene. Mol. Cell. Biol. 1994;14:8058–8070.

Yatsu A, Shimada H, Ohbayashi N, Fukuda M. Rab40C is a novel Varp-binding protein that promotes proteasomal degradation of Varp in melanocytes. Biol Open. (2015) Mar 15; 4(3): 267–275.

Yoshida-Amano Y, Hachiya A, Ohuchi A, Kobinger GP, Kitahara T, Takema Y, Fukuda M. Essential role of RAB27A in determining constitutive human skin color. PLoS One. 2012;7(7):e41160. doi: 10.1371/journal.pone.0041160.

Yu JK, Meulemans D, McKeown SJ, Bronner-Fraser M. Insights from the amphioxus genome on the origin of vertebrate neural crest. Genome Res. 2008 Jul;18(7):1127-32. doi: 10.1101/gr.076208.108.

Zerial M, McBride H. Rab proteins as membrane organizers. Nat Rev Mol Cell Biol. 2001 Feb;2(2):107-17.

Zhang L, Yu K, Robert KW, DeBolt KM, Hong N, Tao JQ, Fukuda M, Fisher AB, Huang S. Rab38 targets to lamellar bodies and normalizes their sizes in lung alveolar type II epithelial cells. Am J Physiol Lung Cell Mol Physiol. 2011 Oct;301(4):L461-77. doi: 10.1152/ajplung.00056.2011.

Zippelius A, Gati A, Bartnick T, Walton S, Odermatt B, Jaeger E, Dummer R, Urosevic M, Filonenko V, Osanai K, Moch H, Chen YT, Old LJ, Knuth A, Jaeger D. Melanocyte

differentiation antigen RAB38/NY-MEL-1 induces frequent antibody responses exclusively in melanoma patients. Cancer Immunol Immunother. 2007 Feb;56(2):249-58.

LIST OF PUBLICATIONS

Coppola U, Annona G, D'Aniello S, Ristoratore F. (2016) Rab32 and Rab38 genes in chordate pigmentation: an evolutionary perspective. BMC Evol Biol DOI: 10.1186/s12862-016-0596-1

Tammaro S, Simoniello P, Ristoratore F, Coppola U, Scudiero R, Motta CM (2016) Expression of caspase 3 in ovarian follicle cells of the lizard Podarcis sicula. Cell Tissue Res. 2017 Feb;367(2):397-404. doi: 10.1007/s00441-016-2506-7

Racioppi C, Valoroso MC, Coppola U, Lowe EK, Brown CT, Swalla BJ, Christiaen L, Stolfi A, Ristoratore F. Evolutionary loss of melanogenesis in the tunicate Molgula occulta. Evodevo. 2017 Jul 18;8:11. doi: 10.1186/s13227-017-0074-x.

Coppola U, Nittoli V, Sepe RM, D'Agostino Y, De Felice E, Palladino A, Vassalli QA, Locascio A, Ristoratore F, Spagnuolo A, D'Aniello S, Sordino P. A comprehensive analysis of neurotrophins and neurotrophin tyrosine kinase receptors expression during development of zebrafish. Journal of Comparative Neurology 2018 DOI: 10.1002/cne.24391 (first equal author)